TECHNISCHE UNIVERSITÄT WIEN
Vienna | Austria

Dissertation

Development of a Novel Handle-Based Wheelchair Propulsion Device

carried out for the purpose of obtaining the degree of Doctor technicae (Dr. techn.),

submitted at TU Wien, Faculty of Mechanical and Industrial Engineering, by

Dipl.-Ing. Markus Puchinger

Mat.Nr.: 00627748

under the supervision of

Univ.Prof.in Dipl.-Ing. Dr.in techn. Margit Gföhler

Institute of Engineering Design and Product Development

Research Unit of Biomechanics and Rehabilitation Engineering

E307-03

Vienna, March 2023

reviewed by

Ao.Univ.Prof. Dipl.-Ing. Dr.med. Dr.techn. Dr.phil.

Thomas Angeli

Institute of Engineering Design
and Product Development

TU Wien

Getreidemarkt 9

1060 Vienna, Austria

Ao.Univ.-Prof. Dipl.-Ing. Dr.techn.

Christian Peham

Department for Companion Animals
and Horses

University of Veterinary Medicine

Veterinärplatz 1

1210 Vienna, Austria

Die approbierte gedruckte Originalversion dieser Dissertation ist an der TU Wien Bibliothek verfügbar.
The approved original version of this doctoral thesis is available in print at TU Wien Bibliothek.
TU WIEN Bibliothek Your knowledge hub

This work was supported by the Austrian Science Fund (FWF)
within the framework of the project P 25507-B24

I confirm, that going to press of this thesis needs the confirmation of the examination committee.

Affidavit

I declare in lieu of oath, that I wrote this thesis and performed the associated research myself, using only literature cited in this volume. If text passages from sources are used literally, they are marked as such.

I confirm that this work is original and has not been submitted elsewhere for any examination, nor is it currently under consideration for a thesis elsewhere.

I acknowledge that the submitted work will be checked electronically-technically using suitable and state-of-the-art means (plagiarism detection software). On the one hand, this ensures that the submitted work was prepared according to the high-quality standards within the applicable rules to ensure good scientific practice "Code of Conduct" at the TU Wien. On the other hand, a comparison with other student theses avoids violations of my personal copyright.

City and Date *Signature*

Die approbierte gedruckte Originalversion dieser Dissertation ist an der TU Wien Bibliothek verfügbar.
The approved original version of this doctoral thesis is available in print at TU Wien Bibliothek.
TU WIEN Bibliothek Your knowledge hub

Danksagung

Ich möchte mich besonders bei Univ.Prof.in Dipl.-Ing. Dr.in techn. Markit Gföhler bedanken, dass ich meine Dissertation in ihrer Arbeitsgruppe durchführen konnte und sie mich stets unterstützte. Sie gab mir die Möglichkeit an vielen spannenden Projekten mitwirken zu können und dabei stets mein Wissen weiter zu vertiefen.

Weiters gilt ein großer Dank an Hermann Wallner und Helmut Taxpointner, welche mich seit der Bachelorarbeit tatkräftig bei der Fertigung sowie dem Zusammenbau vieler unserer Entwicklungen unterstützten und immer für Ratschläge und Hilfe bereitstanden.

Nithin Kurup möchte ich für seine Freundschaft sowie die tolle Zusammenarbeit in diesem gemeinsamen Projekt danken, ohne seine vorhergegangene Forschungsarbeit wäre diese Arbeit nicht möglich gewesen. Zudem möchte ich mich bei all meinen Arbeitskollegen, bedanken, die ich über die Jahre am Institut kennengelernt habe. Sie alle waren unglaublich hilfsbereit und machten jeden Arbeitstag motivierend und unterhaltsam.

Der größte Dank gilt jedoch meiner Familie, die mich auf diesem Weg begleitet und stets unermüdlich unterstützt haben. An letzter, aber prominentester Stelle möchte ich meiner wundervollen Frau Roksana danken, die mir nicht nur meinen Sohn Maximilian schenkte, sondern auch genügend Raum verschaffen hat, um diese Dissertation letztendlich fertigstellen zu können.

Die approbierte gedruckte Originalversion dieser Dissertation ist an der TU Wien Bibliothek verfügbar.
The approved original version of this doctoral thesis is available in print at TU Wien Bibliothek.
TU WIEN Bibliothek Your knowledge hub

Table of Contents

Danksagung I
Table of Contents II
Abstract IV
Kurzfassung V
List of Figures VI
List of Tables VIII
List of Abbreviations IX
Journal Publications X
Conference Publications and Patent XI
Conference Publications XI
Granted Patent XI
Author's Contribution XII
1 Introduction 13
1.1 Motivation 13
1.2 Biomechanical Optimization and Design of a Novel Device for Manual Wheelchair Propulsion 15
1.3 Objectives 16
2 Methods 18
2.1 Propulsion Device Design 18
2.2 Experimental Methods 21
2.2.1 Test Rig [26] 21
2.2.2 Measurement of Muscle Activations 24
2.2.3 Measurement of Hand Contact Forces and Joint Angles 26
2.2.4 Spirometry Measurements 27
2.2.5 Data Analysis and Statistical Testing 29
3 Journal Publication I 30
3.1 Summary 30

Die approbierte gedruckte Originalversion dieser Dissertation ist an der TU Wien Bibliothek verfügbar.
The approved original version of this doctoral thesis is available in print at TU Wien Bibliothek.
TU WIEN Bibliothek Your knowledge hub

3.2 Publication 31

4 Journal Publication II 45

4.1 Summary 45

4.2 Publication 46

5 Journal Publication III 54

5.1 Summary 54

5.2 Publication 55

6 Journal Publication IV 73

6.1 Summary 73

6.2 Publication 74

7 Conclusion and Outlook 89

List of References 91

Appendix 99

Granted Patent 100

Die approbierte gedruckte Originalversion dieser Dissertation ist an der TU Wien Bibliothek verfügbar.
The approved original version of this doctoral thesis is available in print at TU Wien Bibliothek.
TU WIEN Bibliothek Your knowledge hub

Abstract

The wheelchair is one of the most commonly used assistive devices to enhance the mobility of people with lower limb impairments. According to the World Health Organisation (WHO), more than one percent of the world's population is dependent on a wheelchair. More than 90% of all wheelchair users prefer the push-rim, even though it is the least efficient mode of propulsion. Awkward force distribution in non-ergonomic joint angle ranges as well as frequent repetitions are not only strenuous for the musculoskeletal system, they also frequently lead to severe upper limb injuries. Consequently, a project supported by the Austrian Research and Science Fund (FWF) was launched with the aim of developing an ergonomic wheelchair drive which reduces joint strain while maximising power output.

The aim of the present work was to develop and evaluate a mechanical wheelchair drive that follows a motion path optimised for the musculoskeletal system previously obtained by numerical simulation and optimization methods.

A crank mechanism was chosen as the most suitable propulsion variant for this purpose, in which a length-variable crank follows a sliding guide along the optimal path of motion using. Timing belts transmit the propulsion power slip-free to the reduced rear wheels, and the crank position can be adjusted to the user without any tools. A stationary, wheelchair-based test stand has been developed during the course of this work to evaluate different propulsion methods.

Through hand contact force measurement, motion analysis, electromyographic as well as spiroergometric measurements, the novel drive was tested and evaluated at different power levels with a group of wheelchair users as well as a nondisabled control group.

The results showed that this novel drive enables force application over the complete drive cycle, while keeping the joint angles within the ergonomic ranges. Furthermore, the efficiency was significantly increased compared to push-rim propulsion.

The scientific work presented here can contribute significantly to people who are dependent on a wheelchair and can help to preserve or improve their independence and integration in daily life.

Die approbierte gedruckte Originalversion dieser Dissertation ist an der TU Wien Bibliothek verfügbar.
The approved original version of this doctoral thesis is available in print at TU Wien Bibliothek.
TU WIEN Bibliothek Your knowledge hub

Kurzfassung

Der Rollstuhl ist eines der am häufigsten verwendeten Hilfsmittel, um die Mobilität von Menschen mit Einschränkungen der unteren Extremität zu verbessern. Nach Angaben der WHO sind mehr als ein Prozent der Weltbevölkerung auf einen Rollstuhl angewiesen. Obwohl der Greifring die am wenigsten effizienteste Antriebsart darstellt, ist er für mehr als 90 % aller Rollstuhlfahrer die bevorzugte. Ungünstige Kraftverhältnisse in nicht ergonomischen Gelenkwinkelbereichen als auch die vielen Wiederholungen sind nicht nur anstrengend für den Bewegungsapparat, sondern führen häufig zu schweren Erkrankungen der oberen Gliedmaßen. Deswegen wurde ein durch den österreichischen Forschungs- und Wissenschaftsfond (FWF) unterstütztes Projekt ins Leben gerufen, welches das Ziel eines gelenkschonenden, ergonomischen Rollstuhlantriebs bei maximaler Leistungsausbeute hatte. Ziel dieser Arbeit war es, auf Basis einer zuvor durch computerunterstützte Simulation erhaltenen, für den Bewegungsapparat optimierten Bewegungskurve, einen dieser Kurve folgenden, mechanischen Rollstuhlantrieb zu entwickeln als auch zu evaluieren.

Als für diesen Zweck am besten geeignete Antriebsvariante wurde ein Kurbelmechanismus gewählt, der über eine längenveränderliche Kurbel einer Gleitführung mit der optimalen Bewegungskurve folgt. Über Zahnriemen wird die Antriebsleistung zu den verkleinerten Hinterrädern schlupffrei geführt, die Lage der Kurbeln kann ohne Werkzeug auf die Benutzer eingestellt werden. Zur Evaluierung verschiedener Antriebsformen wurde im Zuge dieser Arbeit auch ein stationärer, rollstuhlbasierender Prüfstand entwickelt.

Mittels Handkontaktkraftmessung, Bewegungsanalyse, elektromyographischer als auch spiroergometrischer Messungen wurde der neue Antrieb bei unterschiedlichen Belastungsstufen mit einer Gruppe von Rollstuhlfahrer*innen als auch einer nicht beeinträchtigten Kontrollgruppe getestet.

Die Ergebnisse zeigten, dass diese neue Antriebsform eine Kraftaufbringung über den gesamten Antriebszyklus hinweg ermöglicht, wobei die Gelenkwinkel in den ergonomischen Bereichen bleiben. Darüber hinaus konnte die Effizienz im Vergleich zum Greifring erheblich gesteigert werden.

Die hier vorgestellte wissenschaftliche Arbeit kann einen wesentlichen Beitrag für Menschen, welche auf einen Rollstuhl angewiesen sind, leisten und kann dazu beitragen ihre Unabhängigkeit sowie die Integration im alltäglichen Leben zu erhalten bzw. zu verbessern.

Die approbierte gedruckte Originalversion dieser Dissertation ist an der TU Wien Bibliothek verfügbar.
The approved original version of this doctoral thesis is available in print at TU Wien Bibliothek.
TU WIEN Bibliothek Your knowledge hub

List of Figures

Figure 1: Schematic function of the length-adjusting crank mechanism. 18
Figure 2: Novel handle based propulsion (HBP) device for the right-hand side..... 19
Figure 3: Conventional wheelchair equipped with two HBP devices in different views. 20
Figure 4: Digital mock-up of the wheelchair-based test rig in front and rear view..... 22
Figure 5: Drive-train layout of the wheelchair-based test rig..... 23
Figure 6: SMART^{Wheel} installed on the right side of the test rig during experiments with paraplegic subjects..... 23
Figure 7: Weight and width modified Force Measurement Handle used during experiments 24
Figure 8: EMG surface electrode placement..... 25
Figure 9: Schematic of the experimental setup for EMG measurements in PRP and HBP..... 26
Figure 10: Schematic of the experimental setup for hand contact force and joint angle measurements in PRP and HBP..... 26
Figure 11: Reflective markers placed on the upper limb of each subject and propulsion devices..... 27
Figure 12: Spirometry measurement setup for HBP during incremental exercise..... 28
Figure 13: (a) Musculoskeletal model with right hand linked to the propulsion mechanism (b) Kinematic components of the propulsion mechanism..... 34
Figure 14: Dynamically optimized propulsion path 38
Figure 15: Optimized muscle activity patterns. 39
Figure 16: Net work done by the upper limb muscles during the four zones of propulsion with the optimized handle path..... 40
Figure 17: Comparison of the joint ranges of motion (ROM) of the upper extremity between push-rim propulsion and the HBP technique..... 40
Figure 18: Normalized fiber length and normalized fiber shortening velocity of the muscles spanning the elbow joint during one full crank rotation 41
Figure 18: Peak muscle forces obtained from the computational simulation of HBP compared to dynamic optimization results for push rim propulsion. 41
Figure 13: Standard push-rim wheelchair attached to controllable custom made test rig and handle based propulsion mechanism. 48

Die approbierte gedruckte Originalversion dieser Dissertation ist an der TU Wien Bibliothek verfügbar.
The approved original version of this doctoral thesis is available in print at TU Wien Bibliothek.
TU WIEN Bibliothek Your knowledge hub

Figure 14: Mean muscle activation intervals for the two propulsion modes at 25W and 35W workloads respectively 51
Figure 15: Wheelchair based test rig 58
Figure 16: Handle based propulsion device and its components 59
Figure 17: Biomechanical Model 61
Figure 18: HP resultant and tangential forces 63
Figure 19: HP upper-limb joint angles vs. crank angle 64
Figure 20: Joint angles/joint torques. Averaged normalized joint torque-joint angle trajectories generated with HP for: (A) shoulder elevation-plane, (B) shoulder elevation-angle, (C) shoulder rotation, (D) wrist deviation and (E) wrist flexion. .. 66
Figure 21: Wheelchair-based test rig with mounted HBP devices 79
Figure 22: Handle-based propulsion (HBP) device and its components 79
Figure 23: Dependence of gross mechanical efficiency (*GME*), oxygen uptake per unit distance travelled (VO_2 *efficiency*), weight-related oxygen uptake (VO_2/kg), heart rate (*HR*), ventilation (*Ve*) and oxygen uptake (VO_2) on resistance level measured for PP subjects and ND subjects during HBP and PRP. 83
Figure 24: Mean RER values and standard deviations measured for HBP and PRP in paraplegic and non-disabled subjects. 84

Die approbierte gedruckte Originalversion dieser Dissertation ist an der TU Wien Bibliothek verfügbar.
The approved original version of this doctoral thesis is available in print at TU Wien Bibliothek.
TU WIEN Bibliothek Your knowledge hub

List of Tables

Table 1: Normalized EMG peak magnitude and performance Index across the two workloads for both propulsion modes. 50

Table 2: Characteristics of the 8 subjects with spinal cord injury 60

Table 3: Resultant peak forces during HP and PRP 67

Table 4: Maximum and minimum joint angles in degrees during HP and PRP. 68

Table 5: Peak joint torques in HP and PRP. 71

Table 6: Characteristics of paraplegic (PP) and non-disabled (ND) subjects 78

Table 7: Mean (SD) submaximal values measured for HBP and PRP at 15W constant resistance for the PP and ND groups 82

Table 8: ANOVA results obtained for the maximal exercise tests (15W-35W) for the PP and ND subject groups 84

Table 9: Mean values and standard deviations for peak power output ($PO_{(peak)}$), peak weight-related oxygen uptake ($VO_2/kg_{(peak)}$), peak oxygen uptake ($VO_{2(peak)}$), peak ventilation ($Ve_{(peak)}$), peak respiratory exchange ratio ($RER_{(peak)}$), and peak heart rate ($HR_{(peak)}$). Results obtained from the ANOVA for propulsion mode (HBP vs. PRP), group (ND vs. PP) and interaction effects are also shown. 85

Die approbierte gedruckte Originalversion dieser Dissertation ist an der TU Wien Bibliothek verfügbar.
The approved original version of this doctoral thesis is available in print at TU Wien Bibliothek.
TU WIEN Bibliothek Your knowledge hub

List of Abbreviations

3D	three dimensional
ADL	activities of daily life
ANOVA	analysis of variance
BMI	body mass index
CTS	carpal tunnel syndrome
DOF (DoF)	degree(s) of freedom
EHDM	ergonomic lever propulsion device
EMG	electromyography
En	metabolic expenditure
GME	gross mechanical efficiency
GUI	graphical user interface
HBP	handle-based propulsion
HR	heart rate
MVC	maximum voluntary contraction
ND	non-disabled
PI	performance index
PO	power output, resistance power
PP	paraplegic
PRP	push-rim propulsion
RER	respiratory exchange ratio
SCI	spinal cord injury
SD	standard deviation
sEMG	surface electromyography
VCO_2	carbon dioxide output
Ve	ventilation
VO_2	oxygen uptake
WHO	World Health Organization
Wi-Fi	Wireless Fidelity, WLAN

Die approbierte gedruckte Originalversion dieser Dissertation ist an der TU Wien Bibliothek verfügbar.
The approved original version of this doctoral thesis is available in print at TU Wien Bibliothek.
TU WIEN Bibliothek Your knowledge hub

Journal Publications

This cumulative dissertation is based on the following four publications:

Journal Publication I

Forward dynamic optimization of handle path and muscle activity for handle based isokinetic wheelchair propulsion: A simulation study

Nithin Babu Rajendra Kurup, Markus Puchinger, Margit Gföhler

*Computer Methods in Biomechanics and Biomedical Engineering, **2019**, 22: 55-63.*

DOI: 10.1080/10255842.2018.1527321

Journal Publication II

A preliminary muscle activity analysis: Handle based and push-rim wheelchair propulsion

Nithin B. R. Kurup, Markus Puchinger, Margit Gföhler

*Journal of Biomechanics, **2019**, 89: 119-122.*

DOI: 10.1016/J.JBIOMECH.2019.04.011

Journal Publication III

In Vivo Biomechanical Assessment of a Novel Handle-Based Wheelchair Drive

Markus Puchinger, Pia Stefanek, Karin Gstaltner, Marcus G. Pandy, Margit Gföhler

*IEEE transactions on neural systems and rehabilitation engineering (TNSRE), **2021**, 29: 1669-1678.*

DOI: 10.1109/TNSRE.2021.3105388

Journal Publication IV

Metabolic Cost and Mechanical Efficiency of a Novel Handle-Based Device for Wheelchair Propulsion

Markus Puchinger, Nithin B. R. Kurup, Karin Gstaltner, Marcus G. Pandy, Margit Gföhler

*Journal of Rehabilitation Medicine (JRM), **2022**, 54: jrm00346.*

DOI: 10.2340/JRM.V54.1503

Die approbierte gedruckte Originalversion dieser Dissertation ist an der TU Wien Bibliothek verfügbar.
The approved original version of this doctoral thesis is available in print at TU Wien Bibliothek.
TU WIEN Bibliothek Your knowledge hub

Conference Publications and Patent

Conference Publications

Conference Publication I

Dynamically Optimized Muscle Activity Patterns from a Novel Handle Based Propulsion Movement for a Wheelchair

Nithin B. R. Kurup, Markus Puchinger, Margit Gföhler

*Proceedings of the 35th Conference of the International Society of Biomechanics in Sports (ISBS), **2017**, 35: 698-701*

https://commons.nmu.edu/isbs/vol35/iss1/218

Conference Publication II

Wrist kinematics and kinetics during wheelchair propulsion with a novel handle-based propulsion mechanism

Nithin B. R. Kurup, Markus Puchinger, Thomas Keck, Margit Gföhler

*40th Annual International Conference of the IEEE Engineering in Medicine and Biology Society, **2018,** 2146-2149*

DOI: 10.1109/EMBC.2018.8512658

Granted Patent

Mechanischer Rollstuhlantrieb und Rollstuhl mit einem solchen mechanischen Rollstuhlantrieb

English title: Mechanical Wheelchair Drive and Wheelchair having such a Mechanical Wheelchair Drive

Markus Puchinger, Nithin B. R. Kurup, Margit Gföhler

EP 3 823 576 B1, PCT/AT2019/060235, WO 2020/014720

*Registered: **16.07.2019**, Granted: 16.02.2022*

Die approbierte gedruckte Originalversion dieser Dissertation ist an der TU Wien Bibliothek verfügbar.
The approved original version of this doctoral thesis is available in print at TU Wien Bibliothek.
TU WIEN Bibliothek Your knowledge hub

Author’s Contribution

Journal Publication I

Markus Puchinger evaluated and specified the various parameters of the simulation for a possible mechanical implementation. He reviewed and edited the publication.

Journal Publication II

Markus Puchinger was extensively involved in this work. He built a prototype of the novel handle-based wheelchair drive and constructed a universal slip-free wheelchair test rig for evaluation. Furthermore, he was responsible for the implementation and data acquisition of the tests, including the measurement of EMG signals and MVC as well as motion capture. He processed the collected data in substantial parts. He wrote, reviewed and edited the publication in significant parts.

Journal Publication III

Markus Puchinger planned and conducted the in vivo biomechanical assessment of the novel handle-based wheelchair drive in substantial parts. He was responsible for the implementation and data acquisition of the tests, including the measurement of EMG signals and hand contact forces as well as motion capture. He advised regarding the adaption of the biomechanical model of the upper arm, which allows estimating muscle forces and torques based on the measured data for both, handle-based drive and push-rim. He wrote, reviewed and edited the publication.

Journal Publication IV

Markus Puchinger planned and conducted the metabolic assessment of the novel handle-based wheelchair drive on paraplegic and non-disabled individuals. He was responsible for the implementation of the measurement and data acquisition in both, submaximal and maximal tests, where cardio and respiratory parameters were obtained. He wrote, reviewed and edited the publication.

Die approbierte gedruckte Originalversion dieser Dissertation ist an der TU Wien Bibliothek verfügbar.
The approved original version of this doctoral thesis is available in print at TU Wien Bibliothek.
TU WIEN Bibliothek Your knowledge hub

1 Introduction

1.1 Motivation[1]

The wheelchair is one of the most commonly used assistive devices for enhancing the mobility of physically disabled persons. According to the World Health Organization, an estimated 1% of the world's population, or more than 80 million people worldwide, require the use of a wheelchair [1]. Wheelchair users typically include people with spinal cord injuries, lower limb amputation, stroke, multiple sclerosis, rheumatoid arthritis, spina bifida, poliomyelitis as well as hip fractures and other groups. Nearly 90% of all wheelchairs are propelled manually by using the arms to apply force to the push-rims, even though it is the least efficient pattern of propulsion [2].

Manual wheelchair users use upper extremities mainly for mobility, but also for transfers, pressure relief, and several other daily functional activities. During all these activities, high joint loads are applied to the upper limbs, which are not accustomed to heavy repetitive loading. Thus, manual wheelchair users are at a high risk of upper-limb injury. There is a high prevalence of upper-limb pain and pathology in manual wheelchair users, including the carpal tunnel syndrome at the wrist, shoulder impingement syndrome and rotator cuff injuries, elbow/shoulder tendinitis and osteoarthritis [3–5].

Upper-extremity pain and injury are therefore a major problem for wheelchair dependent persons as use of the arms is essential for independent mobility and participation in the community. Thus, extensive research has been performed to understand the biomechanical and physiological factors of wheelchair propulsion [6].

Limited information is available on joint angle ranges and joint loads during conventional PRP. The applied patterns during PRP are characterized by large variations between subjects and the results are altered by propulsion cadence [7]. However, it can be concluded from literature that PRP leads to non-ergonomic joint excursions, especially for the wrist and shoulder joint and that the highest loads occur in these non-ergonomic areas.

Furthermore, as mentioned before, PRP is energetically inefficient and associated with high cardiopulmonary effort, leading to high metabolic cost, heart rate and oxygen uptake [8–10]. Previous studies show that only 20% of the stroke cycle, the so-called push phase, contributes

[1] Due to the proximity in content of this cumulative dissertation and the publications included therein, this section is based on the review of Publication I-IV.

.

Die approbierte gedruckte Originalversion dieser Dissertation ist an der TU Wien Bibliothek verfügbar.
The approved original version of this doctoral thesis is available in print at TU Wien Bibliothek.
TU Bibliothek Your knowledge hub WIEN

to pushing the wheelchair forward [10]. To benchmark mechanical efficiency of manual wheelchair propulsion, gross mechanical efficiency (GME), the percentage ratio between external power output and energy expenditure, is used. In PRP, GME is usually between 2 10% and rarely exceeds 10% [2, 11].

Alternative modes of manual wheelchair propulsion have been widely considered, the most common alternatives being lever-propulsion and arm-crank-propulsion. Both of these methods increase joint range of motion in the upper limb, particularly at wrist and shoulder joints, compared to PRP [2, 12, 13].

Lever-propelled devices were mainly designed to reduce repetitive strain injuries [2, 12, 14, 15]. Previous studies have shown that lever-propelled wheelchair designs decrease shoulder muscular demands and offer more constant propulsion force application at the hand [2, 12, 14, 16]. In general, GME in lever-propelled devices is found to be higher compared to PRP, and wheelchair users report greater overall satisfaction with lever-propelled wheelchairs, but previous designs do not consider user anthropometrics [2, 15]. However, Zukowski *et al.* [12] compared the metabolic cost of a special so-called ergonomic lever propulsion mechanism (EHDM) with conventional PRP for twelve spinal cord injured adults, and surprisingly, the results for ergonomic lever propulsion showed lower VO_2 efficiency and almost identical HR compared to PRP.

Arm-crank-propelled wheelchairs, so-called handcycles (handbikes), are the most popular crank-propelled alternative to PRP for manual wheelchair propulsion with GME values measured between 8% and 15% [13, 17–20]. Due to a higher energetic efficiency and lower strain on the cardiorespiratory system, several authors recommend the handcycles as an alternative to push-rim wheelchair propulsion for outdoor use [10, 13, 17, 19, 21, 22].

In general, the efficiency of alternative devices for wheelchair propulsion is often higher, especially when gearing is included. A major drawback of all currently available alternative propulsion systems is that they can hinder activities of daily living (ADL), as they are usually bulky, heavy and less manoeuvrable. This can be problematic for essential daily activities, such as transfers, back wheel balancing to overcome steps, moving the chair over a variety of surfaces or sitting at a table [2, 13, 17, 23, 24].

Die approbierte gedruckte Originalversion dieser Dissertation ist an der TU Wien Bibliothek verfügbar.
The approved original version of this doctoral thesis is available in print at TU Wien Bibliothek.
TU WIEN Bibliothek Your knowledge hub

1.2 Biomechanical Optimization and Design of a Novel Device for Manual Wheelchair Propulsion

The work presented here was part of the research project "Biomechanical optimization and design of a novel device for manual wheelchair propulsion" and was supported by the Austrian Science Fund (FWF) under grant number P 25507 B24.

In this project, to overcome the limitations of PRP, the project team[2] set the overall goal to combine musculoskeletal modelling with the principles of wheelchair mechanical design to develop a novel optimized manual wheelchair propulsion device that is compatible with the physiological properties of the human upper-limb musculoskeletal system.

Based on findings of previous studies related to this topic, the design criteria for the optimized devices shall be:

I. Circular hand movement and a continuous upper-arm movement pattern that involves the flexor and extensor muscles, and hence a larger muscle mass compared to a discontinuous push. We hypothesize that the new design will distribute physical strain over a larger number of muscles.

II. No extreme joint excursions

III. Two optimization problems shall be solved using two different cost functions:

   a. Cost Function 1 will minimize muscular effort during manual wheelchair propulsion, thereby improving mechanical efficiency.

   b. Cost Function 2 will minimize upper-limb joint contact forces.

In a first step, a 3D human musculoskeletal model of the upper extremity shall be established to determine a handle-based continuous wheelchair propulsion movement in a forward dynamic optimization simulation that optimizes the handle-path shape and muscle activity patterns for maximum net propulsion power. These results are described in detail in the doctoral thesis of Nithin B. R. Kurup [25] and partially in **[Journal Publication I & II]**.

In a second step, the obtained results from simulation shall be applied and, consequently, two novel optimized propulsion devices (left and right side) shall be developed and evaluated which is the main content of the here presented thesis.

[2] The project team consists of researchers from the Research Division of Biomechanics and Rehabilitation Engineering at TU Wien (Head: Prof. M. Gföhler) and the Department of Mechanical Engineering at the University of Melbourne (Head: Prof. M. G. Pandy)

Die approbierte gedruckte Originalversion dieser Dissertation ist an der TU Wien Bibliothek verfügbar.
The approved original version of this doctoral thesis is available in print at TU Wien Bibliothek.
TU Bibliothek Your knowledge hub WIEN

1.3 Objectives

As part of the residual project, this dissertation aims to develop and evaluate a novel manual wheelchair drive mechanism that follows an ergonomically optimized movement path for the arms, which is expected to be more joint-friendly and efficient compared to conventional manual drives.

The optimized motion path has been obtained from musculoskeletal simulation and optimization [25], thus the focus of this thesis is on the mechanical implementation followed by evaluation and benchmarking of this novel wheelchair drive.

The following objectives were set for a comprehensive evaluation as well as the biomechanical assessment of the novel wheelchair drive:

I. Propulsion parameters required for the mechanical implementation of the drive shall be determined based on simulation results **[Journal Publication I]**.

II. A custom-built instrumented wheelchair ergometer shall be developed to ensure reliability and reproducibility of measured data during experiments with different propulsion devices **[26]**.

III. Muscle activations of the major upper limb muscles shall be measured on non-disabled individuals during different workloads on the physically realised handle-based propulsion drive (HBP) and the push-rim to investigate differences in muscle activation patterns. The assumption of lower peak muscle activations and thus reduced muscular effort during HBP shall be evaluated. **[Journal Publication II]**.

IV. Propulsion forces, upper-limb joint excursions and predicted net joint torques generated by this novel HBP device shall be determined on the instrumented test rig for paraplegic and non-disabled subjects. The hypothesis of higher propulsion force effectiveness, lower average propulsion forces and ergonomic joint excursions during HBP in comparison to PRP shall be validated. Furthermore, the individual force application over an entire cycle shall be investigated to identify changing propulsion patterns. **[Journal Publication III]**.

V. Differences in metabolic cost and mechanical efficiency for HBP in comparison to PRP shall be investigated on the instrumented test rig. Data shall be collected from paraplegic long-term wheelchair users as well as non-disabled individuals, to further investigate effects on propulsion mode and efficiency and to determine how the results differ for long-term wheelchair users who have trained muscle coordination

Die approbierte gedruckte Originalversion dieser Dissertation ist an der TU Wien Bibliothek verfügbar.
The approved original version of this doctoral thesis is available in print at TU Wien Bibliothek.
TU WIEN Bibliothek Your knowledge hub

patterns for PRP and may also have changed relative muscle strengths. Furthermore, the hypothesis that HBP is more energetically efficient and less strenuous compared to PRP shall be validated. **[Journal Publication IV]**.

Die approbierte gedruckte Originalversion dieser Dissertation ist an der TU Wien Bibliothek verfügbar.
The approved original version of this doctoral thesis is available in print at TU Wien Bibliothek.
TU WIEN Bibliothek Your knowledge hub

2 Methods[3]

The present work describes the development of a novel handle based manual wheelchair propulsion device that was evaluated for both mechanical efficiency and metabolic cost. This section describes the methods used. The descriptions are intended to provide a basis for understanding the research findings presented in Chapter 3 (Journal Publication) and Chapter 7 (Conclusion and Outlook).

2.1 Propulsion Device Design

A mechanism must be designed to generate the propulsion path determined by the dynamic optimization solution described in Kurup [25].

Due to the most important design criteria of size and weight, a solution was found that consists of a sliding guide mechanism which follows the optimized handle path and a slip-free power transmission to the back wheels (Figure 1 and Figure 2).

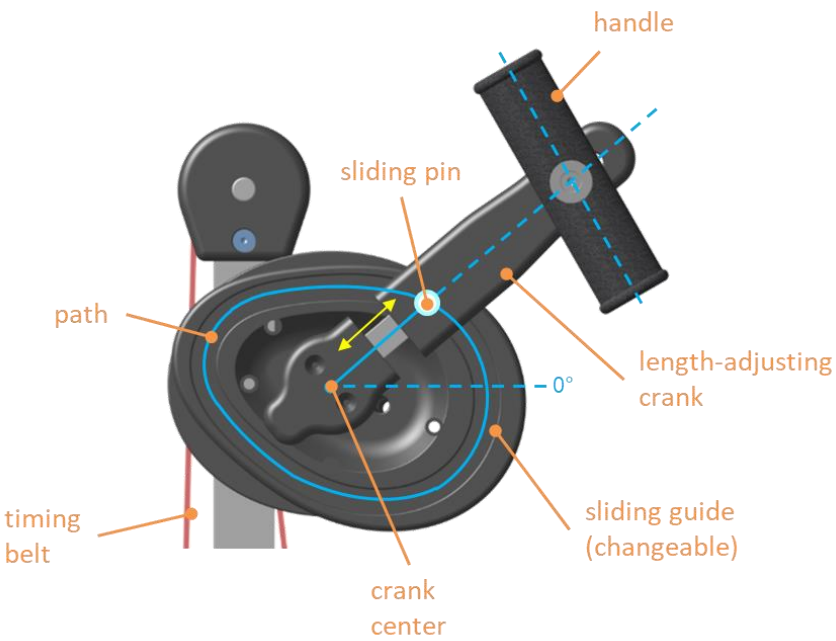

Figure 1: Schematic function of the length-adjusting crank mechanism.

The use of latest manufacturing methods, such as fiber-reinforced 3D printed plastics, enabled a slim design that is optimized for load and allows steady guides with low weight and maximum stiffness. Moreover, the chosen design allows easy testing of different path

[3] The method section is based on the method sections of the publications included in this cumulative dissertation.

Die approbierte gedruckte Originalversion dieser Dissertation ist an der TU Wien Bibliothek verfügbar.
The approved original version of this doctoral thesis is available in print at TU Wien Bibliothek.
TU Bibliothek Your knowledge hub WIEN

solutions obtained from simulation by only changing the sliding guide part, which is an important point for improvements on the prototype.

The novel handle based propulsion (HBP) drive is mounted on each side of a conventional wheelchair instead of the armrests. The drives for the left and the right side are basically the same and were designed in a way that most parts can be used for both sides. Thus, the function is only explained for the right-hand drive.

The handle is mounted to a length-adjusting crank, that rotates around the center point of the path and follows the sliding guide (Figure 1). The propulsion torque is transmitted via timing belts to the back wheels of the wheelchair. A special pulley layout allows to adapt the crank center position horizontally and vertically to the user's anthropometric lengths without changing the belt pretension. With the possibility of a changeable timing belt pully, the gear ratio can be adjusted for different back wheel diameters to guarantee submaximal propulsion at the recommended cadence of 50 revolutions per minute [22].

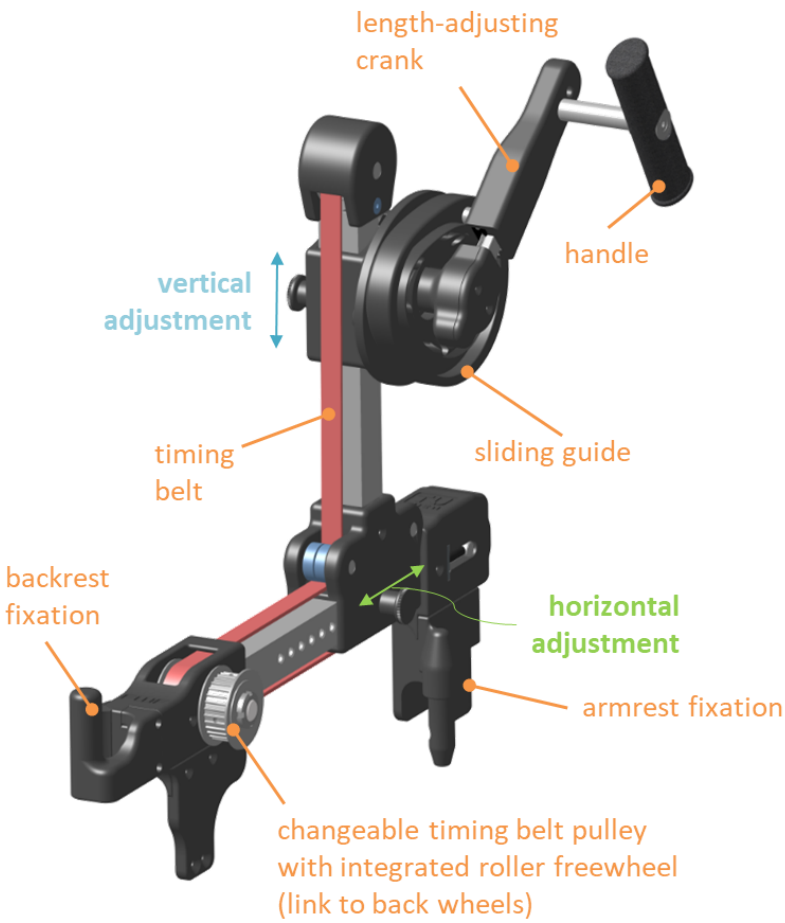

Figure 2: Novel handle based propulsion (HBP) device for the right-hand side

Die approbierte gedruckte Originalversion dieser Dissertation ist an der TU Wien Bibliothek verfügbar.
The approved original version of this doctoral thesis is available in print at TU Wien Bibliothek.

Two sets of prototypes were built, one adapted for the scientific measurements and the other for demonstration of the functionality on a conventional wheelchair.

The scientific prototypes were attached to the wheelchair-based test rig described in Chapter 2.2.1. Thus, the prototypes did not include the objectives of not restricting the working space of the upper extremities, no impeding during transfers and the possibility of braking. Figure 3 shows the HBP devices mounted on a conventional wheelchair to demonstrate the functionality. The back wheels were reduced to 20 inches to avoid collisions with the propulsion mechanism, and a hydraulic bicycle braking system was used with brake levers on each handle. The whole design is described more detailed in **[Granted Patent]**.

Figure 3: Conventional wheelchair equipped with two HBP devices in different views

A short video clip showing the HBP drive in action is available on YouTube® by scanning the QR code below.

https://youtu.be/jUpi1ZzdHBQ

Die approbierte gedruckte Originalversion dieser Dissertation ist an der TU Wien Bibliothek verfügbar.
The approved original version of this doctoral thesis is available in print at TU Wien Bibliothek.
TU WIEN Bibliothek Your knowledge hub

2.2 Experimental Methods

The objective was to investigate differences in metabolic cost, muscle activation patterns, and mechanical efficiency for this novel HBP device compared to the standard PRP. Data were collected from paraplegic subjects, who are long-term wheelchair users, and non-disabled individuals to further investigate effects on propulsion mode and efficiency and to determine how the results differ for long term wheelchair users who have trained muscle coordination patterns for push-rim propulsion and may also have changed relative muscle strengths.

The experiments with paraplegic subjects were performed at the Rehabilitation Center Weisser Hof in Klosterneuburg (Lower Austria), whereas the experiments with non-disabled subjects were performed at the laboratory facility of the Research Unit for Biomechanics and Rehabilitation Engineering at TU Wien. All subjects provided informed consent and approval for all measurements was obtained from the responsible federal state ethics committee (GS1-EK-3/149-2018).

Each group used an instrumented wheelchair-based test rig (described in Section 2.2.1) operating at constant speed and different resistance levels. Three different experiment types were performed to evaluate the novel propulsion device:

I. Comparison of upper extremity muscle activations between PRP and HBP at different workloads **[Journal Publication II]**
II. Determination of hand contact forces and correspondent joint angles to estimate joint torques at shoulder and wrist **[Journal Publication III]**
III. Recording of cardiorespiratory factors to assess metabolic cost and gross mechanical efficiency **[Journal Publication IV]**.

2.2.1 Test Rig [26]

A standard wheelchair represents the basis for the development, the digital mock-up of the test-rig is shown in Figure 4. The base frame, a welded steel tube construction raises the wheelchair to a height where the back wheels are not in contact with the floor. A motor-gearbox unit (EC45, Maxon Motors) mounted under the seat with associated control (EPOS 70/10, Maxon Motors) is connected via a timing belt to a distribution shaft. The distributor-shaft connects timing belt pulleys for the back wheels and front attachment area, where different propulsion devices can be attached. The standard 24-inch back wheels with push-rims have been modified with timing belt pulleys so that they can be connected to the pulleys of the distributor-shaft. A manually operated belt tensioner allows the back wheels to

Die approbierte gedruckte Originalversion dieser Dissertation ist an der TU Wien Bibliothek verfügbar.
The approved original version of this doctoral thesis is available in print at TU Wien Bibliothek.
TU WIEN Bibliothek Your knowledge hub

be attached or detached quickly and easily. With this configuration, the back wheels can be changed in less than two minutes.

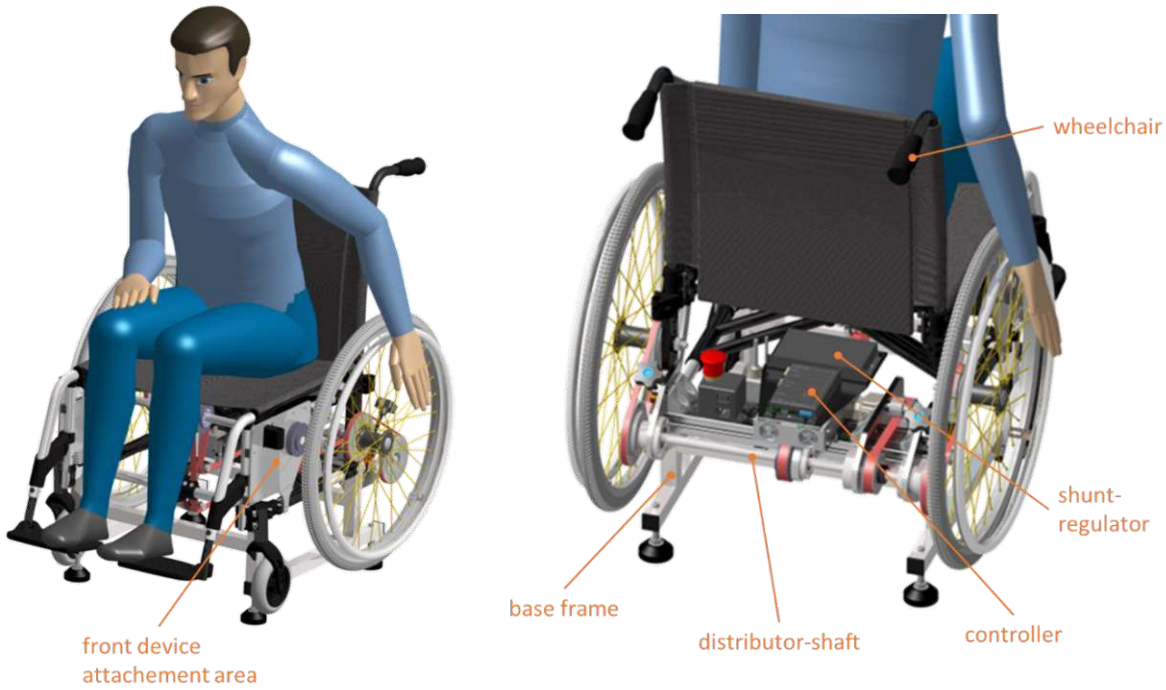

Figure 4: Digital mock-up of the wheelchair-based test rig in front (left) and rear view (right)

The controller of the motor-gear unit can communicate with the programmed LabView® routine on the PC and acts as resistor during propulsion of any device attached to the test rig. The released energy is dissipated via a shunt regulator (DSR70/30, Maxon Motors). A small flywheel is attached to the motor-gearbox unit to flatten control peaks in acceleration and deceleration phases and to imitate inertia (Figure 5).

By starting and stopping measurements on the test rig, the controller sends trigger impulses (+5V twitch), where different measurement systems can be synchronized. The software enables the user to operate the test rig in three different modes:

I. Imitation of real conditions, whereas specific profiles for velocity, inclination and floor conditions over the time can be set and driven.

II. Constant power mode, whereas the resistance torque is permanently adapted to the propulsion speed to keep a predefined power value.

III. Incremental power mode, whereas the resistance torque is changing to predefined power values by time.

Over an additional monitor connected to the PC, visual feedback on resistance power, propulsion speed and experiment time can be given to the probands. Furthermore, the

Die approbierte gedruckte Originalversion dieser Dissertation ist an der TU Wien Bibliothek verfügbar.
The approved original version of this doctoral thesis is available in print at TU Wien Bibliothek.
TU Bibliothek Your knowledge hub WIEN

software is able to record data from both, a commercially available instrumented push-rim wheel (SMART^{Wheel}) and a custom-made wireless force/torque measuring handle.

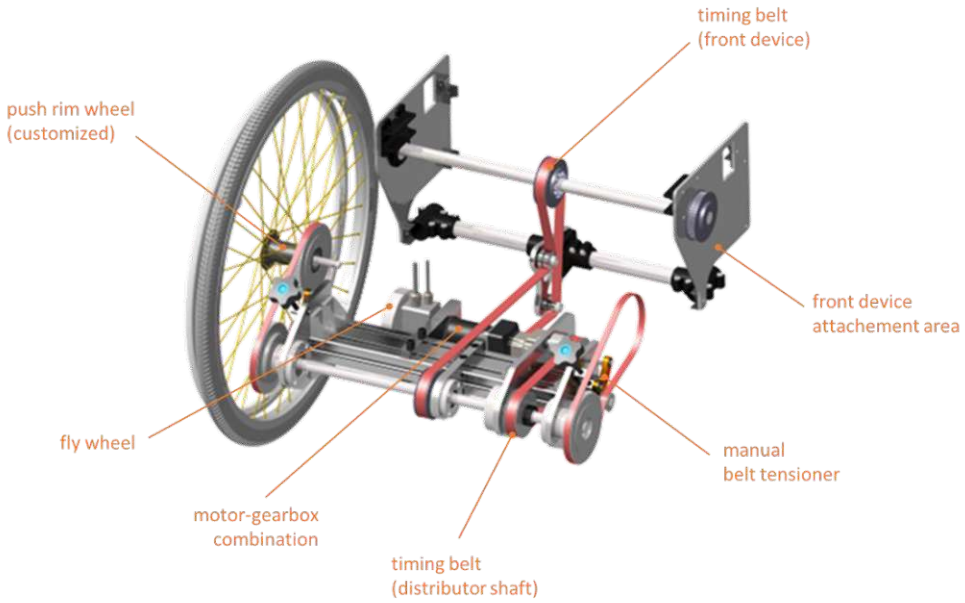

Figure 5: Drive-train layout of the wheelchair-based test rig

2.2.1.1 SMART^{Wheel}

The SMART^{Wheel} (Out-Front, USA), shown in Figure 6, is an instrumented wheel for push-rim propulsion designed for professional use in clinical or research settings [27]. The unit is equipped with an axle mount and replaces the 24-inch back wheel of a manual wheelchair.

Figure 6: SMART^{Wheel} installed on the right side of the test rig during experiments with paraplegic subjects

Die approbierte gedruckte Originalversion dieser Dissertation ist an der TU Wien Bibliothek verfügbar.
The approved original version of this doctoral thesis is available in print at TU Wien Bibliothek.
TU WIEN Bibliothek Your knowledge hub

Over Wi-Fi, information on three-dimensional propulsion forces and torques, applied to the push-rim are sent and can be stored and visualized. Similar to the modified push-rim wheels, a timing belt pulley was added to the hub of the SMART^{Wheel} to connect it with the test rig.

2.2.1.2 Force Measurement Handle

To determinate the applied hand contact forces during propulsion in HBP custom made force measurement handle similar to [28] was used. Different to the existing solution, the 6-axis-force/torque sensor (K6D40, ME-Messsysteme GmbH) was moved out of the center to reduce the overall width to the size of the HBP's handgrip (Figure 7). The sensor handle was integrated into a 3D printed fiber-reinforced low-density plastic housing to minimize the effects of inertia. With a M10 machine thread, the sensor can be mounted on each HBP device by replacing its handgrip. Two measurement amplifiers (GSV-4BT, ME-Messsysteme GmbH) are integrated above and below the handgrip and send the measurement data directly to the test rig software via Bluetooth. Three-dimensional propulsion forces respective to the tilt-angle are measured. The sensor calibration is performed automatically before each measurement.

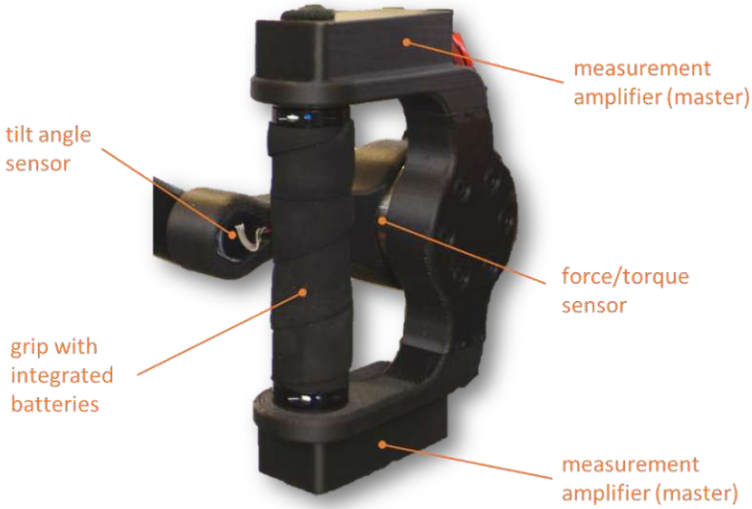

Figure 7: Weight and width modified Force Measurement Handle used during experiments

2.2.2 Measurement of Muscle Activations[4]

Muscle activations were recorded of seven muscles (*deltoid anterior, deltoid medial, deltoid posterior, pectoralis major, biceps brachii, triceps long* and *triceps lateral*) via surface

[4] This section is based on the methods of Journal Publication II

Die approbierte gedruckte Originalversion dieser Dissertation ist an der TU Wien Bibliothek verfügbar.
The approved original version of this doctoral thesis is available in print at TU Wien Bibliothek.
TU Bibliothek Your knowledge hub WIEN

electromyography electrodes (sEMG) using a wireless EMG measurement system (Delsys Trigno). Only the right arm was investigated and used to propel in both propulsion modes, assuming symmetry of propulsion as only subjects without upper extremity injury or pain were selected **[Journal Publication II]**.

After placement of all EMG sensors for each subject (Figure 8), muscle maximum voluntary contraction (MVC) measurements were conducted, to normalize the EMG.

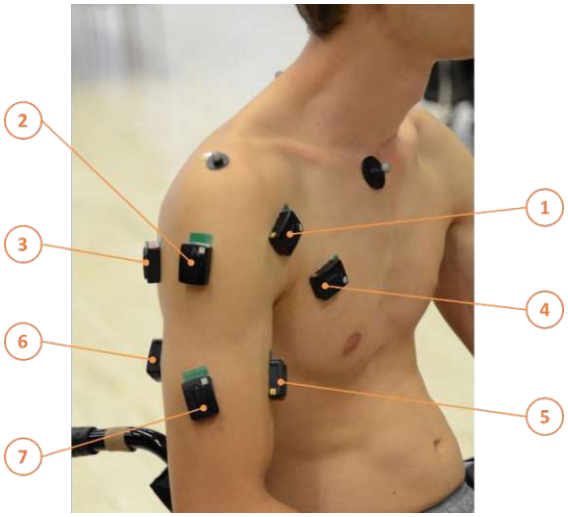

Figure 8: EMG surface electrode placement
(1: deltoid anterior, 2: deltoid medial, 3: deltoid posterior, 4: pectoralis major, 5: biceps brachii, 6: triceps long and 7: triceps lateral)

For the tests, two workloads at 25W and 35W had to be performed with both HBP and PRP. Therefore, the test rig was set to constant power mode, where the propulsion resistance can be predefined via the software [26].

Figure 9 left shows the schematic experimental setup of the muscle activation measurements for PRP. The same setup was used for the HBP measurements, only on the test rig the back wheels were detached and an HBP unit was installed instead of the armrest (Figure 9 right). During tests, visual feedback was given to the participants to aid keeping the target propulsion speed of 1.1m/s.

The subjects performed the tests at two workloads for each of the propulsion systems in a randomized order to minimize effects of training or fatigue on the results. To determine propulsion cycles from motion, an 8-camera motion capture system (Motion Analysis Corporation, Kestrel 2200/Cortex 7) along with reflective markers placed on the propulsion units of HBP and PRP at 120Hz capture frequency was used. The data collection of all systems was synchronized by the test rig software.

Die approbierte gedruckte Originalversion dieser Dissertation ist an der TU Wien Bibliothek verfügbar.
The approved original version of this doctoral thesis is available in print at TU Wien Bibliothek.
TU WIEN Bibliothek Your knowledge hub

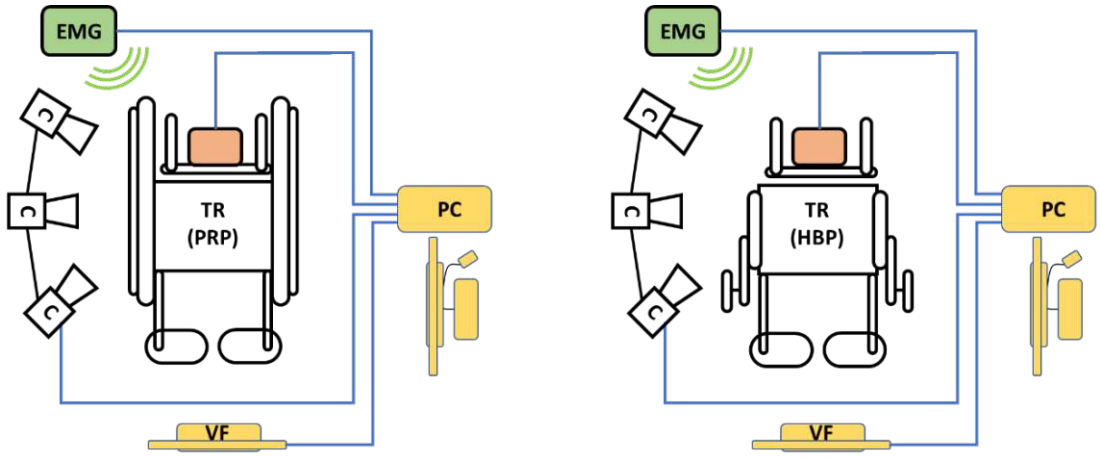

Figure 9: Schematic of the experimental setup for EMG measurements in PRP (left) and HBP (right)
{PC: Computer, TR: Test Rig, VF: Visual Feedback, EMG: EMG Base Station, C: Motion Capturing}

2.2.3 Measurement of Hand Contact Forces and Joint Angles[5]

The subjects were asked to complete two workloads at 25W and 35W with both HBP and PRP on the test rig. Therefore, test rig which operated in constant power mode. Due to the assumption of symmetric propulsion, the hand contact forces were measured on the right side for both propulsion modes. For HBP, the hand contact forces were measured with the force measuring handle, for PRP with the SMART^{Wheel}. All trials were performed at a wheelchair linear velocity of 1.1m/s and visual feedback on actual and target speed was provided to each participant, ensuring a constant speed during each trial. Figure 10 shows the schematic experimental setup of the contact force and joint angle measurements for PRP and HBP.

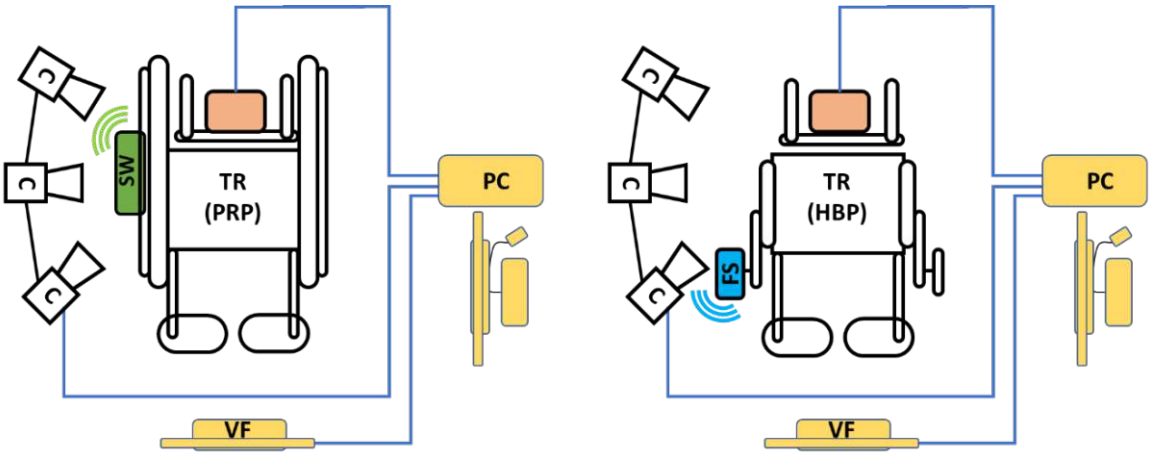

Figure 10: Schematic of the experimental setup for hand contact force and joint angle measurements in PRP (left) and HBP (right)
{PC: Computer, TR: Test Rig, VF: Visual Feedback, SW: SMART^{Wheel}, FS: Force Sensor, C: Motion Capturing}

[5] This section is based on the methods of Journal Publication III

Die approbierte gedruckte Originalversion dieser Dissertation ist an der TU Wien Bibliothek verfügbar.
The approved original version of this doctoral thesis is available in print at TU Wien Bibliothek.
TU WIEN Bibliothek Your knowledge hub

Ten propulsion cycles at each workload were recorded and a two-minute rest interval between the two trials was given. With an 8-camera motion capture system (Motion Analysis Corporation, Kestrel 2200/Cortex 7) the upper limb trajectories of ten reflective markers placed on the participant's upper limb and trunk (*clavicle, acromion, 7th cervical vertebrae, biceps, lateral epicondyle and medial epicondyle, forearm, radial styloid, ulnar styloid, 2nd metacarpophalangeal*) were recorded. Three additional markers were placed on the handle as well as on the SMART^{Wheel} to simultaneously capture the position of the propulsion device (Figure 11).

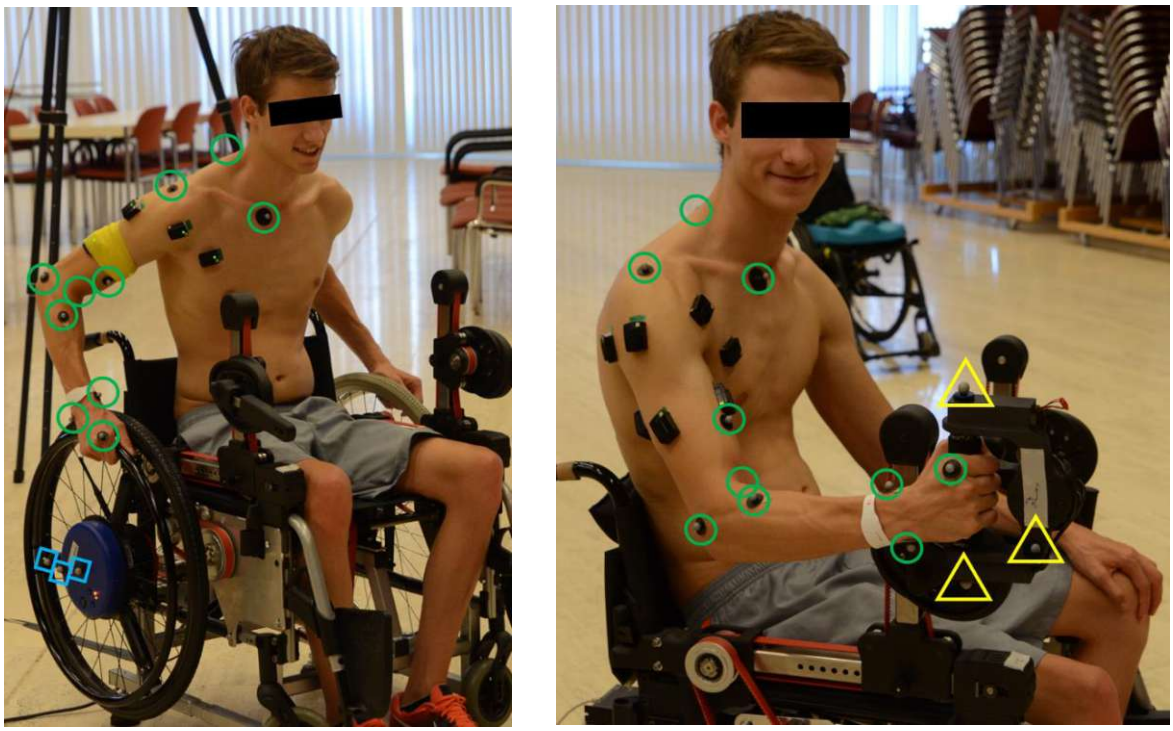

Figure 11: Reflective markers placed on the upper limb of each subject and propulsion devices {CIRCLE: upper limb or trunk marker, SQUARE: SMART^{Wheel} marker, TRIANGLE: HBP marker}

The data thus obtained were processed with Matlab® and converted to the respective joint angles. For post processing and data analysis only cycles after reaching steady propulsion at the target speed were used, acceleration and deceleration phases were not included. The data collection of all systems was synchronized by the test rig software.

2.2.4 Spirometry Measurements[6]

All participating subjects had to perform an exercise test on both HBP and PRP device. The exercise test consisted of two parts: a two-minute submaximal exercise test performed at

[6] This section is based on the methods of Journal Publication IV

Die approbierte gedruckte Originalversion dieser Dissertation ist an der TU Wien Bibliothek verfügbar.
The approved original version of this doctoral thesis is available in print at TU Wien Bibliothek.
TU WIEN Bibliothek Your knowledge hub

15W constant resistance power, followed by a maximal exercise test in which the resistance power was increased by 5W every minute. Both parts were performed consecutively with no break in between. The test was terminated when either 55W of resistance power was reached or when the subject reached physical exhaustion and could not continue. To simulate a common propulsion speed, subjects were asked to maintain a propulsion speed in the range 1.20-1.65m/s for both HBP and PRP.

During each test, the actual resistance power and linear velocity were measured concurrently. For PRP, conventional 24-inch diameter push-rim wheels were mounted on the test rig whereas for crank propulsion two HBP devices were utilized instead of the armrests (Figure 12). The test rig operated in incremental power mode, where the resistance progressively increased according to a predefined resistance increment and time interval. In all trials, visual feedback allowed the participant to maintain the target speed during propulsion. All subjects performed the same exercise with both PRP and HBP on the same day with a minimum rest period of 10 minutes between each trial. Subjects were assigned to alternately start with PRP or HBP to prevent any influence from fatigue.

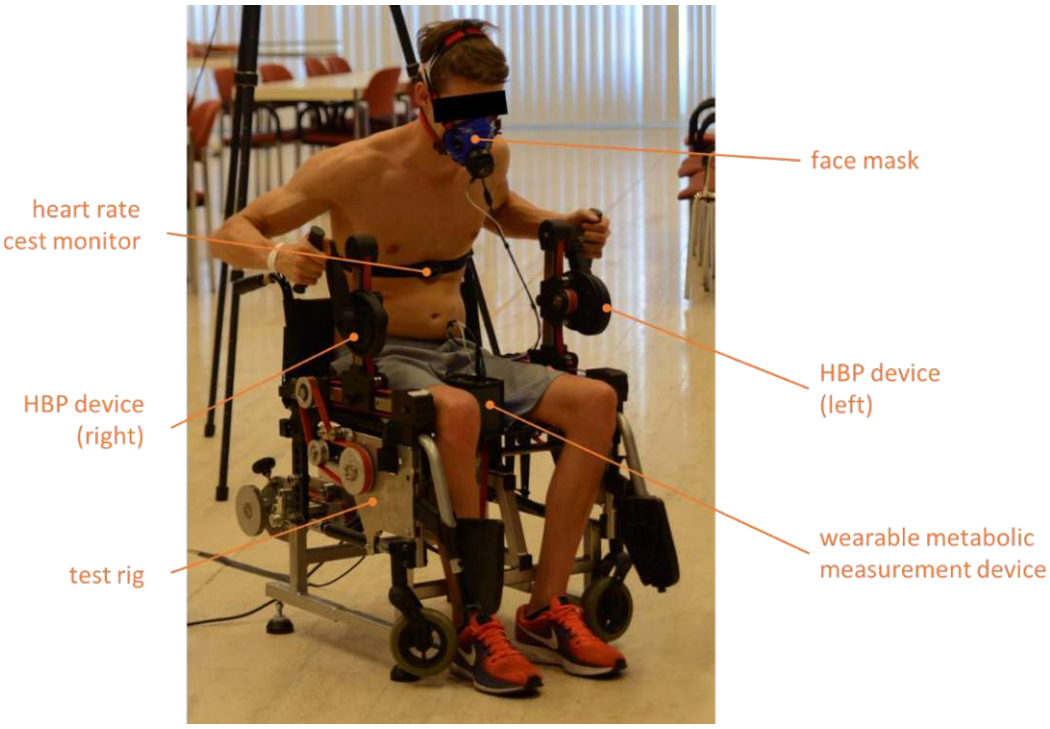

Figure 12: Spirometry measurement setup for HBP during incremental exercise

Oxygen uptake (VO_2), carbon dioxide output (VCO_2) and ventilation (Ve) were measured continuously using a wearable metabolic measurement system (Cosmed K5, Cosmed GmbH, Germany). The spirometry system was matched to the subjects with respect to ethnicity

Die approbierte gedruckte Originalversion dieser Dissertation ist an der TU Wien Bibliothek verfügbar.
The approved original version of this doctoral thesis is available in print at TU Wien Bibliothek.
TU Bibliothek Your knowledge hub WIEN

(Caucasian) and calibrated with a reference gas after each subject. The heart rate was measured with a heart rate monitor (Polar H10 ANT+, Polar Electro Inc., Finland). Linear velocity and cadence were obtained from the test rig control and were also measured using cadence sensors (B00JLMS848 ANT+/B00JLMRXCQ ANT+, Garmin Ltd., Switzerland) mounted on both HPB cranks and the back wheels.

2.2.5 Data Analysis and Statistical Testing

All data recorded data were processed using Matlab® (The MathWorks, Inc., USA) and statistical analysis was performed using SPSS (IBM, USA). For all tests, statistical significance was set at $p < 0.05$ with no adjustment for multiple comparisons. The following statistical tests were performed to compare subject group and propulsion method:

I. T-test was performed to find any significant differences between the performance index of the muscles in the two propulsion modes **[Journal Publication II]**.

II. Levene's test was applied to test for the homogeneity of variances between two groups **[Journal Publication IV]**.

III. Analysis of variance (ANOVA) with different designs (2×2, 2×4×2) was used to determine effects between propulsion mode, subject group, and different workloads **[Journal Publication II, Journal Publication IV]**.

Die approbierte gedruckte Originalversion dieser Dissertation ist an der TU Wien Bibliothek verfügbar.
The approved original version of this doctoral thesis is available in print at TU Wien Bibliothek.
TU WIEN Bibliothek Your knowledge hub

3 Journal Publication I

3.1 Summary

Title: Forward dynamic optimization of handle path and muscle activity for handle based isokinetic wheelchair propulsion: A simulation study

In this study, a musculoskeletal model of the upper extremity is established to determine a handle-based continuous wheelchair propulsion movement. The focus was on finding a new, optimized propulsion shape for wheelchair users, which is within the upper limb ergonomic ranges of joint motion, thus reducing the probability of injuries. With a forward dynamic optimization approach the handle-path shape and muscle activity patterns for maximum net propulsion power were optimized. Therefore, the musculoskeletal model was linked to a handle-based propulsion mechanism, having shape and muscle excitations as optimization variables.

For the possible implementation into a mechanical drive, the result with a circularity ratio of 0.95 and a produced net propulsion power of 34.7W for an isokinetic propulsion cycle at 50rpm was considered suitable for the purpose. A comparison of the joint ranges of motion gathered by simulation between PRP and HBP clearly indicates, that the HBP mechanism leads to motions which are in the ergonomic ranges for all joints, thus avoiding over-exertion of joints during the propulsion movement.

The limitations of the study indicated that the promising results obtained by simulation should be supported in a further study with experimentally determined data.

Die approbierte gedruckte Originalversion dieser Dissertation ist an der TU Wien Bibliothek verfügbar.
The approved original version of this doctoral thesis is available in print at TU Wien Bibliothek.
TU WIEN Bibliothek Your knowledge hub

3.2 Publication

Forward dynamic optimization of handle path and muscle activity for handle based isokinetic wheelchair propulsion: A simulation study

Nithin B. R. Kurup, Markus Puchinger, Margit Gföhler

Research Division of Biomechanics and Rehabilitation Engineering, Department of Engineering Design and Product Development, Technische Universität Wien (TU Wien), 1060 Vienna, Austria;

Abstract

Push-rim wheelchair propulsion is biomechanically inefficient and physiologically stressful to the musculoskeletal structure of human body. This study focuses to obtain a new, optimized propulsion shape for wheelchair users, which is within the ergonomic ranges of joint motion, thus reducing the probability of injuries. To identify the propulsion movement, forward dynamic optimization was performed on a 3D human musculoskeletal model linked to a handle based propulsion mechanism, having shape and muscle excitations as optimization variables. The optimization resulted in a handle path shape with a circularity ratio of 0.95, and produced a net propulsion power of 34.7W (Watts) for an isokinetic propulsion cycle at 50 rpm. Compared to pushrim propulsion, the compact design of the new propulsion mechanism along with the ergonomically optimized propulsion shape may help to reduce the risk of injuries and thus improve the quality of life for wheelchair users.

Keywords - Wheelchair propulsion; musculoskeletal modelling; handle-based propulsion; dynamic optimization

Die approbierte gedruckte Originalversion dieser Dissertation ist an der TU Wien Bibliothek verfügbar.
The approved original version of this doctoral thesis is available in print at TU Wien Bibliothek.
TU WIEN Bibliothek Your knowledge hub

Introduction

Significant research work has been performed over the decades, to understand the biomechanical and physiological factors involved in wheelchair propulsion [6], as wheelchairs are considered an important necessity for the daily mobility and ambulation for physically disabled and injured persons. van der Woude *et al.* [2] reported that the hand-rim was the most favoured mode of propulsion by a large percentage of wheelchair users even though it follows the least efficient pattern of propulsion. The use of the hand-rim may lead to severe upper limb injuries mainly in the shoulder joint such as rotator cuff tear and injuries in the wrist region caused by the discontinuous and complex upper limb movements during propulsion [9]. Studies focused on the kinematic aspects of push rim propulsion, have shown that the joints of the upper limb exhibit large ranges of motion and at certain extreme joint limits, the muscles may need to produce relatively large forces to maintain the propulsion cycle. In such situations the muscles operate in unfavourable regions of their force–length curves, resulting in limited force production and subsequently leading to musculoskeletal injury and pain [29, 30]. In addition, studies on the kinematics and kinetics of wheelchair propulsion have reported that increasing the velocity of propulsion leads to increase in shoulder forces and moments [8, 31]. The increased magnitude of reaction forces at high speeds due to low contact duration [32, 33] can impose high mechanical demand on the shoulder muscles which control stabilization and rotation and this may contribute to acute shoulder pain and injury. Boninger *et al.* [7] noted that stroke patterns at decreased cadence resulted in lower cases of medial nerve injuries due to longer contact duration with the push-rim. Jayaraman *et al.* [34] had reported that push-rim propulsion can lead to higher jerk forces due to sharp direction changes and abrupt speed changes associated with propulsion. Hence restricting the joint motion to ergonomic limits as in this study can prevent injuries due to simultaneous occurence of peak forces and peak shoulder angles with increasing speed as observed in push-rim propulsion [35]. Arm-cranking and hub-crank wheelchairs are the only available devices that use a continuous cyclic motion for wheelchair propulsion. These devices have geometrical restrictions (e.g. large frame size) that make them unacceptable for use in daily living as they severely restrict the maneuverability in small spaces [23, 24]. But cyclic form of propulsion is quite efficient as the force is uniformly applied to the handle over the full rotation resulting in lower peak force [10]. Whereas under hand-rim propulsion, additional braking moments are produced during the hand-rim contact and release periods, which hinder

Die approbierte gedruckte Originalversion dieser Dissertation ist an der TU Wien Bibliothek verfügbar.
The approved original version of this doctoral thesis is available in print at TU Wien Bibliothek.
TU Bibliothek Your knowledge hub WIEN

the forward propulsion movements [36]. These forces reduce propulsion efficiency and increase the loading on the joints [9, 10, 37]. In addition, the continuous circular propulsion helps to distribute the propulsion load over more muscle groups, mainly by involving the flexor and extensor muscle groups, thereby reducing the chances of overuse injuries of specific muscles [6]. Based on the above concepts there is a significant shortage of propulsion techniques, which incorporate the cyclic propulsion pattern of hand cycling while compact enough to be adapted to a conventional wheelchair for daily living. Several studies have utilized three-dimensional upper extremity models and optimization techniques to estimate the muscle forces and joint variables involved in hand-rim wheelchair propulsion [9, 37, 38]. Forward dynamic simulations have been widely used even though computationally expensive to understand the intermuscular coordination during hand-rim based wheelchair propulsion [39–41]. To the best of our knowledge, no studies have targeted path shape optimization for wheelchair propulsion so far. Few studies dealt with shape optimizations using 3D human models and its concerned variables for dynamic chain-ring optimizations for cycle pedalling, a very similar problem for the lower instead of the upper extremity. Kautz and Hull [42] performed forward dynamic optimization using a torque driven 3D model to identify an optimal non-circular chain ring shape for pedalling, but the study lacked the important intrinsic properties of muscles such as muscle length and shortening velocity which have an influence on the resultant optimal chain ring shapes. A subsequent study by Rankin and Neptune [43] included a complete musculoskeletal model of the lower limb attached to a pedal setup for identifying chain ring shape using dynamic optimization. The results indicate that the muscle activation/deactivation dynamics play a vital role in determining the optimized chain ring shape. The aim of this study is to establish a musculoskeletal model of the upper extremity and determine a handle-based continuous wheelchair propulsion movement in a forward dynamic optimization approach that optimizes the handle-path shape and muscle activity patterns for maximum net propulsion power.

Die approbierte gedruckte Originalversion dieser Dissertation ist an der TU Wien Bibliothek verfügbar.
The approved original version of this doctoral thesis is available in print at TU Wien Bibliothek.
TU WIEN Bibliothek Your knowledge hub

Methods

Musculoskeletal model

The dynamic musculoskeletal model was developed in the OpenSim [44] platform, involving the anthropometry and muscle force-generating properties of a 50th percentile adult male based on the work by Saul *et al.* [45]. The rigid segments of the model included the fixed thorax segment (no spine movement), the right upper arm, the right forearm defined by individual components of ulna and radius, and the hand segment. The model was not bilaterally symmetric and only included the right shoulder and hand segments. The shoulder was modelled as a 3 DOF (Degree of freedom) joint comprising of the elevation plane, the shoulder elevation angle (thoracohumeral angle) and the shoulder rotation angle. The elbow joint is defined by 1 DOF with 0° (extension) to 130° (flexion). The wrist joint is modelled with 2 DOF, wrist flexion and wrist deviation [46]. The hand supination had to be constrained to restrict the motion of the hand in the plane during the path optimization. The collective motion of the shoulder girdle (*humerus, clavicle and scapula*) determines the motion of the shoulder joint. Humerus and scapula are articulated by a ball and socket joint, while regressive equations determine the motion of the shoulder girdle, which moves only with the elevation angle. The model included 15 musculotendon actuators, spanning the shoulder, elbow and the wrist joints as shown in Figure 13.

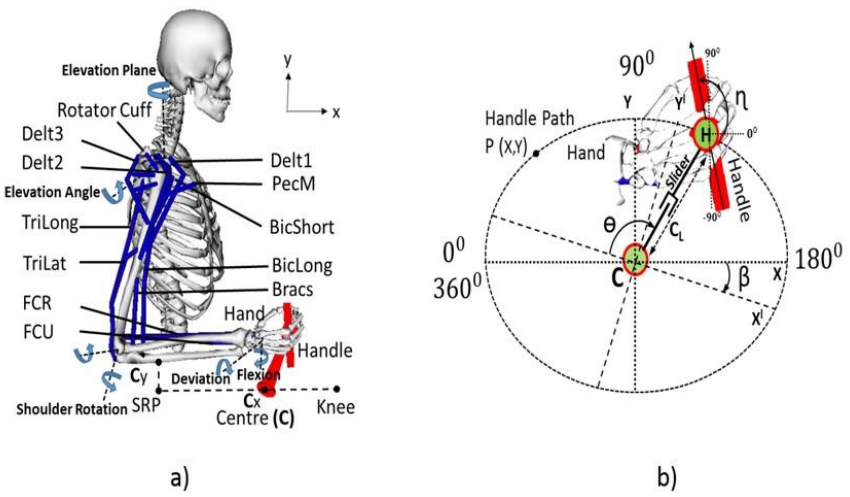

Figure 13: (a) Musculoskeletal model with right hand linked to the propulsion mechanism, with the 15 muscle actuators, Delt1(AnteriorDeltoid), Delt2(MiddleDeltoid), Delt3(PosteriorDeltoid), BicLong(BicepsLong), BicShort(BicepsShort), TriLong(TricepsLong), TriLat(TricepsLateral), Bracs(Brachialis), FCR(FlexorCarpiRadialis),FCU(FlexorCarpiUlnaris),PecM(Pectoralis Major) and Rotator cuff muscles(Supraspinatus (SUPRA), subscapularis (SUBSC), infraspinatus (INFRA), teresminor (TMIN)) with the major DOF such as Elevation Plane, Elevation angle, Elbow flexion, Shoulder rotation, Wrist deviation and flexion. (b) Kinematic components of the propulsion mechanism, with major DOF such as crank angle (θ), effective crank length (C_L), tilt angle (β) and handle angle (η).

Die approbierte gedruckte Originalversion dieser Dissertation ist an der TU Wien Bibliothek verfügbar.
The approved original version of this doctoral thesis is available in print at TU Wien Bibliothek.
TU Bibliothek Your knowledge hub WIEN

A Hill type muscle model, defined by Thelen [47] was used in this study, including both active and passive muscle force generation characteristics based on the muscle force–velocity and force–length relationships. The lumped muscle model included the 4 parameters (optimal fibre length, maximum isometric force, tendon slack length and pennation angle) used to represent the generic properties of musculotendon units [48]. Elastic and damping joint torques were applied to the model to enforce the joint limits [49]. The novel handle based propulsion (HBP) mechanism is located in the parasagittal plane that contains the shoulder joint, with the crank centre coordinate C_{XY} fixed in the global frame (global frame origin at the sternum of the upper extremity model). C_x is the mid-point between the seat reference point (SRP) of the wheelchair and knee joint position of the model, considering the model is in a seated position on the wheelchair. C_Y is the vertical height from the SRP to the forearm of the model with elbow joint being flexed at 90°. The propulsion mechanism consists of the crank that rotates around the origin C and a sliding segment which moves with respect to the crank and can change the effective crank length (C_L) during rotation. The handle is linked to the sliding segment by a pin joint (H). The propulsion mechanism has 4 variables, the crank angle (θ), the effective crank length (C_L), the tilt angle (b) and handle angle (η). During propulsion the movement is defined by 2 DOF (crank angle and handle angle). The crank rotates in clockwise direction as depicted in Figure 13b. The crank's effective length can have values between 0.030m and 0.155m. To connect the arm and the propulsion system, the hand and the handle segments are rigidly welded.

Optimization

Dynamic optimization and forward dynamic simulation were performed using OpenSim 3.2. For the optimization the Interior point optimization algorithm (IPOPT) on an Intel® Xeon® CPUE5-1650 with 6 cores and clock speed of 3.50 GHz, on a 64-bit operating system was used. The dynamic optimization routine followed is a "fully forward" approach [50]. The neural muscle excitations u(t), and the shape parameters of the path (A, B, n, and β) (Equation (1 and (2) act as the control signals. The optimal solutions of these controls are found using dynamic optimization, in combination with solving the muscle dynamics and multibody system dynamics by integration at each iteration. A variable step size Runge–Kutta–Merson integrator [51] was used in this study.

Die approbierte gedruckte Originalversion dieser Dissertation ist an der TU Wien Bibliothek verfügbar.
The approved original version of this doctoral thesis is available in print at TU Wien Bibliothek.
TU WIEN Bibliothek Your knowledge hub

Optimization criterion

Instantaneous power is obtained as the product of instantaneous torque around the crank times the crank speed at each point of the optimization, the average over one propulsion cycle gives the net propulsion power (Watts). The cost function is designed to maximize the net propulsion power over one complete propulsion cycle at each iteration, with added penalties to limit the joint motion within the physiological human limits as defined in the model and to the parasagittal plane defined by the wheels.

Optimization parameters

For muscle excitation optimization, 10 control points at equal time intervals over a full crank rotation i.e., between the initial time (t_0) and the final time (t_f) were selected for each muscle. At each control point the neural excitation u(t), was optimized with values ranging between 0 for least excited muscle state to 1 for maximum excited state. A cubic spline function was used to interpolate the control nodes as cubic functions reduced the oscillations between the data points, and produce smoother interpolated data set when compared to other polynomial interpolators. For handle shape optimization, the path of the handle was parameterized as a function of the crank angle (θ) as represented in the parametric Equation ((1 and (2). The equations helps to prevent concave regions in the path, and also facilitates the generation of varied shapes for optimization [52].

$$P_X(\theta) = \boldsymbol{A}\ \mathrm{COS}(\theta) \tag{1}$$

$$\begin{aligned} P_Y(\theta) &= \boldsymbol{B}\ \mathrm{SIN}(\theta)\ \mathrm{SIN}^{\boldsymbol{n}}(0.5\,\theta) \\ P(X^1Y^1) &= R_z(\boldsymbol{\beta})\,P_{XY}(\theta) \end{aligned} \tag{2}$$

Four optimization variables (A, B, n, and β) define the shape of the path. The scaling factors denoted by A and B were constrained by the limits of the crank effective length C_L. The shape factor n can have values ranging from 0 to 1. The final variable β (Equation (22) defines the tilt angle of the path $P_{XY}(\theta)$ in clockwise direction with respect to the origin C. R_z indicates the rotation matrix to rotate the path in the x–y plane. In total 154 optimization variables were used: 150 variables for muscle excitation, 4 variables from the parametric Equations (1 and 2). P_X and P_Y represent the x and y Cartesian coordinates of the shape (P_{XY}).

During each forward simulation the motion of the HBP was realized by converting the Cartesian coordinates of the optimized path $P_{X^1Y^1}(\theta)$, (Equation (2) to polar form and then

Die approbierte gedruckte Originalversion dieser Dissertation ist an der TU Wien Bibliothek verfügbar.
The approved original version of this doctoral thesis is available in print at TU Wien Bibliothek.
TU Bibliothek Your knowledge hub WIEN

prescribing the effective crank length (C_L) as a function of crank angle (θ). In OpenSim, the prescribed motion of the slider joint is generated by inputting a linearly interpolated function of above parameters at each iteration of the optimization.

Test setup

The initial variables for the optimization were randomly generated for both shape and muscle excitation parameters, and were optimized to maximize the cost function for each crank cycle. For the muscle parameters, the initial excitation (control signal) and the activation values at time (t_0) were set as 0.050, and 3 complete cycles were simulated to reach a steady state. After the third cycle, a constraint was enabled to set the muscle excitation values at time (t_0) equal to the excitation values at time (t_f), thereby creating a periodic muscle activity pattern for hand propulsion. In addition, a terminal constraint was applied such that at time (t_f) the crank angle is 360°. In this study the angular velocity (x) of the crank was set as constant (50rpm) to emulate an isokinetic ergometer. The set constant 50rpm speed, is the value required for over ground propulsion for daily living [6]. Crank speed in handcycling around 50rpm lead to increased mechanical efficiency [20]. Further increasing velocity of propulsion can lead to reduced efficiency, increased joint accelerations and torque, and consequently lead to injuries [8]. Certainly, normal wheelchair propulsion has acceleration and deceleration phases and not only steady state speed as assumed in this optimization study. But here the chosen steady state speed is higher than the normal self-selected cadence, which is between 25 and 35rpm [40], and the authors believe that the selected 50rpm steady state speed may lead to joint parameters equivalent to the short acceleration and deceleration phases experienced by users during propulsion at lower cadences. The dynamic optimization simulations were performed using the OpenSim-C++ API by accessing the OpenSim and Simbody libraries. The obtained simulation states files were further analyzed (e.g. muscle work and the normalized muscle force–length and force–velocity values) and processed in the OpenSim GUI and MS Excel.

Die approbierte gedruckte Originalversion dieser Dissertation ist an der TU Wien Bibliothek verfügbar.
The approved original version of this doctoral thesis is available in print at TU Wien Bibliothek.
TU WIEN Bibliothek Your knowledge hub

Results

The dynamic optimization of the control variables at constant angular velocity of 50rpm resulted in a shape as shown in Figure 14, with a circularity ratio (i.e. function of perimeter and area of the shape, a circle has a circularity of 1) of 0.951 and the optimized shape parameters A=0.151 m, B=0.152m and n=0.700.

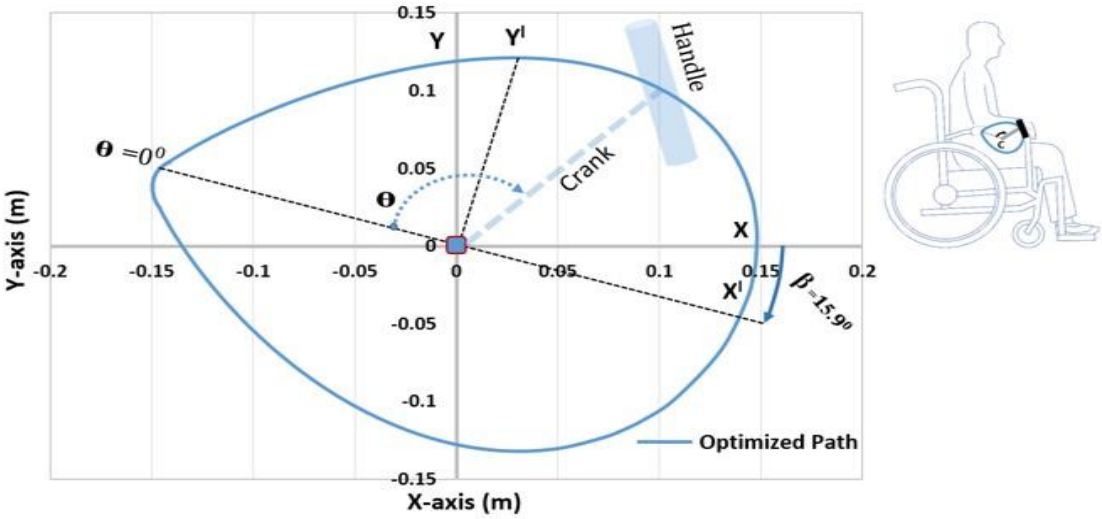

Figure 14: Dynamically optimized propulsion path with the centre C for HBP in the parasagittal plane defined by the wheels.

The propulsion path is tilted in clockwise direction (β=15.950°) with respect to the ground frame. The optimization for the HBP resulted in a net propulsion power of 34.650W at 50rpm. The optimized muscle excitation patterns from the simulation are shown in Figure 15.

During push (zones 2, 3) mainly Delt1, Trilong, PecM, Infraspinatus, Teres Minor showed excitation, whereas during pull (zones 1, 4) mainly the muscles Delt3, BicShort, Biclong, Subscapularis were excited. Delt2 and Supraspinatus were active during parts of both, pull and push phases. Calculation of the net muscle work (in Joules) produced by the muscles during the four zones of propulsion (Figure 16) shows that Delt1, Delt3, PecM, Infraspinatus, Biclong, Bicshort, Brachialis, Trilong and Trilat contributed most to the net positive work during propulsion. The highest amount of positive work, 0.680 Joules, is produced by Delt1. Considerable amount of negative work was observed by Delt1 and BicLong in the regions of eccentric motion.

Die approbierte gedruckte Originalversion dieser Dissertation ist an der TU Wien Bibliothek verfügbar.
The approved original version of this doctoral thesis is available in print at TU Wien Bibliothek.
TU WIEN Bibliothek Your knowledge hub

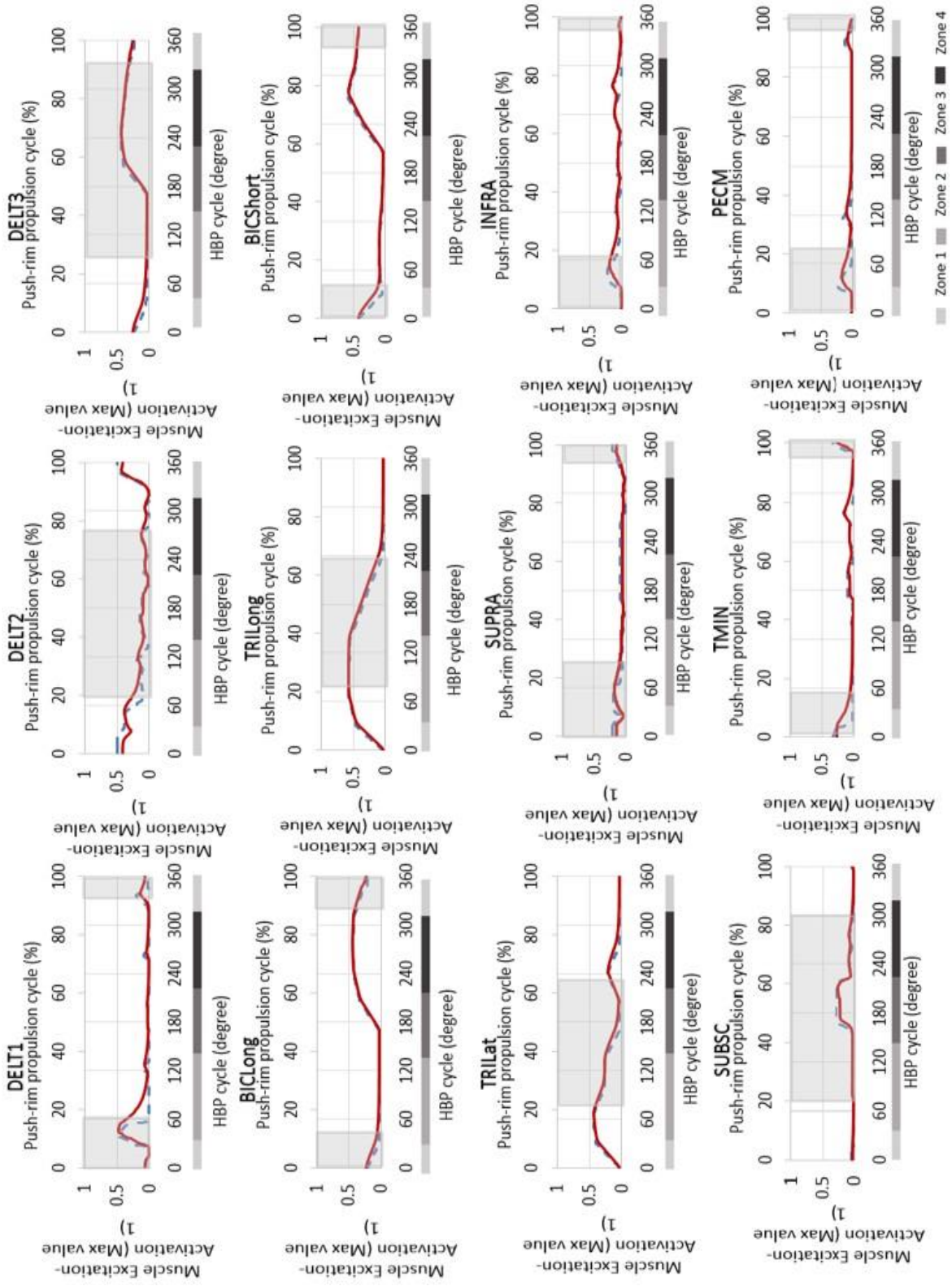

Figure 15: Optimized muscle activity patterns (only muscles for which a comparison to push rim propulsion is available), with the dark solid lines (muscle activations) and the dotted lines (muscle excitations) over one full propulsion cycle. The shaded regions indicate the phases in which the respective muscles were active during push-rim propulsion [53]. The shaded bars below the diagrams show the propulsion zones.

Die approbierte gedruckte Originalversion dieser Dissertation ist an der TU Wien Bibliothek verfügbar.
The approved original version of this doctoral thesis is available in print at TU Wien Bibliothek.

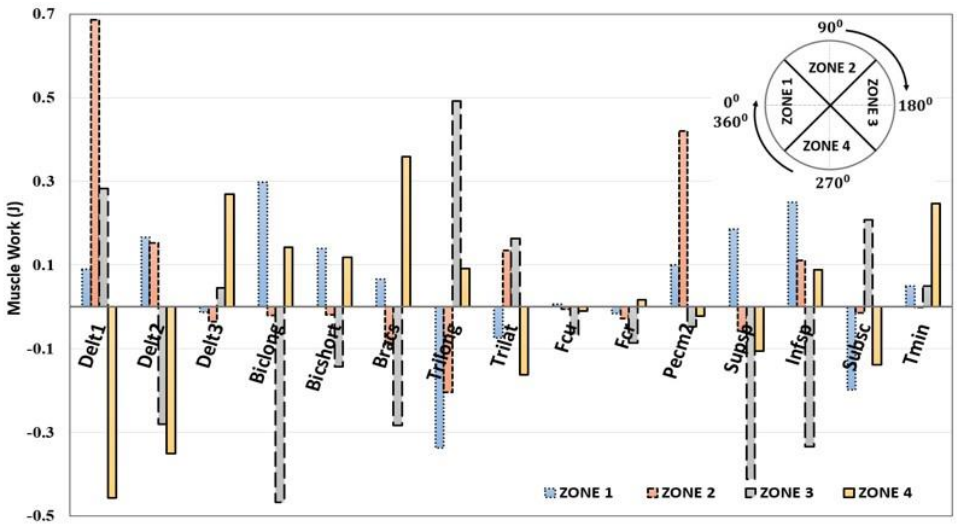

Figure 16: Net work done by the upper limb muscles (in Joules) during the four zones of propulsion with the optimized handle path.

A comparison of the joint ranges of motion during standard push-rim propulsion and propulsion with the optimized shape shows that for the optimized shape, all joint ranges stay within their ergonomic regions, whereas during push-rim propulsion shoulder rotation and wrist deviation move outside the ergonomic ranges (Figure 17).

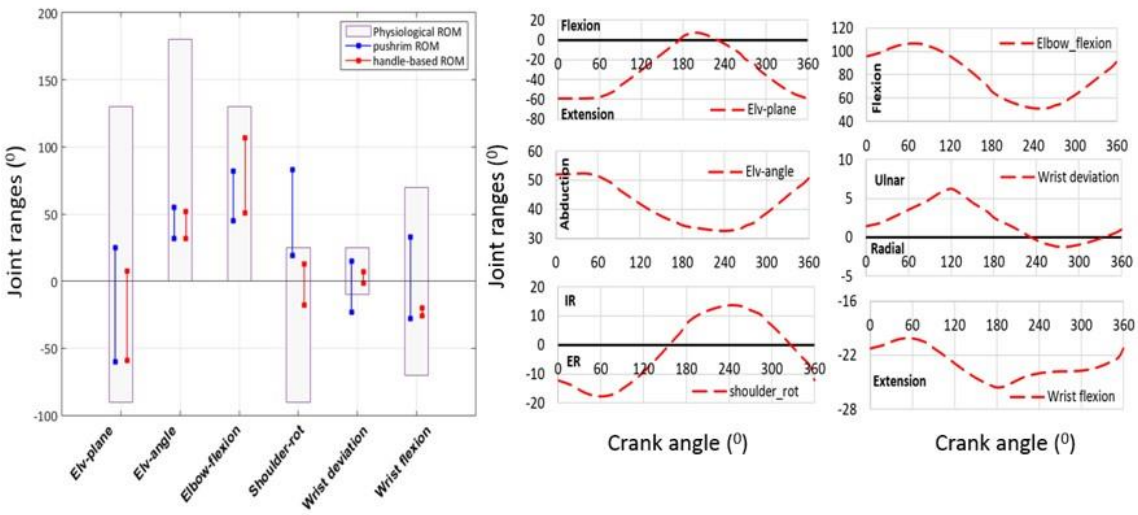

Figure 17: Comparison of the joint ranges of motion (ROM) of the upper extremity between push-rim propulsion and the HBP (handle-based propulsion) technique [38, 49]. Shoulder rotation Int/Ext(+/-).Wrist deviation Ulna/Radial(+/-) and wrist flexion Ext/Flex(-/+). The physiological range represents the anatomical joint range. The figures on the right side indicate the joint motion during HBP.

Due to the fact that the joint motions from optimization were well within the ergonomic ranges and not at extreme limits, the effect of the coordinate restraining torques were not analysed explicitly as it will be minimal. Figure 18 shows that all four muscles spanning the elbow joint were working close to their optimal fiber lengths, where they can generate highest

Die approbierte gedruckte Originalversion dieser Dissertation ist an der TU Wien Bibliothek verfügbar.
The approved original version of this doctoral thesis is available in print at TU Wien Bibliothek.
TU Bibliothek Your knowledge hub WIEN

active muscle forces, and with negative fiber velocity (contraction), meaning that they can generate positive muscle power, in the regions with activity above 20% (grey shaded regions).

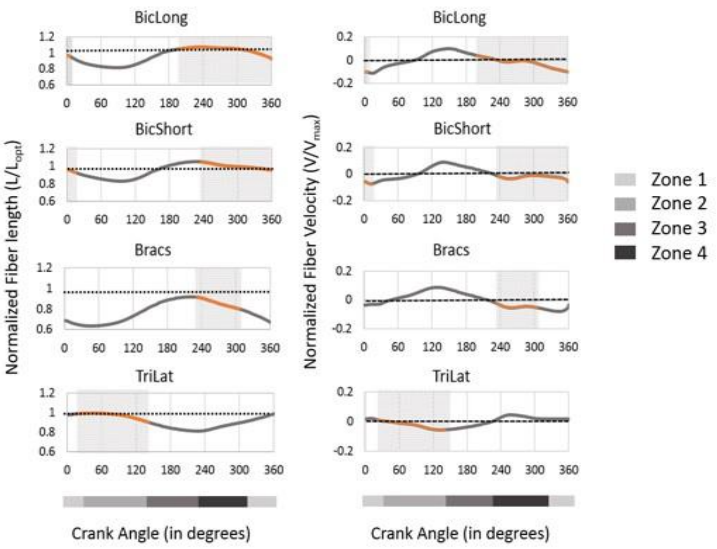

Figure 18: Normalized fiber length and normalized fiber shortening velocity of the muscles spanning the elbow joint during one full crank rotation. The dotted lines represent the optimal fiber length (L_{opt}). In the normalized fiber velocity graph the muscle contraction is negative and muscle lengthening is positive. The maximum shortening velocity of each muscle was assumed to be 10 optimal fiber lengths per second (V_{max}=10 L_{opt} s^{-1}). The dark shaded areas in the graphs represent the regions with more that 20 percent of muscle activation.

In addition, Figure 19 shows a comparison of the peak muscle forces during propulsion with HBP and push-rim at self-selected speeds (35 ± 8rpm). Both propulsion modes produced near equal peak muscle forces, especially for the deltoid and the elbow muscle groups. Even though the comparison was performed to a lower cadence propulsion, the *Infra* and *Tmin* generated higher peak force when compared to HBP.

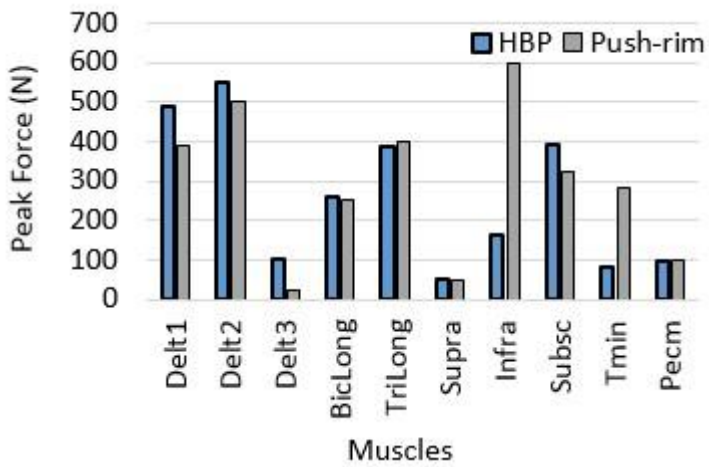

Figure 19: Peak muscle forces obtained from the computational simulation of HBP compared to dynamic optimization results for push rim propulsion [38].

Die approbierte gedruckte Originalversion dieser Dissertation ist an der TU Wien Bibliothek verfügbar.
The approved original version of this doctoral thesis is available in print at TU Wien Bibliothek.

Discussion

This study opens up for a new wheelchair propulsion movement, which is optimized for the musculoskeletal architecture of the upper extremity. The optimization at the chosen angular velocity of 50rpm, resulted in a unique propulsion pattern for the HBP, having a circularity shape factor less than 1. This resembles the hand stroke pattern generated during wheelchair racing [54] and a semi-circular pattern observed in the classic wheelchair stroke [36]. This pattern for the HBP is continuous, cyclic and improves hand contact during full propulsion cycle in contrary to push-rim propulsion. In addition, this dynamic movement pattern with alternate activation of agonist and antagonist muscles, increases dynamic muscle activity, which may increase blood circulation and help to postpone local muscle fatigue of the upper limb. Furthermore, the net propulsion power of 34.65W generated from the HBP optimization supports the hypothesis that the HBP can produce sufficient power to propel a conventional wheelchair for daily life activities. This remains in agreement with previous studies that have indicated that a minimum of 30W is required for a person to propel on a 3°–6° inclined slope, which demands higher muscular effort [55]. A comparison of the joint ranges of motion (ROM) between the stages of hand-rim propulsion [38, 49] and HBP, clearly indicates that the HBP mechanism leads to motions which are in the ergonomic ranges for all joints, thus avoiding over-exertion of joints during the propulsion movement. In HBP, during the onset of the propulsion motion (pull phase) the shoulder is extended, abducted and externally rotated by the activation of muscles such as delt3, delt2, infraspinatus and supraspinatus. This motion subsequently leads to the push phase where the shoulder is flexed, adducted and internally rotated. The pattern of shoulder rotation is different to that observed in push-rim. The subscapularis in HBP has lower duration of activation when compared to push-rim and also facilitates greater contribution of the external rotators such as infraspinatus and teres minor, which may prevent the muscle imbalances leading to sub acromial impingement [53]. Major joint excursions during wrist movements, which may cause CTS (Carpal Tunnel Syndrome) [56], are considerably reduced in HBP. The groups of muscles activated in pull and push zones were similar to wheelchair propulsion [57]. The major elbow muscles, *BicLong* and *TriLong* exhibit large ranges of both positive and negative work during the propulsion zones in both HBP and push-rim propulsion [40]. In pushrim propulsion during the pull phase, *BicLong* – positive work and *TriLong* – negative work are observed and vice versa in push phase with *BicLong* absorbing force from the push-rim. In HBP, similar pattern of work done by *BicLong*

Die approbierte gedruckte Originalversion dieser Dissertation ist an der TU Wien Bibliothek verfügbar.
The approved original version of this doctoral thesis is available in print at TU Wien Bibliothek.
TU Bibliothek Your knowledge hub WIEN

and *TriLong* as in push-rim is noted [58]. The kinematics of the elbow joint moves from flexion to extension with the elbow flexor-extensor muscles shortening in regions, where the muscles are close to their optimal fiber length and velocity, which may result in increased muscle force production.

There are a few limitations in this study, which need to be addressed. First, the results were obtained in a simulation study using an experimentally validated 3D musculoskeletal model of a 50th percentile adult male but are not yet supported with experimental data. However, several studies have reported that the use of dynamic optimization techniques on 3D models closely resembled the experimental results [38, 43, 45, 50, 59]. Second, the function of the trunk muscles has not been investigated in this study as the authors consider the HBP can be used over a larger population, not only persons with limited trunk function (SCI with higher lesion) but also disabled persons with intact trunk control (as e.g. leg amputees). Thirdly, the angular velocity of the crank was fixed to replicate an isokinetic propulsion since the constant velocity profile was needed to obtain a unique propulsion shape during the path optimization process. Assuming steady state propulsion at a low constant speed, straight forward over a leveled tiled surface the inertia of wheelchair and the related crank drive train dynamics were not explicitly modeled. As the objective function was designed to maximize the power for the optimal shape, the derived 34.65W at handle is sufficient to overcome the minimum resistive forces experienced during wheelchair propulsion for the assumed conditions [60]. Studies on cycling have reported that the crank inertial loads have minimum influence on the joint kinematics of users at a constant cadence of propulsion [43]. The effects of the rolling resistance and air resistance will be minimal [6] on the assumed conditions and the addition of minor weights to the system has no effects on the joint kinematics [61] for wheelchair propulsion.

This study offers some short and long term perspectives, a thorough experimental study is needed on the future developed HBP mechanism to test its functionality and efficiency on novice and veteran wheelchair users. There is also a wide scope in the industrial sector to develop a new wheelchair propulsion device for the disabled users.

Die approbierte gedruckte Originalversion dieser Dissertation ist an der TU Wien Bibliothek verfügbar.
The approved original version of this doctoral thesis is available in print at TU Wien Bibliothek.
TU WIEN Bibliothek Your knowledge hub

Conclusion

This study describes the computational optimization of a novel handle based mechanism for wheelchair propulsion, which might be an interesting alternative to pushrim propulsion especially for long term wheelchair users, due to ergonomical joint angle ranges and lower muscle loads that might help to prevent injuries due to wheelchair propulsion.

Disclosure statement

The authors report that there are no conflicts of interests.

Funding

This work was financially supported by a grant (P 25507-B24) from the Austrian Science Fund (FWF).

Die approbierte gedruckte Originalversion dieser Dissertation ist an der TU Wien Bibliothek verfügbar.
The approved original version of this doctoral thesis is available in print at TU Wien Bibliothek.
TU WIEN Bibliothek Your knowledge hub

4 Journal Publication II

4.1 Summary

Title: A preliminary muscle activity analysis: Handle based and push-rim wheelchair propulsion

This work is a follow up of our simulation study **[Journal Publication I]** and compared the upper extremity muscle activations of subjects on the now physically realized HBP and PRP. Surface EMG data of the major upper limb muscles from healthy male subjects were recorded for both HBP and conventional PRP at a workload of 25W and 35W on a wheelchair-based test rig (Section 2.2.1). To determine the propulsion cycles, a motion capture system along with reflective markers placed on both propulsion units was used.

The analysis of the peak muscle activations indicated that the increase of workload leads to an increase in muscle activity for both propulsion modes, which is consistent with other studies from literature.

The results showed, highly mismatched peak activities of agonist and antagonist muscles of the elbow region in PRP, whereas in HBP the muscles had more balanced durations. This means that the use of HBP may improve the load distribution of agonists and antagonists, which can help to postpone local muscle fatigue in the arms due to better blood circulation.

Furthermore, the activity of the pectoralis in HBP was lower than in PRP which may help to prevent injuries.

The study suggests that the HBP may be a suitable alternative to the push-rim, especially for users with shoulder injuries, but at the same time it is stated that the unexperienced subjects may have influenced the results.

Die approbierte gedruckte Originalversion dieser Dissertation ist an der TU Wien Bibliothek verfügbar.
The approved original version of this doctoral thesis is available in print at TU Wien Bibliothek.
TU WIEN Bibliothek Your knowledge hub

4.2 Publication

A preliminary muscle activity analysis: Handle based and push-rim wheelchair propulsion

Nithin B. R. Kurup, Markus Puchinger, Margit Gföhler

Research Division of Biomechanics and Rehabilitation Engineering, Department of Engineering Design and Product Development, Technische Universität Wien (TU Wien), 1060 Vienna, Austria;

Die approbierte gedruckte Originalversion dieser Dissertation ist an der TU Wien Bibliothek verfügbar.
The approved original version of this doctoral thesis is available in print at TU Wien Bibliothek.

Abstract

Approximately ninety percent of the wheelchair users worldwide prefer the conventional push rim mode of propulsion for daily mobility and rehabilitation. Even though push-rim wheelchairs help to promote a healthy life style, the high muscular demand and the non-continuous push motions can lead to serious upper extremity injuries. In this study, muscle EMG data of ten healthy subjects were recorded for a newly introduced handle based propulsion mechanism (HBP) and compared to conventional push-rim propulsion at two workloads, 25W and 35W respectively. The results for the mean peak muscle activations at both workloads demonstrate that push-rim propulsion leads to higher peak muscle activity compared to HBP at a similar wheelchair forward velocity of 1.11m/s. The generation of these high peak muscle activations with increasing loads in push-rim propulsion over time can lead to overuse injuries. Overall, the use of the HBP mechanism is less straining to the muscles and may reduce fatigue during prolonged propulsion.

Keywords - Wheelchair propulsion, Handle based propulsion, Muscle activity

Introduction

Wheelchairs are commonly used as a mode of ambulation and rehabilitation for persons suffering from injuries such as spinal cord injury (SCI) [2, 6, 56]. Studies on muscle activity during wheelchair propulsion with various styles have shown that there is a high muscular demand on a few specific muscles involved in wheelchair propulsion mainly due to low contact durations with the push-rim [62], and the muscles used during the push phase become stronger over the course of time while the muscles used in the recovery phase remain at the same strength. These muscular imbalances can lead to fatigue and overuse injuries in the long term [63]. Studies on hand cycling (tricycle wheelchair arm crank propulsion) have shown that the continuous propulsion pattern used in this technique is less straining to the muscles and also facilitates to distribute the propulsion load to greater number of muscles [6, 9, 37]. Even though hand cycling is more biomechanically efficient and less physically straining, majority of the users prefer the pushrim over hand cycling as it is more easy to maneuver in small indoor spaces while hand cycles are better suited for outdoor activities due to their large frame size and difficultly in steering [56]. Using the above concepts, an alternative form of wheelchair propulsion mechanism was introduced in our simulation study and the results were promising as the new hand propulsion pattern followed ergonomic ranges of joint motion thus limited the chances of injuries when compared to push-rim [64].

As a follow up of our simulation study, this study aims to compare the upper extremity muscle activations of subjects on the physically realised Handle Based Propulsion (HBP) and push-rim propulsion drive at two different workloads.

Methods

Participants

Ten able-bodied, nonskilled male subjects (mean±SD; 27±5yrs, 1.81±0.06m, 88±12kg) were recruited for this study. All subjects were right handed and had no known history of joint injuries or movement limitations. All the subjects provided voluntary informed consent for the experimental trials, which was approved by the Institutional Review Board.

Experimental setup

A standard lightweight manual wheelchair was used for the study. The dimensions of this wheelchair are 0.420m seat depth, altered backrest height of 0.220m and a seat width of

Die approbierte gedruckte Originalversion dieser Dissertation ist an der TU Wien Bibliothek verfügbar.
The approved original version of this doctoral thesis is available in print at TU Wien Bibliothek.
TU Bibliothek Your knowledge hub WIEN

0.500m. The size of the wheel was changed based on the test setup: for the HBP test a reduced wheel size of 20in. was used and for the normal push-rim test, an instrumented SMART^{Wheel} with standard wheel dimensions of 24 inches was used [27]. The wheel with smaller diameter was used for HBP to avoid collision of the rotating crank or hand with the wheel. Future designs of HBP mechanism may solve this problem. In order to maintain a constant propulsion power output and constant linear velocity of the wheels during propulsion a custom-made test rig, controlled by a LabVIEW (National Instruments Corp., Austin TX) program was built and attached to a standard wheelchair (Figure 20). The test rig includes a controlled motor linked to a flywheel. During propulsion, the instantaneous angular velocity of the wheels was recorded and the corresponding instantaneous torque was calculated. In order to maintain a steady state of constant power, the magnitude of this torque was applied as a resistive torque by the motor linked to the wheels through timing belts [26].

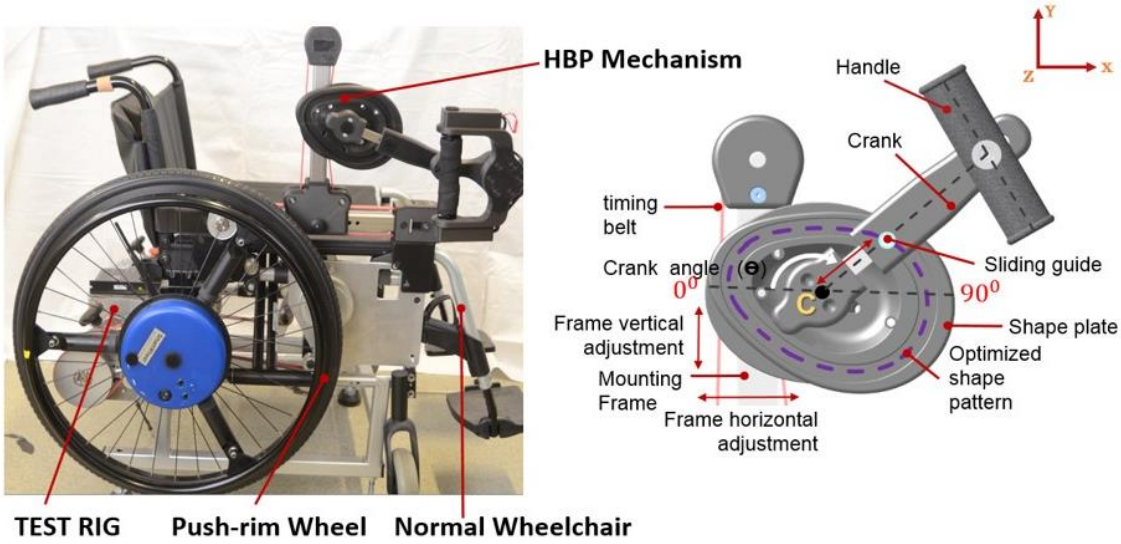

Figure 20: Standard push-rim wheelchair attached to controllable custom made test rig (left) and handle based propulsion mechanism (right).

Figure 20The handle based propulsion unit was attached to the wheelchair in the parasagittal plane of the wheels and consists of a crank centre, attached to a sliding guide on which a handle was mounted as shown in (Figure 20). The optimized propulsion shape with a shape factor of 0.95 was engraved into the shape plate. During propulsion, the crank changes its effective length forced by the sliding guide capable of moving back and forth in the shape plate, resulting in the novel propulsion movement for the HBP mechanism. The gear ratio of the HBP mechanism to the wheel is set as 2:1. The lower gear ratio was set for the HBP mechanism because the gear ratio of 1:1 will need greater exertion of force to the handle

Die approbierte gedruckte Originalversion dieser Dissertation ist an der TU Wien Bibliothek verfügbar.
The approved original version of this doctoral thesis is available in print at TU Wien Bibliothek.
TU WIEN Bibliothek Your knowledge hub

while the hand velocity and the muscle contraction drop and this may lead to fatigue [6]. Also increasing the gear ratio may decrease the mechanical efficiency of the propulsion [65]. In addition, an adjustable mounting frame allows to set the position of the crank centre in the parasagittal plane. The centre was set for all subjects based on the protocol followed in our optimization study, thus ensuring all the subjects have similar arm kinematics during propulsion. A timing belt transfers the propulsion torque from the HBP to the wheels.

In this study, propulsion was unilateral. Even though the wheelchair attached to the test rig had wheels on both sides, only the right arm was used to propel in both propulsion modes, assuming symmetry of propulsion as the subjects were without any secondary injury or pain [66], naturally unilateral propulsion will be more demanding on the muscles when compared to bilateral propulsion where the propulsion work will be shared by both limbs. Hence the muscle activities observed in this study will be higher compared to values collected from bilateral propulsion. As the subjects in this study had very good trunk control and stability we assume that muscle activity of the shoulder muscles is not significantly influenced by the unilateral propulsion [6].

Muscle activations were recorded using DELSYS Trigno wireless surface electromyography (sEMG) electrodes. An 8-camera motion capture system (Motion Analysis Corporation) along with reflective markers placed on the propulsion units of HBP and SMART^{Wheel} at 120Hz were used to manually determine the propulsion cycles. Further details of upper limb joint kinematics are not described in this paper.

Experiments

Prior to the experimental trials, the subjects were instructed about the propulsion modes (push-rim and HBP) and the testing protocols. Then the subjects were allowed to familiarize with both HBP and push-rim by propelling each of them for 5min without any resistance provided by the test rig and further 5 min were given to the subjects to test the drives on each propulsion load with varying resistances provided by the test rig. For the tests with both the HBP and the push-rim, 2 workloads of 25W (Watts) and 35W at a wheelchair linear velocity of 1.1m/s were set using the test rig. A visual interactive feedback was provided to the users to visually monitor the wheelchair speed and propulsion power and aid the users to reach the target propulsion power and speed for the tests. The subjects performed the experiments at 2 workloads for each of the propulsion systems in a randomized manner in order to minimize

Die approbierte gedruckte Originalversion dieser Dissertation ist an der TU Wien Bibliothek verfügbar.
The approved original version of this doctoral thesis is available in print at TU Wien Bibliothek.
TU Bibliothek Your knowledge hub WIEN

effects of training or fatigue on the results. Muscle activations of Anterior deltoid, Posterior deltoid, Pectoralis major, Biceps brachii and Triceps brachii were monitored. Further details on data acquisition and processing can be found in Appendix A.

A performance index (PI), was used to identify the change in the muscle recruitment between the workloads 25W and 35 W, and the calculated values were compared between the two modes of propulsion. Equation (3, represents the formula used to calculate the PI value in percentage for each individual muscle (ranging from -100 to +100) [67] with EG_{peak} representing the mean peak EMG values from 3 individual propulsion cycles from each subject at each of the workloads.

$$PI = \frac{EG_{Peak}^{35W} - EG_{Peak}^{25W}}{EG_{Peak}^{35W} + EG_{Peak}^{25W}} \times 100 \qquad (3)$$

The statistical analysis includes the determination of mean and standard deviation of the EMG_{peak} values for all the individuals across both workloads for each propulsion type. A two-way (propulsion-groups × workloads) analysis of variance (ANOVA) along with Bonferroni post-hoc correction was applied for the EMG_{peak} for both groups across the two workloads. In addition, a T-test was performed to find any significant differences between the PI values of the muscles in the two propulsion modes.

Results

From the study, the mean peak muscle activities of the subjects were calculated for both propulsion modes. A general trend of increase in the peak muscle magnitude was observed across the workloads (Table 1).

Table 1: Normalized EMG peak magnitude and performance Index (PI) across the two workloads for both propulsion modes (mean ± SD).

Workload (W)	25 W		35 W	
Propulsion	HBP	Push-rim	HBP	Push-rim
Anterior Deltoid*	28.72 (16.60)	58.84 (15.32)	36.07 (16.28)	80.20 (8.56)
Posterior Deltoid*	23.88 (10.01)	54.77 (18.43)	29.96 (13.23)	68.56 (22.79)
Pectoralis Major*	24.95 (13.65)	65.72 (15.61)	34.21 (23.29)	82.60 (10.11)
Biceps Brachii*	36.57 (7.50)	10.61 (5.67)	48.23 (13.76)	14.15 (9.29)
Triceps Brachii*	24.77 (9.00)	40.15 (10.56)	34.61 (12.36)	51.12 (10.92)
Muscles	HBP (PI) (%)	Push-rim (PI) (%)		
Anterior Deltoid	+16.36 (27.87)	+18 (12.40)		
Posterior Deltoid	+10.81 (8.65)	+11.33 (7.26)		
Pectoralis Major	+12.59 (15.20)	+12.38 (9.24)		
Biceps Brachii	+13.12 (7.40)	+12.12 (12.37)		
Triceps Brachii	+14.22 (10.91)	+12.27 (11.81)		

Note:
* Significance was set as *P* value less than 0.050 for all analyses.

Die approbierte gedruckte Originalversion dieser Dissertation ist an der TU Wien Bibliothek verfügbar.
The approved original version of this doctoral thesis is available in print at TU Wien Bibliothek.
TU WIEN Bibliothek Your knowledge hub

The highest EMG_{peak} was exhibited by the Pectoralis major muscles (82.60±10.11%) while propelling the push-rim wheelchair at 35W power. A significant difference in EMG_{peak} ($p<0.050$) was observed between all the muscles when compared between the HBP and push rim groups at 25W and 35W respectively. Push rim propulsion produced higher EMG_{peak} values at both workloads for *Anterior deltoid, Posterior deltoid, Pectoralis major* and *Triceps brachii* muscles, while Biceps brachii was the only notable muscle group with higher activity during the propulsion with HBP. No significant differences were found between the average PI of muscles when compared with HBP and push rim. A two percent increase in muscle recruitment was observed by the *Anterior deltoid* muscle in push rim when compared to HBP, due to increase in workloads. Conversely, *Triceps brachii* exhibited a greater PI value when propelling the HBP.

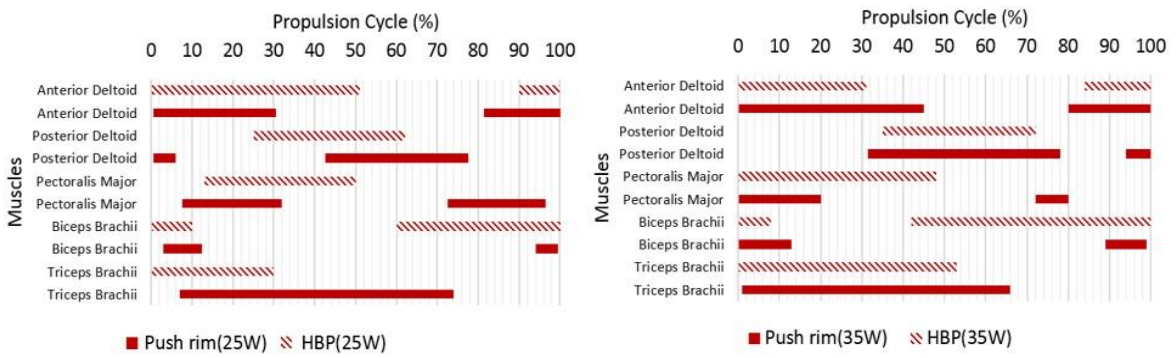

Figure 21: Mean muscle activation intervals for the two propulsion modes at 25W and 35W workloads respectively

Figure 21 shows the muscle's activity intervals over a whole propulsion cycle for both HBP and push-rim propulsion. For both propulsion modes, muscles were active over the whole propulsion cycle, however the activation patterns were different. In HBP, the *Biceps brachii* muscle group is active over a much longer interval than in push-rim propulsion. The length of the activity intervals increases with increasing workload for both propulsion modes, with notable differences in the *Triceps brachii* and *Biceps brachii* muscle groups. In addition, with the increase in workload the onset of muscle activity is earlier in the propulsion cycle (*Anterior deltoid, Posterior deltoid, Pectoralis major, and Biceps brachii*). When comparing the onset and offset values of experienced push-rim users from literature to the values observed in our study, the *anterior deltoid* in our study showed a similar pattern as in literature but with a late offset after 20% of the propulsion cycle and an early onset in the later phase of the propulsion cycle for both workloads [53], while the *deltoid posterior* showed a reduced duration of

Die approbierte gedruckte Originalversion dieser Dissertation ist an der TU Wien Bibliothek verfügbar.
The approved original version of this doctoral thesis is available in print at TU Wien Bibliothek.
TU WIEN Bibliothek Your knowledge hub

activity at 25W compared to 35W. The onset of the *pectoralis major* was a bit late at 25W, while activity duration was shorter at 35W when compared to literature [53]. The activity of *biceps* was similar to literature while the *triceps* had an earlier onset in both propulsion modes.

Discussion

Experiments on wheelchair propulsion with healthy subjects using an optimized handle based propulsion unit and standard push rim at two different workloads were performed, and the data were analyzed to compare muscle activations.

Analysis of the peak muscle activations indicates that the increase of workload leads to an increase in muscle activity for both propulsion modes, and is consistent with previous studies [68]. The peak EMG values in push-rim propulsion indicate that for both workloads 25W and 35W, *Anterior deltoid, Pectoralis major* and *Triceps Brachii* were maximally recruited during the push phase of propulsion and Posterior deltoid for the recovery phase in this study. Whereas in HBP, all muscles contributed evenly to the propulsion. Positive values of the performance index PI gave an understanding of the percent of muscle fibers recruited with increasing workloads. As expected, in push-rim propulsion, the peak activities of agonist and antagonist muscles of the elbow region were highly mismatched, i.e., muscle groups of *Triceps brachii* had greater activity (see Table 1) and duration (63%(25W) and 74%(35W)) than *Biceps brachii* (8%(25W) and 25%(35W)) during the propulsion stages. In HBP, on the contrary, the muscles had more balanced durations with *Biceps brachii* (50%(25W) and 48%(35W)) and *Triceps brachii* (31%(25W) and 52%(35W)). This suggests that the use of HBP can improve the load distribution on agonist and antagonist muscle groups of the elbow joint. The activity of these muscle groups can improve blood circulation and help to postpone the local muscle fatigue in the arms [19, 63]. In addition, the over-exertion of the prime movers, especially *Pectoralis major* along with other rotator cuff muscles (not described in this study), in push-rim propulsion can lead to reduced muscle endurance which directly decreases the humeral head depression forces, which can lead to shoulder impingements [14]. *Pectoralis* activity in HBP is lower when compared to push-rim propulsion, this may help to prevent injuries.

There are a few limitation that need to be addressed. Firstly, all the subjects tested were non-wheelchair users, results of muscle activity may differ for prolonged wheelchair users who have already adapted to the push rim propulsion movement, but studies comparing experienced to novice push-rim users have shown that there is no significant difference in the

Die approbierte gedruckte Originalversion dieser Dissertation ist an der TU Wien Bibliothek verfügbar.
The approved original version of this doctoral thesis is available in print at TU Wien Bibliothek.
TU WIEN Bibliothek Your knowledge hub

movement pattern across the two groups [69] and the abled bodied subjects in our study performed homogenous exercise at both propulsion modes as they had no restriction due to disability and they were equally inexperienced on both modes of propulsion. Secondly, the users were allowed to propel the push rim at self-selected styles, this can have an influence on the propulsion cycles, the muscle activity and the efficiency. Thirdly, quantification of muscle activity from surface EMG signals is problematic when movement is involved and motion artefacts and other electromagnetic noises may influence the signal levels. We tried to minimize disturbances by the applied signal processing and filtering routines, still artefacts may have small impact on the derived maximum muscle activations (Table 1).

This preliminary study of muscle activity on both propulsion modes suggests that HBP might be a suitable alternative to the push-rim, especially for prolonged wheelchair users who are suffering from joint injuries. The HBP mechanism can also be used for indoor rehabilitation purposes by long term wheelchair users, who are not physically active to use hand cycles and lack proper trunk control due to SCI. The HBP can help to improve their overall muscle strength, muscle imbalances and decrease their risk for overuse injuries.

Conflict of interest

The authors report that there are no conflicts of interests.

Acknowledgments

This research work was supported by Austrian Science Fund (FWF), grant (P 25507- B24).

Appendix A. Supplementary material

Supplementary data to this article can be found online at

https://doi.org/10.1016/j.jbiomech.2019.04.011

Die approbierte gedruckte Originalversion dieser Dissertation ist an der TU Wien Bibliothek verfügbar.
The approved original version of this doctoral thesis is available in print at TU Wien Bibliothek.
TU WIEN Bibliothek Your knowledge hub

5 Journal Publication III

5.1 Summary

Title: In Vivo Biomechanical Assessment of a Novel Handle-Based Wheelchair Drive

In this study hand contact forces, upper-extremity joint excursions and joint torques generated by the novel HBP device were measured on paraplegics and non-disabled controls and compared to results for PRP reported in literature. Therefore, movement patterns of the shoulder and wrist joints were investigated to determine whether high loads occurred at the extreme positions of the joints. The measurements were conducted on a wheelchair-based test rig at two different workloads (25 W and 35 W) and focused mainly on the kinematics and kinetics of the shoulder and wrist joints because these are the joints most often affected by propulsion-related injuries.

Compared to PRP the effectiveness of the propulsion forces was higher in HBP which led to lower average propulsion forces and 20% reduced average peak forces.

In addition, joint excursions in HBP are within their recommended ergonomic ranges, resulting in a reduced range of motion of up to 30% at the shoulder and up to 80% at the wrist. Furthermore, lower net torques at both the shoulder and wrist were found highlighting the potential of this novel propulsion system to reduce the risk of upper-extremity injuries.

Die approbierte gedruckte Originalversion dieser Dissertation ist an der TU Wien Bibliothek verfügbar.
The approved original version of this doctoral thesis is available in print at TU Wien Bibliothek.
TU WIEN Bibliothek Your knowledge hub

5.2 Publication

In Vivo Biomechanical Assessment of a Novel Handle-Based Wheelchair Drive

Markus Puchinger[a], Pia Stefanek[a], Karin Gstaltner[b], Marcus G. Pandy[c] and Margit Gföhler[a]

[a]Research Division of Biomechanics and Rehabilitation Engineering, Department of Engineering Design and Product Development, Technische Universität Wien (TU Wien), 1060 Vienna, Austria;

[b]AUVA Rehabilitation Centre Meidling, 1120 Vienna, Austria;

[c]Department of Mechanical Engineering, University of Melbourne, Parkville, VIC 3010, Australia.

Die approbierte gedruckte Originalversion dieser Dissertation ist an der TU Wien Bibliothek verfügbar.
The approved original version of this doctoral thesis is available in print at TU Wien Bibliothek.
TU WIEN Bibliothek Your knowledge hub

Abstract

Push-rim wheelchair propulsion frequently causes severe upper limb injuries in people relying on the wheelchair for ambulation. To address this problem, we developed a novel handle-based wheelchair propulsion method that follows a cyclic motion within ergonomic joint ranges of motion. The aim of this study was to measure hand propulsion forces, joint excursions and net joint torques for this novel propulsion device and to compare its performance against traditional push-rim wheelchair propulsion. We hypothesized that under similar conditions, joint excursions of this novel handle-based device will remain within their ergonomic range and that the effectiveness of the propulsion forces will be higher, leading to lower average propulsion forces compared to push-rim propulsion and reducing the risk of injury. Eight paraplegic subjects propelled the new device at two different loads on a custom-made wheelchair-based test rig. Video motion capture and force sensors were used to monitor shoulder and wrist joint kinematics and kinetics. Shoulder and wrist loads were calculated using a modified upper-extremity Wheelchair Propulsion Model available in OpenSim. The results show that with this novel propulsion device joint excursions are within their recommended ergonomic ranges, resulting in a reduced range of motion of up to 30% at the shoulder and up to 80% at the wrist, while average resultant peak forces were reduced by up to 20% compared to push-rim propulsion. Furthermore, the lower net torques at both the shoulder and wrist demonstrate the potential of this novel propulsion system to reduce the risk of upper-extremity injuries.

Index Terms - ergonomics, handle, propulsion, shoulder, upper-limb, wheelchair, wrist.

Introduction

The wheelchair is an important aid for the mobility of physically disabled and injured persons, and the push-rim is the preferred mode of propulsion for a large percentage of wheelchair users even though it is associated with the least efficient pattern of propulsion [2]. Extensive research has been performed to understand the biomechanical and physiological factors of wheelchair propulsion [6].

The ergonomics literature indicates that push-rim propulsion (PRP) can lead to severe upper-limb injuries mainly at the shoulder and wrist joints, caused by the discontinuous, highly repetitive and complex upper-limb movements, which reportedly occur during PRP [8–10]. Furthermore, high loads at joint excursions exceeding 20°-45° from the neutral position should be avoided for shoulder movements, and even lower joint excursions (18°-30° from the neutral position) are reported to be detrimental at the wrist [70]. Limited information is available on joint angle ranges and joint loads during conventional PRP. Veeger *et al.* [71] measured a mean propulsion force of 30.0N ±7.1N and a peak propulsion force of 69.4N ±26.1 N for 20W constant PRP at 1.39m/s linear velocity on a wheelchair dynamometer. Koontz *et al.* [72] simulated wheelchair propulsion over a level, smooth floor at two different speeds – 0.9m/s and 1.8m/s – and reported mean resultant peak propulsion forces of 58.9N ±11.6N at 0.9m/s and 94.3N ±26.4N at 1.8m/s. Large variations in upper-limb joint torques are also reported for PRP. Koontz *et al.* [72] analysed kinetics in 27 paraplegic subjects during PRP propulsion on a tile surface at a speed of 0.9m/s and found a peak shoulder abduction/adduction torque of 21.3Nm and shoulder rotation peak torques of 21.6Nm. Collinger *et al.* [73] and Gil-Agudo *et al.* [74] performed measurements under similar conditions and reported peak torques of 7.1Nm/15.3Nm (Collinger *et al.* / Gil-Agudo *et al.*) and 5.8Nm/3.5Nm for shoulder ab-/adduction and shoulder rotation, respectively. Different methods used in these studies to compute joint torques may have contributed to the large variations in the kinetic results. Koontz *et al.* [35] applied a local coordinate system approach whereas Collinger *et al.* [73] and Gil-Agudo *et al.* [74] used custom inverse dynamics models. In addition, PRP patterns are characterized by large variations between subjects and the results are altered by propulsion cadence [7].

Upper-extremity pain and injury represent a major problem for wheelchair dependent persons as use of the arms is essential for independent mobility and participation in the community. Alternative modes for wheelchair propulsion, such as lever-propelled, hub-crank

Die approbierte gedruckte Originalversion dieser Dissertation ist an der TU Wien Bibliothek verfügbar.
The approved original version of this doctoral thesis is available in print at TU Wien Bibliothek.
TU Bibliothek Your knowledge hub WIEN

and arm-crank devices, use a continuous cyclic movement for propulsion, which offers higher efficiency compared to conventional PRP [2, 9].

The straightforward upper-arm movement during lever-propulsion involves a much larger muscle mass, offers longer push phases and leads to lower strain compared to PRP [75]. Disadvantages are limited top speed of propulsion related to the frequency of the push and recovery phases combined with the absence of pausing between the pushing and pulling phases [75, 76]. The hub-crank mechanism uses cranks that are directly mounted on the hubs of the rear wheels and so allow a continuous motion of the hands. Gross mechanical efficiency (GME) is higher than in PRP, but the position of the hands combined with difficulties in steering and braking make this device impractical [2]. Arm-cranking devices use a continuous cyclic motion for propulsion [2, 9]. The most familiar example of arm-cranking devices is the hand bike, which is a tricycle with the front wheel driven by hand cranks. Handcycling devices are bulky and used mainly outdoors, making them unsuitable for daily living [23, 24]. However, the propulsion form is quite efficient, as propulsion forces are continuously applied over the full cycle, thus resulting in higher efficiency and lower peak forces at the hand and lower loads transmitted to the joints compared to lever propulsion and PRP methods [9, 10, 37].

Arnet *et al.* [10] compared propulsion forces and net shoulder torques during handcycling and PRP at different inclines. The results showed significantly lower mean and peak propulsion forces and lower peak net shoulder torques during handcycling at all inclines.

A major drawback of all currently available alternative propulsion systems is that they can hinder activities of daily living (ADL), as they are usually bulky, heavy and less manoeuvrable. This can be problematic for essential daily activities, such as transfers, backwheel balancing (wheelies) to overcome steps (kerbs), moving the chair over a variety of surfaces or sitting at a table [2, 13, 23, 24, 37].

To overcome the limitations of PRP, we applied a similar optimization approach to the one described by Rasmussen *et al.* [77] for pedalling. We developed a novel handle-based wheelchair propulsion (HP) device with an ergonomically optimized propulsion shape that offers a continuous cyclic motion at ergonomic joint ranges and is suitable for ADL [64]. The mechanism does not affect the physical width of the wheelchair and was proven to decrease joint excursions and maximum joint torques developed at the wrist [78].

The aim of the present study was to determine the mean and peak propulsion forces, upper-limb joint excursions and net joint torques generated by this novel HP device on an

Die approbierte gedruckte Originalversion dieser Dissertation ist an der TU Wien Bibliothek verfügbar.
The approved original version of this doctoral thesis is available in print at TU Wien Bibliothek.
TU WIEN Bibliothek Your knowledge hub

instrumented wheelchair-based test rig. Measurement results from paraplegic subjects propelling the HP device at different loads were compared with PRP data available in the literature. The measurements focussed mainly on the kinematics and kinetics of the shoulder and wrist joints because these are the joints most often affected by propulsion-related injuries [10]. We hypothesized that under similar conditions, HP joint excursions will remain within their ergonomic range and that the effectiveness of the propulsion forces will be higher, leading to lower average propulsion forces compared to PRP. Furthermore, we expected to find lower peak propulsion forces for the HP device due to force application over the full cycle. Based on our previous results [78], we also expected lower net shoulder and wrist torques during HP.

Methods

Experimental Setup

All experiments were performed on a wheelchair-based test rig that operated in constant power mode [26] (Figure 22). Two HP devices [78, 79] were mounted on the test rig instead of the armrests (Figure 23). Each HP device consisted of a rotating crank on which a handle was mounted. During propulsion, a sliding guide changed the length of the crank over the rotation, and the handle followed the optimized propulsion path.

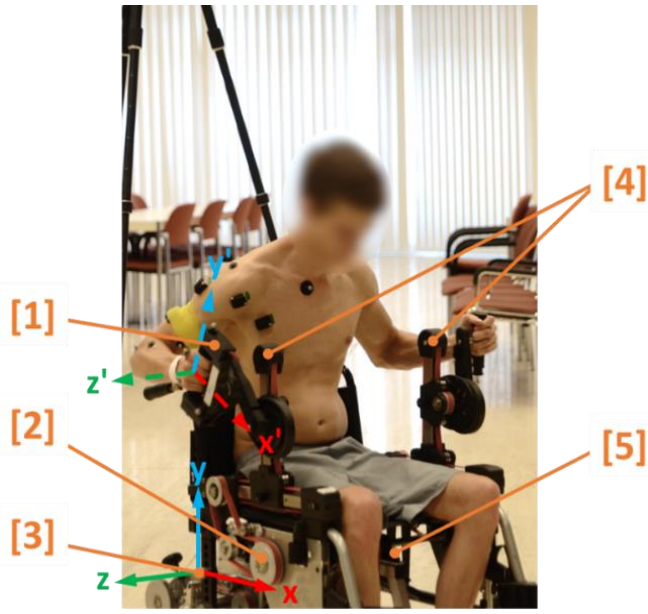

Figure 22: Wheelchair based test rig. Subject sitting in the wheelchair-based test rig with attached HP devices.
[1] handle with integrated force/torque sensor and local coordinate system, [2] resistance power transmission from motor-gear unit to HP devices, [3] global (fixed) coordinate system, [4] HP devices, [5] motor-gear unit.

Die approbierte gedruckte Originalversion dieser Dissertation ist an der TU Wien Bibliothek verfügbar.
The approved original version of this doctoral thesis is available in print at TU Wien Bibliothek.
TU Bibliothek Your knowledge hub WIEN

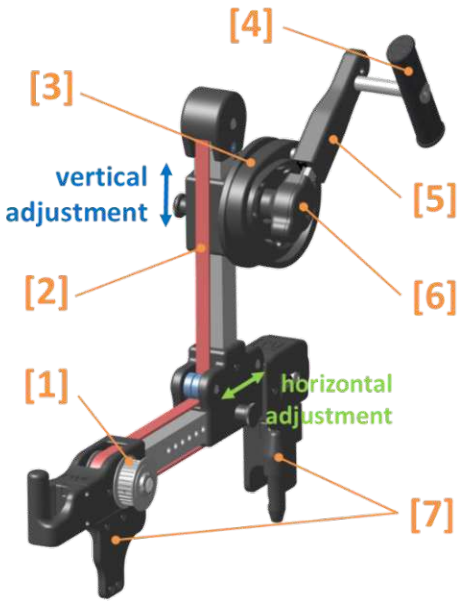

Figure 23: Handle based propulsion (HP) device and its components. Horizontal and vertical position of the crank centre can be adjusted to the users body measures; [1] timing belt pulley (to the back wheel), [2] timing belt, [3] curve disc, [4] handle, [5] variating crank, [6] crank centre, [7] brackets (fit in armrest mounting).

In accordance with Kurup *et al.* [78] the horizontal positon of the crank centre was set to the midpoint between the backrest of the wheelchair and the knee joint position of the subject. For the vertical position, the centre of the crank was set to the height of the elbow joint for upper arm vertically pointing down when seated.

Similar to other studies [22, 80], the test rig was set to simulate linear velocity of 1.1m/s, which simulated the average wheelchair speed used in daily life. The gear ratio of the HP device was fixed at 1.2 for the duration of the experiment, which resulted in an average cadence of ~50rpm. This cadence has been found suitable for submaximal handcycling [22].

A custom wireless force-measuring handle with an integrated 3-axis force/torque sensor (K6D40, ME Messsysteme GmbH, Germany) was used to measure propulsion forces and torques. The device was connected to the test rig and the measured data were recorded using Bluetooth. An 8 camera video motion capture system (Kestrel 2200/Cortex 7, Motion Analysis Corporation, USA) was used to record upper-limb kinematics from each participant.

Die approbierte gedruckte Originalversion dieser Dissertation ist an der TU Wien Bibliothek verfügbar.
The approved original version of this doctoral thesis is available in print at TU Wien Bibliothek.
TU WIEN Bibliothek Your knowledge hub

Subjects

Eight right-handed individuals with paraplegia and no history of upper-limb injury participated in this study. Subject characteristics are listed in Table 2. All subjects provided informed consent and approval for the study was obtained from the responsible federal state ethics committee (GS1-EK-3/149-2018).

Table 2: Characteristics of the 8 subjects with spinal cord injury

Subject (Sex)	Age [yrs]	Weight [kg]	Height [cm]	BMI [kg/m²]	SCI Level
1 (f)	54	62	179	19	T11-12
2 (m)	27	80	188	23	T6-7
3 (f)	43	75	160	29	T10-L1
4 (f)	56	63	158	25	T12-L1
5 (m)	52	65	175	21	T12-L2
6 (m)	45	85	192	23	T11-L1
7 (m)	21	62	185	18	T8-9
8 (m)	51	93	173	31	T12-L2
mean	44	73	176	24	
±SD	±12	±11	±12	±5	

SD: standard deviation; SCI: spinal cord injury

Testing Protocol and Data Collection

The force measurement handle was installed on the right side of the wheelchair test rig and side-to-side symmetry was assumed during propulsion. Prior to the experimental trials each participant received instructions regarding the propulsion exercises and was given an opportunity to familiarize themselves with the equipment by propelling the wheelchair for 2 minutes without resistance. All trials were performed at two different workloads of 25W and 35W and the same wheelchair velocity of 1.1m/s. Visual feedback on actual and target speed was provided to each participant during propulsion to ensure that a constant speed was maintained during each trial. Each participant performed 10 propulsion cycles at each workload with a two-minute rest interval between the two trials. Ten reflective markers were placed on the participant's trunk and right upper limb and three additional markers were placed on the handle (Figure 24). Cycles were recorded only after reaching steady propulsion at the target speed, and acceleration and deceleration phases were not included.

Die approbierte gedruckte Originalversion dieser Dissertation ist an der TU Wien Bibliothek verfügbar.
The approved original version of this doctoral thesis is available in print at TU Wien Bibliothek.
TU WIEN Bibliothek Your knowledge hub

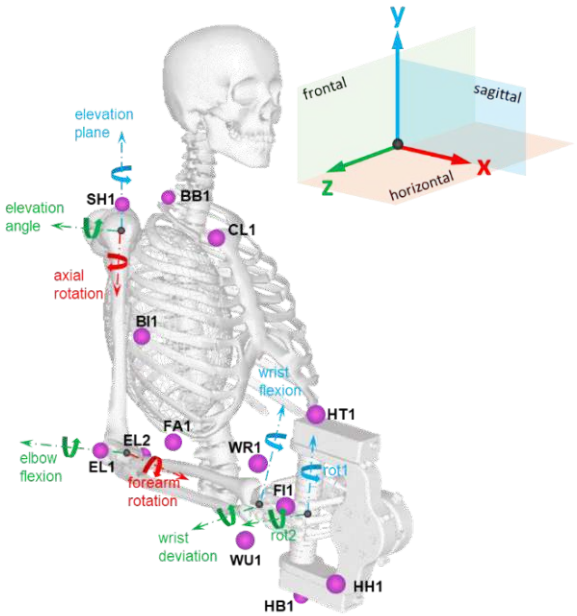

Figure 24: Biomechanical Model. Upper extremity model with nine degrees of freedom showing the global (fixed) coordinate system and virtual marker placements. Markers were placed at the following locations: clavicle (CL1), acromion (SH1), 7th cervical vertebrae (BB1), biceps (BI1), lateral epicondyle (EL1) and medial epicondyle (EL2), forearm (FA1), radial styloid (WR1), ulnar styloid (WU1), 2nd metacarpophalangeal (MCP) joint (FI1), handle help (HH1), handle top (HT1) and handle bottom (HB1).

Biomechanical Model

The upper-extremity model used in this study is based on the *Wheelchair Propulsion (WCP) Model* [81, 82] available in OpenSim [44] and was modified by adding two rotational degrees-of-freedom (DoF) (rot1, rot2) to simulate handle movement. The model comprised of seven rigid bodies (*spine and rib cage, clavicle, scapula, humerus, ulna, radius and hand*) whose positions and orientations were described by nine degrees of freedom (DoF) (Figure 24). The kinematic convention recommended by the International Society of Biomechanics (ISB) [45, 83, 84] was used to describe the three rotations at the shoulder (elevation-angle, elevation-plane, axial rotation), elbow flexion, forearm rotation and wrist deviation and flexion. Due to the installed HP devices on both sides and the resulting simultaneous movements of both arms, we expected minor thorax rotations around the x- and y-axes. Rotations of the thorax about the x and y axes were neglected in the model because they were less than ±3° during experiment, whereas thorax rotations around the z-axis were included because they reached ±10° at the higher workload.

For calculation of joint angles and torques, OpenSim 3.3 was used [44]. The simulation process involved the use of three tools available in OpenSim: Scaling, Inverse Kinematics and Inverse

Die approbierte gedruckte Originalversion dieser Dissertation ist an der TU Wien Bibliothek verfügbar.
The approved original version of this doctoral thesis is available in print at TU Wien Bibliothek.
TU Bibliothek Your knowledge hub WIEN

Dynamics. First, the model was scaled to each participant's anthropometry based on the measured marker positions when the angular position of the crank was 135°. The scaled model was then used to perform Inverse Kinematics to determine the generalized coordinates (joint angles) at each time step of the motion. Finally, Inverse Dynamics was performed using the reaction forces measured at the handle to compute the generalized net joint torques.

Data Analysis

Three-dimensional propulsion forces were measured at the handle bearing using the instrumented handle (Figure 22). All forces were expressed in the global reference frame of the test rig. The resultant propulsion force ($\mathrm{F_{res}}$) was calculated as the vector norm of the three measured global force components ($\mathrm{F_x}, \mathrm{F_y}, \mathrm{F_z}$) during propulsion. For each participant, three cycles with the highest values of F_{res} were used to compute the mean and standard deviation of the resultant force (F_{res_mean})$\mathrm{F_{res_mean}}$. The average resultant peak force ($\hat{F}_{res_avg}\hat{\mathrm{F}}_{\mathrm{res_avg}}$) was defined as the average of the highest peak values of F_{res} $\mathrm{F_{res}}$in all participants across the three cycles. Forces tangential to the handle path (F_{tan}) were calculated with respect to the crank angle (Figure 25). Mean tangential forces (F_{tan_mean}) $\mathrm{F_{tan_mean}}$with standard deviations were calculated from the same three cycles used to compute F_{res_mean}. The computed net joint torques T_{i,n_0} were normalized by dividing by body weight times body height [85, 86], thus:

$$T_{i,n} = \frac{T_{i,n_0}}{m_n \cdot g \cdot h_n} \tag{4}$$

$i = 1\ldots10$generalized coordinate index, $n = 1\ldots8$ participant index

where $T_{i,n}$ $\mathrm{T_{i,n}}$is the dimensionless net joint torque, m_n is the participant's body mass in kg, g is the gravitational constant (9.81 m/s^2), and h_n is the participant's body height in meters. The average of the dimensionless normalized joint torque ($T_{i,n}$) or each generalized coordinate calculated across all participants was defined as the averaged normalized joint torque (T_{i_avg}). Peak torque values for every generalized coordinate and participant ($\hat{T}_{i,n}$) were obtained by averaging the ten highest absolute net torque values (T_{i,n_0}) for the three cycles analyzed. The average peak torque ($\hat{T}_{i_avg}$) was defined as the average across all participants' peak torques ($\hat{T}_{i,n}$) for each generalized coordinate.

Die approbierte gedruckte Originalversion dieser Dissertation ist an der TU Wien Bibliothek verfügbar.
The approved original version of this doctoral thesis is available in print at TU Wien Bibliothek.
TU WIEN Bibliothek Your knowledge hub

Shoulder joint angles and torques were also expressed in an anatomical meaningful way. Shoulder flexion/extension was defined between the global y-axis (Figure 24) and the projection of the upper arm onto the sagittal plane whereas shoulder abduction/adduction occurred between the global y-axis and the projection of the upper arm onto the frontal plane. Shoulder horizontal flexion/extension was equivalent to shoulder elevation-plane movement and shoulder internal/external rotation was equivalent to the axial rotation of the shoulder joint. Sagittal flexion, horizontal flexion, abduction, and internal rotation angles were defined as positive. All angles were determined with reference to a neutral anatomic position; that is, with the arm positioned alongside the body and the palm facing medially.

Results

Handle-based propulsion force

Seven out of the eight participants completed all the trials. One female participant was excluded due to problems with balance during testing. The average of F_{res_mean} across all subjects with respect to a full cycle was 36.9N ±4.1N (mean ±SD) for 25W and 45.8N ±5.7N for 35W (Figure 25, left panel). The average of the applied tangential forces$\mathrm{F}_{\mathrm{tan_mean}}$ F_{tan_mean} across all participants over a complete cycle was 24.4N ±5.4N at 25W and 30.6N ±6.7N at 35W. The participants' individual peak values (>30N) of F_{tan} were applied at crank angle intervals from 10° to 110° and from 190° to 280° for both workloads (Figure 25, right panel, green highlighted zone). The average resultant peak force ($\hat{F}_{res_avg}$) was 55.7N ±11.6N at 25W and 65.4N ±7.6N at 35W.

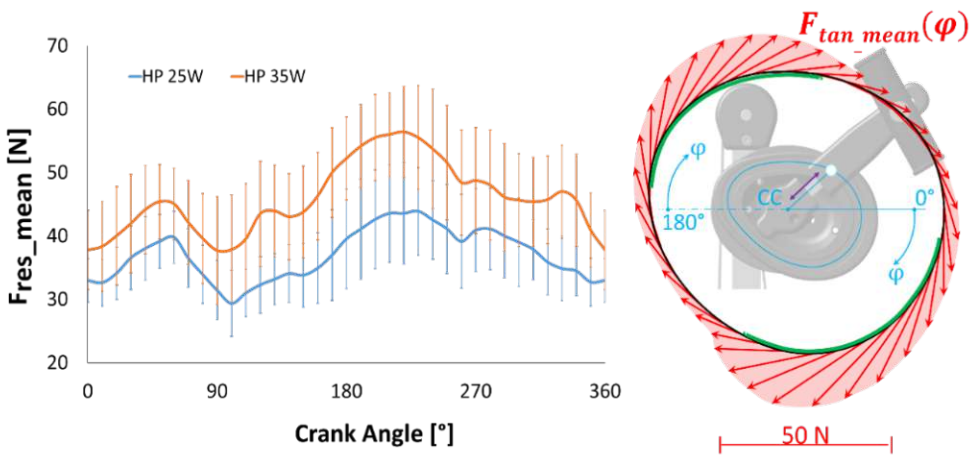

Figure 25: HP resultant and tangential forces. Left panel: Mean resultant force (F_{res_mean}) and standard deviation for all subjects applied at 25W and 35W. Right panel: Mean tangential forces for all subjects applied at 25W constant resistance with 1.1m/s linear velocity and 50Hz cadence. (CC…crank centre, φ…crank angle, green highlighted zone F_{tan}>30N)

Die approbierte gedruckte Originalversion dieser Dissertation ist an der TU Wien Bibliothek verfügbar.
The approved original version of this doctoral thesis is available in print at TU Wien Bibliothek.
TU Bibliothek Your knowledge hub WIEN

Joint kinematics

For both workloads, the range of motion, maximum joint angles and time histories of the joint angles of the shoulder and elbow were almost identical over the full propulsion cycle (Figure 26 and Table 4).

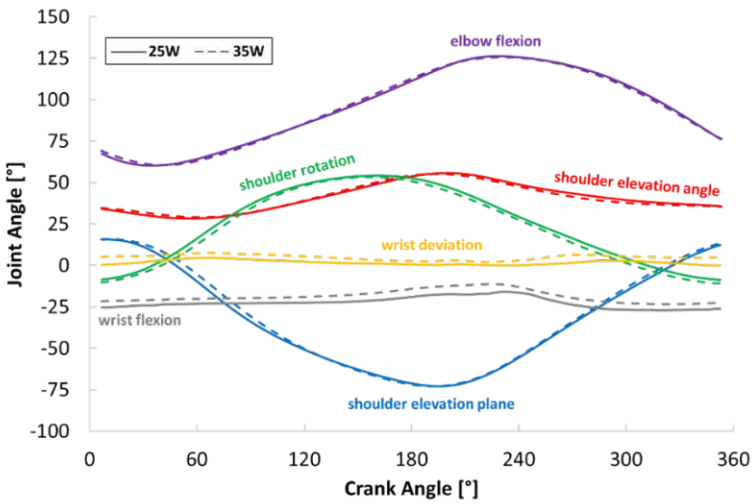

Figure 26: HP upper-limb joint angles vs. crank angle. Trajectories of the mean upper-limb joint angles averaged across all subjects and all selected cycles over one full crank angle rotation and both workloads. Results shown for HP with resistance levels of 25W (solid lines) and 35W (dashed lines).

The maximum shoulder elevation-plane angle (15.7°/16.0° at 25W/35W) occurred when the handle was in the foremost position at crank angles between 0° and 10°. The minimum elevation-plane angle (-73.0°/-72.9° at 25W/35W) occurred at the handle's rearmost position at crank angles between 180° to 200°. Peak angles of shoulder elevation (55.8°/55.1° at 25W/35W) occurred at a crank angle of approximately 190°, where the handle was exactly in the rearmost position. The lowest angles of shoulder elevation (28.1°/29.0° at 25W/35W) occurred near the bottom handle position at a crank angle of approximately 80°. Maximum internal rotation was observed shortly before reaching the rearmost position of the handle (135° - 170°). Peak values of external rotation occurred from -10° to 10°, where the handle moved around its foremost position. Elbow flexion increased continually from its lowest value (60.1°/60.6° at 25W/35W) at 45° crank angle to its peak value (126.1°/125.6° at 25W/35W) at 230°, and then decreased in a similar fashion. At the wrist joint, the time histories of joint angles were again identical for both workloads, but the higher load at 35W led to a larger ulnar deviation and a slightly reduced wrist extension over the whole crank rotation. Peak values for ulnar deviation (4.6°/7.5° at 25W/35W) occurred when the crank reached its highest and lowest positions (270° and 70°, respectively) while minimum angles of ulnar deviation (0.0°/2.0° at 25W/35W) occurred at crank angles of 230° and 350°. Peak values of wrist

Die approbierte gedruckte Originalversion dieser Dissertation ist an der TU Wien Bibliothek verfügbar.
The approved original version of this doctoral thesis is available in print at TU Wien Bibliothek.
TU WIEN Bibliothek Your knowledge hub

extension (27.0°/23.4° at 25W/35W) occurred at a crank angle of 320° while minimum wrist extension (15.8°/10.9° at 25W/35W) was reached at a crank angle of 230°. When the handle reached its foremost position (crank angle of 0°), the shoulder was maximally flexed in the horizontal direction, outwardly rotated, and elevated to about 35°. The wrist was extended and slightly deviated in the ulnar direction. With increasing crank angle, the shoulder became more horizontally extended, elevated, and rotated inwardly. Wrist extension was reduced whereas ulnar deviation increased rapidly to its maximum at about 80° crank angle and then decreased more slowly to its rearmost position. At the rearmost position (crank angle of 180°), the shoulder was maximally extended in the horizontal direction, elevated, and inwardly rotated. The wrist was minimally extended and in a deviation position close to neutral. As the crank angle increased further, the shoulder flexed in the horizontal direction, reduced in elevation, and was outwardly rotated. The wrist extended and ulnar deviation increased.

Joint Torques

The patterns of shoulder joint torque were similar at both workloads (Figure 27A-C), with higher torques measured at the higher workload as expected. The highest torques for horizontal flexion/extension occurred shortly before and after the peak extension angle when the handle was at its rearmost position. The shoulder elevation torque reached its peak magnitudes during the pull phase, when the handle passed the lowest position, and in the middle of the push phase when the handle was near its uppermost position. In the foremost position of the handle, where the shoulder elevation angle peaked, the elevation torque was relatively low. For shoulder axial rotation, peak values of joint torque occurred in both the push and pull phases, when the shoulder was internally rotated by approximately 20°. When the shoulder was near its maximum and minimum axial rotation angles, the joint torque was again relatively low.

The shapes of the wrist deviation torque trajectories were similar for both workloads (Figure 27D-E), but the curve representing HP at 35W appeared to be shifted to higher deviation angles. Peak torques occurred when the handle reached its foremost and rearmost positions, where wrist deviation was almost neutral. Wrist flexion showed a different motion pattern at 25W and 35W, with the wrist less extended at the higher load. Peak torque values occurred in foremost and rearmost crank positions at the lower (25W) propulsion resistance, whereas at the higher resistance of 35W peak wrist torques occurred during the pull and push phases.

Die approbierte gedruckte Originalversion dieser Dissertation ist an der TU Wien Bibliothek verfügbar.
The approved original version of this doctoral thesis is available in print at TU Wien Bibliothek.
TU WIEN Bibliothek Your knowledge hub

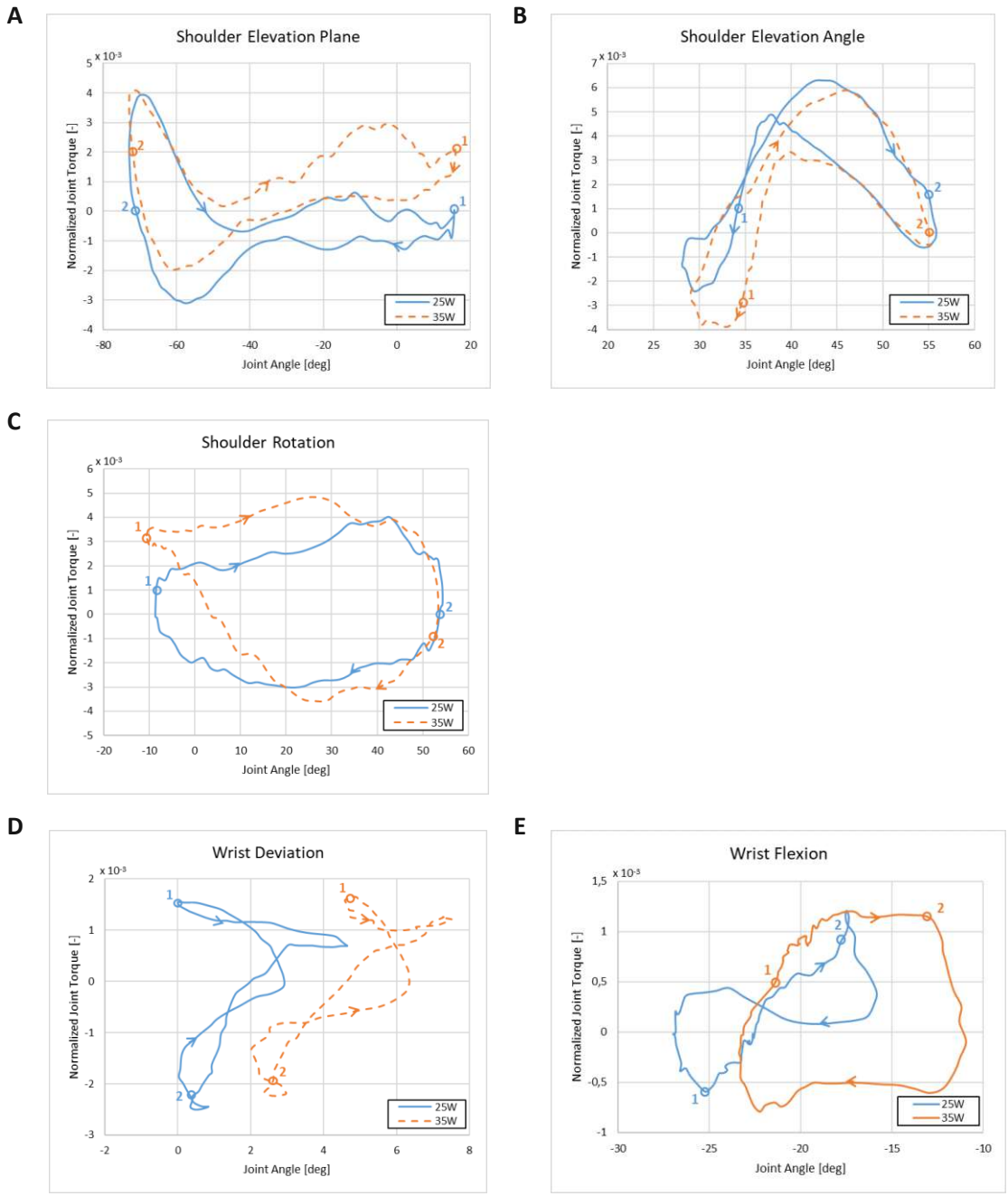

Figure 27: Joint angles/joint torques. Averaged normalized joint torque-joint angle trajectories generated with HP for: (A) shoulder elevation-plane, (B) shoulder elevation-angle, (C) shoulder rotation, (D) wrist deviation and (E) wrist flexion. The curves illustrate the mean values of all subjects and all selected cycles for each crank angle. HP with resistance levels of 25W (solid blue line) and 35W (dashed orange line) are shown. Position 1 represents a crank angle of 0 degrees while position 2 represents the point when the crank angle reached 180 degrees.

Die approbierte gedruckte Originalversion dieser Dissertation ist an der TU Wien Bibliothek verfügbar.
The approved original version of this doctoral thesis is available in print at TU Wien Bibliothek.
TU Bibliothek Your knowledge hub WIEN

Discussion

The aim of this study was to measure hand contact forces and upper-extremity joint excursions and joint torques generated by a novel HP device and to compare the results to literature data reported for PRP. We also investigated movement patterns of the shoulder and wrist joints to determine whether high loads occurred at the extreme positions of the joints. Compared to PRP at similar workloads, we found that joint excursions for HP remained within their ergonomic range and that the effectiveness of the propulsion forces was higher, leading to lower average propulsion forces. Thus, our hypothesis was supported. Whilst the model used in this study was based on the WCP Model in OpenSim, we modified its structure by adding two DoFs for movement of the handle. We also provided upper limb kinematic data and hand propulsion forces from experiments as inputs to the model [81, 82]. We found that the model produced torque and moment patterns that were consistent, similar, and repeatable across strokes, speeds and resistance levels.

The average resultant peak forces ($\hat{F}_{res_avg}$) measured for HP were significantly lower than those reported by Veeger *et al.* [71] and Koontz *et al.* [72] for PRP at lower resistance (Table 3).

Table 3: Resultant peak forces during HP and PRP

	Peak	± SD [N]
This study in HP 25W$^{(1.1m/s)}$	**55.7**	**± 11.6**
This study in HP 35W$^{(1.1m/s)}$	**65.4**	**± 7.6**
PRP Koontz 2006 (smooth floor, 0.9m/s)	58.9	± 11.6
PRP Koontz 2006 (smooth floor, 1.89m/s)	94.3	± 26.4
PRP Veeger 2002 (20W, 0.83m/s)	59.3	± 10.7
PRP Veeger 2002 (20W, 1.39m/s)	69.4	± 26.1

Comparison of resultant peak hand propulsion forces ($\hat{F}_{res_avg}$) in HP and PRP reported in the literature [7, 8]
Test condition is listed in parentheses if multiple conditions were tested

Arnet *et al.* [10] performed a similar study and compared joint angle ranges and loads in handcycling with conventional PRP. Their results showed reduced contact forces and continuous force application in handcycling compared to PRP. The reason for this difference between handcycling and PRP relates to the propulsion mode. Propulsion forces can be applied constantly during the whole propulsion cycle in handcycling while in PRP there is always an idle period where no force is applied to the push rim (recovery phase). Similar to

Die approbierte gedruckte Originalversion dieser Dissertation ist an der TU Wien Bibliothek verfügbar.
The approved original version of this doctoral thesis is available in print at TU Wien Bibliothek.
TU WIEN Bibliothek Your knowledge hub

TU WIEN Bibliothek Your knowledge hub
Die approbierte gedruckte Originalversion dieser Dissertation ist an der TU Wien Bibliothek verfügbar.
The approved original version of this doctoral thesis is available in print at TU Wien Bibliothek.

the findings of Arnet et al. for handcycling, our novel HP device also offers continuous propulsion force application, which results in lower contact forces compared to PRP. Regarding the applied tangential forces with respect to the crank angle, we found that the highest magnitudes were applied shortly after the rearmost and foremost positions of the handle, indicating that our subjects favoured the push and pull phases.

Table 4 shows comparable results for joint ranges measured during PRP and recommended low impact ergonomic joint excursions.

Table 4: Maximum and minimum joint angles in degrees (°) during HP and PRP.

	Shoulder elevation-plane[°]			Shoulder elevation-angle[°]			Shoulder flexion [°]			Shoulder abduction [°]			Shoulder rotation [°]			Wrist deviation [°]			Wrist flexion [°]		
	Min	Max	RoM	Min	Max	RoM	Min	Max	RoM	Min	Max	RoM	Min	Max	RoM	Min	Max	RoM	Min	Max	RoM
Normal joint RoM*	-80,0	135,0	215,0	0,0	180,0	180,0	-60,0	170,0	230,0	0,0	180,0	180,0	-70,0	90,0	160,0	-20,0	35,0	55,0	-70,0	80,0	150,0
Ergonomic low impact RoM Keyserling *et al.* 2007	-20,0	45,0	75,0	0,0	45,0	45,0	-20,0	45,0	65,0	0,0	45,0	45,0	-20,0	45,0	75,0	0,0	18,0	18,0	-45,0	30,0	75,0
This Study in HP 25W (1.1m/s)	**-73,0**	**15,7**	**88,7**	**28,1**	**55,8**	**27,7**	**-27,1**	**21,7**	**48,8**	**23,2**	**38,5**	**15,3**	**-8,7**	**54,3**	**63,0**	**0,0**	**4,6**	**4,6**	**-27,0**	**-15,8**	**11,2**
This Study in HP 35W (1.1m/s)	**-72,9**	**16,0**	**88,9**	**29,0**	**55,1**	**26,1**	**-53,9**	**10,7**	**64,6**	**22,9**	**37,0**	**14,1**	**-10,8**	**53,3**	**64,1**	**2,0**	**7,5**	**5,5**	**-23,4**	**-10,9**	**12,4**
Mean of PRP studies	**-58,2**	**26,5**	**88,3**	**22,5**	**56,6**	**34,1**	**-55,4**	**14,9**	**72,1**	**24,3**	**46,3**	**24,1**	**33,1**	**74,6**	**42,5**	**-7,3**	**23,8**	**31,1**	**-30,9**	**17,9**	**48,8**
PRP Koontz *et al.* 2002 (0.9 m/s)	-50,2	34,4	84,6	-	-	-	-43,2	19,1	62,3	26,0	42,0	16,0	24,5	52,1	27,6	-	-	-	-	-	-
PRP Koontz *et al.* 2002 (1,8 m/s)	-52,4	41,2	93,6	-	-	-	-45,4	23,2	68,6	25,0	42,0	17,0	22,8	51,4	28,6	-	-	-	-	-	-
PRP Boninger *et al.* 1998 (1.3 m/s)	-64,9	11,3	86,0	-	-	-	-64,0	6,2	74,8	24,5	47,0	26,1	55,2	90,7	37,3	-	-	-	-	-	-
PRP Boninger *et al.* 1998 (2.2 m/s)	-66,0	22,2	96,9	-	-	-	-68,8	11,1	82,6	21,6	54,2	37,4	51,3	92,8	44,4	-	-	-	-	-	-
PRP Rao *et al.* 1996 (1.5 m/s)	-57,3	23,2	80,5	22,5	56,6	34,1	-	-	-	-	-	-	11,6	86,2	74,6	-7,3	23,8	31,1	-30,9	17,9	48,8
PRP Boninger *et al.* 1997 (1.3 m/s)	-	-	-	-	-	-	-	-	-	-	-	-	-	-	-	-20,0	25,1	41,5	-38,6	7,1	45,7
PRP Boninger *et al.* 1997 (2.2 m/s)	-	-	-	-	-	-	-	-	-	-	-	-	-	-	-	-22,0	21,4	43,4	-34,2	7,4	41,6
PRP Veeger *et al.* 1998 (different inclines & speed)	-	-	-	-	-	-	-	-	-	-	-	-	-	-	-	-24,0	12,0	36,0	-28,0	20,0	48,0
PRP Wei *et al.* 2003 (high middle position)	-	-	-	-	-	-	-	-	-	-	-	-	-	-	-	-26,0	17,0	43,0	-35,0	10,0	45,0

Comparison of maximum and minimum joint angles and range of motion (RoM) at the shoulder and wrist [29, 30, 35, 70, 87–89]
Test condition is listed in parentheses if multiple conditions were tested
*values are according to the American Academy of Surgeons (AAOS)

Shoulder elevation-plane movement in HP appears to be slightly shifted to increased horizontal extension and axial rotation to increased external rotation compared to PRP. For both workloads, shoulder abduction and flexion-extension ranges of motion were reduced while maximum values for abduction were lower than in PRP. Compared to PRP, shoulder extension was lower at both workloads, while shoulder flexion appeared slightly higher at 25W and lower at 35W. Wrist movement changed from a flexion-extension pattern to a full extension movement, and the range of motion was much smaller for HP than for PRP. In comparison to the recommended ergonomic excursions reported in the literature, HP remained within the ergonomic ranges at the wrist, and only for horizontal flexion, abduction and external rotation at the shoulder. Maximum values of the shoulder angles tended to occur at or near a crank angle of 180°, where the handle was near its rearmost position. Highest range of motion values were found in the shoulder elevation-plane and shoulder rotation movement while lower values were observed in the elevation-angle. This finding was consistent for both workloads and explains firstly, that the movement pattern of the arm is guided by the design of the HP, unaffected by the load; and secondly, that the maximum shoulder joint excursions also depend on the subject's seated position relative to the crank centre. All participants were evaluated in the same test wheelchair and no adjustments were made to emulate their current wheelchair setup. Only the horizontal and vertical position of the HP crank centre was modified for each subject to accommodate their body dimensions. If the wheelchair did not fit the subject properly (i.e., the seat was too narrow or too wide, the handle position was too close or too far, or the handle position was too low or too high), this could have resulted in a shifted and inferior shoulder range of motion than would have been the case had the wheelchair fitted the subject optimally. Koontz *et al.* [35], Boninger *et al.* [87] and Rao *et al.* [29] performed a shoulder kinematic analysis for PRP at a lower resistance and a slightly different speed. The comparison of the shoulder joint movements showed no marked differences in horizontal flexion/extension and lower values for both flexion/extension and abduction range of motion. However, shoulder rotation range of motion in HP was about 20° higher and shifted to a more externally rotated position, alternating movement around the neutral position, compared to PRP. This can be explained by the fact that in HP the handle always keeps the hand in front of the subject, in contrast to PRP, where the shoulder is rotated strongly outwards at the beginning of the push phase to ensure an early hand contact with the push rim, and then remains rotated until the end of the

Die approbierte gedruckte Originalversion dieser Dissertation ist an der TU Wien Bibliothek verfügbar.
The approved original version of this doctoral thesis is available in print at TU Wien Bibliothek.
TU Bibliothek Your knowledge hub WIEN

push phase [35]. Wrist deviation is very small in HP with a maximum value of 7.5°, whereas large joint angles (12°-23.8°) and range of motion have been reported for PRP. The in literature in HP for wrist flexion was ~70% lower compared to PRP and ~80% lower for wrist deviation. Previous studies [87–89] also report alternating values between wrist flexion-extension and wrist radial-ulnar deviation for PRP, whereas in HP we observed only ulnar deviation close to neutral and wrist extension below 27°.

As shown in Table 5, our average peak shoulder joint torques at 25W are much lower than those reported by Veeger *et al.* [71] and Koontz *et al.* [35] for propulsion at 20W. For both workloads at the wrist, our average peak torque for wrist flexion is below 2Nm and for deviation around 3Nm, which are 7 times lower than the results reported by Boninger *et al.* [87] for similar conditions during PRP. These findings suggest that HP may lead to a reduction in upper-limb injuries compared to PRP [8–10]. The normalized torque-crank angle curves at the shoulder joint for both workloads were similar, with only minor propulsion torque differences observed. This effect is seen in Figure 27, which displays normalized averaged torque values for seven different subjects. There were small differences between subjects in their propulsion patterns, which led to individuals applying peak torques at different joint angles. However, these peaks tended to disappear when the data were averaged across subjects. Average peak torque values as well as peak contact forces values (Table 3) of single subjects showed an increase from 25W to 35W. The wrist joint generally showed different torque/angle curves for both resistance levels. Regarding wrist deviation, the propulsion pattern was similar but the range of motion shifted to a more deviated position with increasing workload. This shift can be explained by the fact that at higher resistance forces the subjects tended to grab the handle tighter and hence keep their wrist joints stiffer. Consequently, the range of motion of the wrist moved to a more extended position. Both the propulsion pattern and range of motion for wrist flexion were altered by changing the workload. Because propulsion at 35W increased wrist flexion, higher push and pull forces, which led to a rotation of the wrist during propulsion, were likely caused by the characteristic of the HP drive. Figure 6 shows that the highest joint torques occurred directly after and shortly before the rearmost grip position, where horizontal shoulder extension and internal shoulder rotation also reached their maximum values. As a result, the elbows were directed slightly outwards, forcing the wrist towards extension during propulsion in both the pull and push phases. This fact is also reinforced by the lowest value of flexion in the foremost handle position (Position 2).

Die approbierte gedruckte Originalversion dieser Dissertation ist an der TU Wien Bibliothek verfügbar.
The approved original version of this doctoral thesis is available in print at TU Wien Bibliothek.
TU WIEN Bibliothek Your knowledge hub

Conducting further tests at maximum load would likely force subjects into similar propulsion patterns and could strengthen this hypothesis.

Table 5: Peak joint torques in HP and PRP.

	Shoulder elevation-plane	Shoulder elevation-angle	Shoulder rotation	Wrist deviation	Wrist flexion
	Peak ± SD [Nm]	Peak ± SD [Nm]	Peak ± SD [Nm]	Peak ± SD [Nm]	Peak ± SD [Nm]
This study in HP 25W	**5.2 ± 2.1**	**7.2 ± 3.2**	**5.2 ± 2.8**	**2.8 ± 1.5**	**1.5 ± 0.9**
This study in HP 35W	**5.5 ± 2.0**	**7.9 ± 3.3**	**6.1 ± 3.3**	**3.1 ± 1.6**	**1.6 ± 0.6**
PRP Koontz *et al.* 2002 (9.24W, 0.9m/s)	10.9 ± 6.3	21.3 ± 12.0	21.6 ± 5.9	-	-
PRP Koontz *et al.* 2002 (21.85W, 1.3m/s)	21.0 ± 10.2	31.1 ± 14.1	31.9 ± 10.7	-	-
PRP Veeger *et al.* 2002 (20W, 0.83m/s)	21.7 ± 3.7	12.1 ± 4.9	9.8 ± 1.4	-	-
PRP Veeger *et al.* 2002 (20W, 1.39m/s)	21.1 ± 0.9	16.0 ± 8.6	11.7 ± 3.1	-	-
PRP Boninger et al. 1997 (14W, 1.3m/s)	-	-	-	16.6 ± 8.8	10.4 ± 4.8
PRP Boninger *et al.* 1997 (23W, 2.2m/s)	-	-	-	21.3 ± 11.7	13.6 ± 5.1

Average peak torques during HP calculated for 25W and 35W workloads and compared to peak torque values for PRP reported in the literature [35, 71, 88].
Test condition is listed in parentheses if multiple conditions were tested

From an ergonomic standpoint, it is recommended to keep joint angles close to their neutral positions for the duration of the movement [70]. Considering the propulsion pattern and the torque curves for HP, our results indicate that propelling the wheelchair with this novel propulsion device produces a more ergonomic range of motion of the upper-limb joints compared to PRP.

There are limitations of our study that ought to be considered when interpreting the results. First, the crank handle of the test wheelchair was not adjustable in the medial-lateral (z) direction to account for individual differences in body anthropometry, which may have influenced the performance (i.e., kinematics and kinetics) of the HP device. Second, the sample size (n=8) was relatively small. Force application during wheelchair propulsion is highly individualized, particularly for PRP, thus a larger number of test subjects would be required for greater statistical strength. However, the sample size used in the present study was limited by the availability of paraplegic patients who were willing and able to participate in these experiments. Future studies should consider performing maximum power tests at different power levels with a larger group of individuals to obtain a statistically significant inter-subject comparison of HP and PRP.

Die approbierte gedruckte Originalversion dieser Dissertation ist an der TU Wien Bibliothek verfügbar.
The approved original version of this doctoral thesis is available in print at TU Wien Bibliothek.
TU Bibliothek Your knowledge hub WIEN

In this study, we focus on kinematic and kinetic variables during steady propulsion, using the novel wheelchair drive device which has been computationally optimised for maximum power output [64]. Due to the possibility of applying propulsion forces over the entire cycle in combination with the selected gear ratio, we also expect that mobility will be significantly improved in practical use. Especially activities in daily life which require higher drive torques, such as start-up, acceleration, uneven ground or driving on ramps, are much easier to handle with the novel wheelchair propulsion device, which has also been confirmed by first tests. Furthermore, it is possible to propel both in synchronous and asynchronous mode, which can be advantageous for different situations in everyday life. With the brakes integrated for everyday use, the wheelchair can be decelerated in controlled fashion whereas for certain situations, such as overcoming steps, the push-rims on the wheelchair wheels can still be used. Future HP devices should offer a reverse gear and the possibility to lower the cranks, which is most important for transfers or driving under tables. However, we see our HP device as more suitable for indoor use, but it can also be used in an urban environment.

Conclusion

Overall, we found that our novel HP device improved wrist motion during wheelchair propulsion. In addition, shoulder rotation motion was optimized while shoulder elevation-plane motion remained relatively unchanged compared to PRP. However, our results indicate that HP is associated with reduced joint torques and lower joint excursions compared to PRP. Future work should focus on optimizing handle positions and determining whether improved joint ranges of motion may be achieved, especially for the shoulder elevation-plane, by increasing the distance between the crank centre and the body.

Acknowledgments

This work was supported by Austrian Science Fund (FWF) under Grant P 25507-B24.

Die approbierte gedruckte Originalversion dieser Dissertation ist an der TU Wien Bibliothek verfügbar.
The approved original version of this doctoral thesis is available in print at TU Wien Bibliothek.
TU WIEN Bibliothek Your knowledge hub

6 Journal Publication IV

6.1 Summary

Title: Metabolic Cost and Mechanical Efficiency of a Novel Handle-Based Device for Wheelchair Propulsion

This work conducted the measurement of cardiorespiratory responses to investigate differences in metabolic cost and mechanical efficiency for this novel HBP device compared with the standard PRP. Data were collected from long-term paraplegic subjects and non-disabled individuals, to further investigate effects on propulsion mode and efficiency and to determine how the results differ for long-term wheelchair. Each group performed a combined submaximal and maximal exercises using a wheelchair-based test rig which operated at constant speed and different resistance levels over time. Respiratory responses were measured with a wearable metabolic measurement system.

The results demonstrated for both subject groups significantly higher peak power output, higher mechanical efficiency, and lower physiological responses during HBP compared with PRP. Moreover, the results indicated that propelling the wheelchair with the HBP device is less strenuous and more efficient than conventional push-rim propulsion.

It was shown that the performance of the HBP exceeded the performances of lever-propelled and push-rim wheelchairs.

Die approbierte gedruckte Originalversion dieser Dissertation ist an der TU Wien Bibliothek verfügbar.
The approved original version of this doctoral thesis is available in print at TU Wien Bibliothek.
TU WIEN Bibliothek Your knowledge hub

6.2 Publication

Metabolic cost and mechanical efficiency of a novel handle-based device for wheelchair propulsion

Markus Puchinger, MSc,[a] Nithin Kurup, PhD,[a] Karin Gstaltner[b], Marcus G. Pandy, PhD,[c] and Margit Gföhler, PhD[a]

[a]Research Division of Biomechanics and Rehabilitation Engineering, Department of Engineering Design and Product Development, Technische Universität Wien (TU Wien), 1060 Vienna, Austria;

[b]AUVA Rehabilitation Centre Meidling, 1120 Vienna, Austria;

[c]Department of Mechanical Engineering, University of Melbourne, Parkville, VIC 3010, Australia.

Lay Abstract

The push-rim is the preferred mode of propulsion for more than 90% of all self-propelled wheelchair users, even though it is the least efficient. Furthermore, push-rim propulsion is highly strenuous for the musculoskeletal system and often leads to severe upper limb injuries. Alternative modes of manual wheelchair propulsion are available (e.g. arm-crank propulsion (handbikes) and lever-propulsion) but most of these are bulky, heavy and mostly suitable for outdoor use. The aim the present study was to investigate differences in metabolic cost and mechanical efficiency for a novel handle-based and ergonomically optimized device and to compare its performance to conventional push-rim propulsion. Eight paraplegic subjects and 10 non-disabled controls performed exercises at different power resistances. The results show that the performance of the handle-based device is below that of the handbike but that it out-performs lever-propelled and push-rim wheelchairs, suggesting that this novel design is more suited to indoor use and may therefore be an attractive alternative to push-rims for activities of daily living.

Keywords - wheelchairs, upper extremity, metabolism, rehabilitation, ADL

Die approbierte gedruckte Originalversion dieser Dissertation ist an der TU Wien Bibliothek verfügbar.
The approved original version of this doctoral thesis is available in print at TU Wien Bibliothek.

Abstract

Objective: To investigate differences in metabolic cost and gross mechanical efficiency of a novel handle-based wheelchair propulsion device and to compare its performance to conventional push-rim propulsion.

Design: Double-group comparative study between two different propulsion methods.

Participants: Eight paraplegic individuals and 10 non-disabled persons.

Methods: Participants performed the same exercise using a push-rim device and the novel handle-based device on a wheelchair-based test rig. The exercise consisted of a combined submaximal and maximal test. Power output, oxygen uptake, ventilation, respiratory exchange ratio and heart rate were recorded continuously during the tests. Analysis of variance was performed to determine effects of group, mode and on power output.

Results: Submaximal exercise resulted in a higher efficiency for the novel device and significant main effects of propulsion mode on all investigated parameters, except heart rate. On the respiratory exchange ratio, a significant interaction effect was found for both mode and group. The maximal exercise resulted in a higher peak power output and lower peak heart rate during propulsion using the handle-based device. A significant main effect on mode for mean peak power output, ventilation and heart rate was also observed.

Conclusion: Wheelchair propulsion using the handle-based device resulted in lower physical responses and higher mechanical efficiency, suggesting that this novel design may be well suited for indoor use, thereby offering an attractive alternative to push-rim wheelchairs.

Die approbierte gedruckte Originalversion dieser Dissertation ist an der TU Wien Bibliothek verfügbar.
The approved original version of this doctoral thesis is available in print at TU Wien Bibliothek.
TU WIEN Bibliothek Your knowledge hub

Introduction

Manual wheelchair propulsion is the most favored mode of propulsion adopted by a large percentage of wheelchair users: more than 90% of all self-propelled wheelchairs are propelled manually by using the arms to apply force to the push-rim [2]. Push-rim propulsion (PRP) is energetically inefficient, highly strenuous for the musculoskeletal system, and associated with high cardiopulmonary effort [2, 13, 14, 16, 90, 91]. Furthermore, PRP often leads to severe upper limb injuries, especially at the shoulder and wrist joints [29, 30, 92].

Gross mechanical efficiency (*GME*), defined as percentage the ratio between external power output (*PO*) and energy expenditure (*En*), is often used to benchmark mechanical efficiency of manual wheelchair propulsion. Oxygen uptake per unit time (VO_2), heart rate (*HR*) and propulsion frequency are the parameters typically used to assess the metabolic cost and efficiency of wheelchair propulsion [12, 93]. Due to high physical strain during PRP most of the expended energy dissipates, for example in heat loss, the rest contributes to propulsion. Thus, GME is typically measured to be in the range 2-10% and rarely exceeds 10% [2, 94]. Despite similar power output conditions, reported values for *GME* vary widely, which may be explained by individual differences in the physical ability of wheelchair users and by the influence of propulsion speed and surface properties [2, 94] .

Alternative modes of manual wheelchair propulsion have been tested, the most common alternatives being lever-propulsion and arm-crank-propulsion. Compared to PRP, both of these methods increase the joint range of motion in the upper limb, particularly at the wrist and shoulder joints [2, 12, 13]. Lever-propelled devices were mainly designed to reduce repetitive strain injuries [2, 12, 14, 15]. In general, *GME* in lever-propelled devices is reported to be higher compared to PRP, and wheelchair users report greater overall satisfaction with lever-propelled wheelchairs, but previous designs often do not consider user anthropometrics [2, 15, 16]. Handbikes are the most popular arm-crank-propelled alternative to PRP for manual wheelchair propulsion, with values for *GME* reported to range from 8% to 15% [13, 17–20]. Due to a higher energetic efficiency and lower strain on the cardiorespiratory system, several investigators have recommended the handbike as an alternative to push-rim wheelchair propulsion for outdoor use [10, 13, 17–19, 21, 22]. Although the efficiency of alternative devices for wheelchair propulsion is often higher, most of these are limited to outdoor use because they are bulky, heavier, less friendly for transferring, and less maneuverable [2, 13, 17].

Die approbierte gedruckte Originalversion dieser Dissertation ist an der TU Wien Bibliothek verfügbar.
The approved original version of this doctoral thesis is available in print at TU Wien Bibliothek.
TU WIEN Bibliothek Your knowledge hub

Our group has developed a novel handle-based propulsion (HBP) mechanism for conventional wheelchairs as a compact indoor alternative to PRP [64]. With an ergonomically optimized propulsion movement and the ability to continuously apply propulsive force, HBP offers a continuous cyclic motion at ergonomic joint ranges of motion and has been shown to decrease joint excursions and maximum joint torques during propulsion [64, 78, 95]. The objective of the present study was to investigate differences in metabolic cost and mechanical efficiency for this novel HBP device compared to the standard PRP. Data were collected from paraplegic subjects, who are long-term wheelchair users, and non-disabled individuals to further investigate effects on propulsion mode and efficiency and to determine how the results differ for long term wheelchair users who have trained muscle coordination patterns for push-rim propulsion and may also have changed relative muscle strengths. Each group used an instrumented wheelchair-based test rig operating at constant speed and different resistance levels. We hypothesized that under similar conditions HPB would be more energetically efficient and less strenuous compared to conventional PRP due to continuous force application.

Methods

Subjects

Eight right-handed paraplegic (PP) subjects were recruited from the spinal cord injury (SCI) rehabilitation centre “Weisser Hof” in Klosterneuburg, Austria. PP subjects were eligible for the study if they had an SCI level between L1 and T12, no permanent medication and no history of upper-limb injury.

The 10 non-disabled (ND) students (controls), who participated in this study (Table 6), were eligible if they were right-handed, had no history of upper limb injury, and no permanent medication. The significantly younger ND group had no experience with PRP, whereas all PP subjects were long-term wheelchair users with a minimum experience of 3 years. The sample size was defined by the maximum number of PP subjects available, rather than based on statistical considerations. All subjects provided informed consent and approval for the study was obtained from the responsible federal state ethics committee Ethikkommission für das Land Niederösterreich (NÖ Ethikkommission), Landhausplatz 1, Haus 15B, 3109 St. Pölten, Austria (GS1-EK-3/149-2018).

Die approbierte gedruckte Originalversion dieser Dissertation ist an der TU Wien Bibliothek verfügbar.
The approved original version of this doctoral thesis is available in print at TU Wien Bibliothek.
TU WIEN Bibliothek Your knowledge hub

Table 6: Characteristics of paraplegic (PP) and non-disabled (ND) subjects

Participants	Subject (Sex)	Age [yrs]	Weight [kg]	Height [cm]	BMI [kg/m²]	SCI Level
paraplegic (PP)	1 (f)	54	62	179	19	T11-12
	2 (m)	27	80	188	23	T6-7
	3 (f)	43	75	160	29	T10-L1
	4 (f)	56	63	158	25	T12-L1
	5 (m)	52	65	175	21	T12-L2
	6 (m)	45	85	192	23	T11-L1
	7 (m)	21	62	185	18	T8-9
	8 (m)	51	93	173	31	T12-L2
	mean (SD)	**44 (12)**	**73 (11)**	**176 (12)**	**24 (5)**	
non-disabled (ND)	1 (f)	23	70	165	26	
	2 (f)	21	63	170	22	
	3 (m)	21	92	185	27	
	4 (f)	21	54	162	21	
	5 (m)	23	58	181	18	
	6 (m)	24	70	169	25	
	7 (f)	26	58	175	19	
	8 (m)	36	99	181	30	
	9 (f)	35	64	176	21	
	10 (m)	19	61	187	17	
	mean (SD)	**25 (5)**	**69 (14)**	**175 (8)**	**22 (4)**	

SD: standard deviation; SCI: spinal cord injury

Experimental Setup

All subjects were tested using a previously developed test rig [26] (Figure 28) consisting of a lightweight manual wheelchair (Eurochair Vario,XXL, Meyra Orthopedics, Kalletal, Germany) with 0.42m seat depth, 0.50m seat width, and an adjusted seat height of 0.51m. The wheelchair was mounted on a square tube frame to avoid direct contact between the wheels and floor and to facilitate mounting of different hand-driven propulsion devices. A controlled brushless motor combined with gearbox and flywheel mounted under the seat of the wheelchair provided torques that simulated resistances during wheelchair propulsion. Timing belts were used to promote a slip-free power transmission to the wheels and front connection points. For this study, the test rig operated in maximal power mode, where the resistance progressively increased according to a predefined resistance increment and time interval. In all trials, visual feedback allowed the participant to maintain the target speed during propulsion.

Die approbierte gedruckte Originalversion dieser Dissertation ist an der TU Wien Bibliothek verfügbar.
The approved original version of this doctoral thesis is available in print at TU Wien Bibliothek.
TU WIEN Bibliothek Your knowledge hub

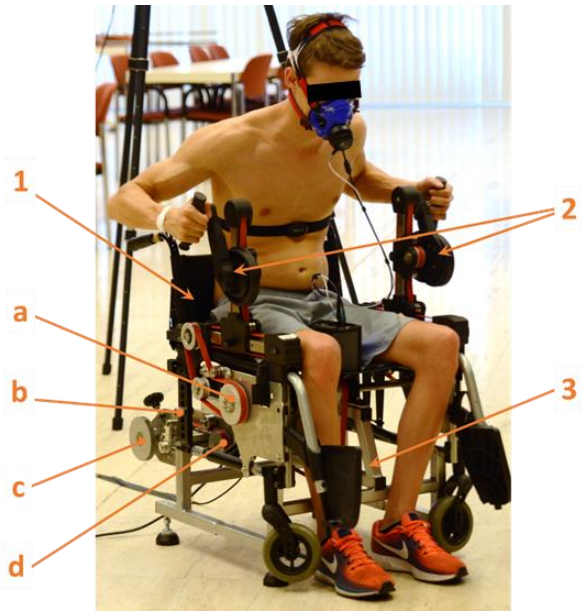

Figure 28: Wheelchair-based test rig with mounted HBP devices: [1] wheelchair, [2] HBP devices, [3] mounting frame, [a] front attachment pulley, [b] back wheel hub, [c] rear attachment pulley, [d] resistance power unit.

Propulsion devices

For PRP, conventional 24-inch (609,6mm) diameter push-rim wheels were mounted on the test rig whereas for crank propulsion two handle-based propulsion (HBP) devices [79] were utilized instead of the armrests (Figure 28 and Figure 29). Each HBP device consisted of a rotating crank on which a handle was mounted. During propulsion, a sliding guide changed the length of the crank during each rotation, allowing the handle to follow the optimized propulsion path [78]. The gear ratio of the HBP device was fixed at 1.2.

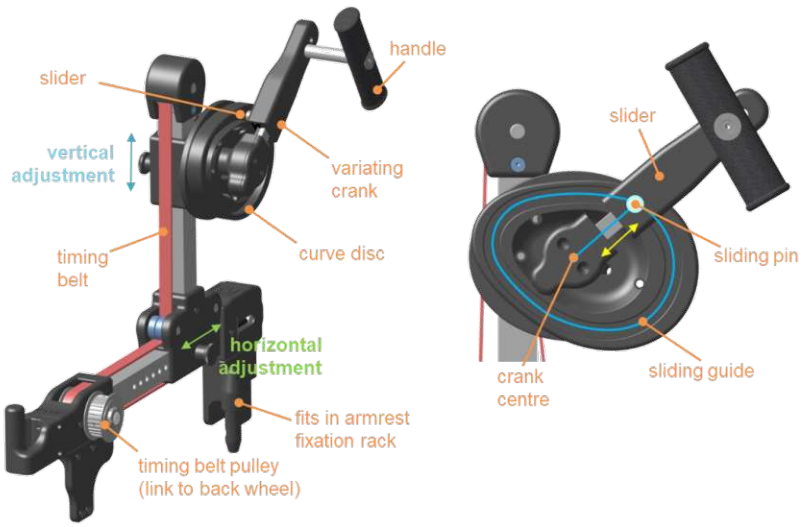

Figure 29: Handle-based propulsion (HBP) device and its components. The horizontal and vertical positions of the crank centre can be adjusted according to the user's body anthropometry.

Die approbierte gedruckte Originalversion dieser Dissertation ist an der TU Wien Bibliothek verfügbar.
The approved original version of this doctoral thesis is available in print at TU Wien Bibliothek.
TU WIEN Bibliothek Your knowledge hub

Test Protocol

All participants performed the same exercise with both PRP and HBP consecutively on the same day with a least 10 minutes of rest between exercises. The subjects were instructed to refrain from smoking for at least two hours before testing, to not consume any caffeinated or alcoholic beverages, and to void their bladder shortly before the measurements. To control the influence of fatigue on the effect of mode, subjects were assigned to alternately start with PRP or HBP, i.e. even-numbered subjects started the exercises with PRP, and odd-numbered subjects with HBP. To ensure familiarization with all equipment, subjects participated in a short preliminary session in which both HBP and PRP were used with low resistance (5W). The exercise test consisted of two parts: a two-minute submaximal exercise test performed at 15W constant resistance power, followed by a maximal exercise test in which the resistance power was increased by 5W every minute. Both parts were performed consecutively with no break in between. The test was terminated when either 55W of resistance power was reached or when the subject reached physical exhaustion and could not continue. To simulate a common propulsion speed, subjects were asked to maintain a propulsion speed in the range 1.20-1.65m/s for both HBP and PRP, similar to the range of speeds used in previous studies [10, 19, 96]. Sixteen of the 18 subjects completed all exercises. One female participant was excluded due to problems with balance during testing while one male ND subject was excluded because the required speed range was not achieved during the experiments.

Data Collection

Actual resistance power (*PO*, W) and linear velocity (*v*, m/s) were measured concurrently during each test. In addition, oxygen uptake (VO_2, ml/min), carbon dioxide output (VCO_2, ml/min) and ventilation (*Ve*, ml/min) were measured continuously using a wearable metabolic measurement system (Cosmed K5, Cosmed GmbH, Fridolfing, Germany), while heart rate (*HR*, beats/min) was measured using a mobile chest heart rate monitor (Polar H10 ANT+, Polar Electro Inc., Kempele, Finland). The spirometry system was matched to the subjects with respect to ethnicity (Caucasian) and calibrated with a reference gas after each subject. Linear velocity (*v*, m/s) and cadence (*RPM*, 1/min) were obtained from the test rig control and were also measured using cadence sensors (B00JLMS848 ANT+/B00JLMRXCQ ANT+, Garmin Ltd., Schaffhausen, Switzerland) mounted on both HPB cranks and the back wheels.

Die approbierte gedruckte Originalversion dieser Dissertation ist an der TU Wien Bibliothek verfügbar.
The approved original version of this doctoral thesis is available in print at TU Wien Bibliothek.
TU WIEN Bibliothek Your knowledge hub

Data Analysis

Respiratory exchange ratio (*RER,* -) was calculated as the ratio between carbon dioxide output (*VCO_2,* ml/min) and oxygen uptake (*VO_2,* ml/min). Metabolic expenditure (*En,* W) was obtained from *VO_2* and *RER* using the equation reported by Garby et al. [97]:

$$En = (4.94 \cdot RER + 16.04) \cdot \frac{VO2}{60} \text{ [W]} \tag{5}$$

Gross mechanical efficiency (*GME,* %) was defined as the ratio between the actual resistance power (*PO,* W) provided by the test rig and energy expenditure (*En*) of the subject:

$$GME = \frac{PO}{En} \cdot 100 \text{ [\%]} \tag{6}$$

Weight-specific oxygen uptake (*VO_2/kg*, ml/min/kg) was obtained from oxygen uptake (*VO_2*) and the weight of the subject. Oxygen uptake per unit distance traveled (*VO_2 efficiency*, ml/kg/m) was found from the measured VO_2/kg and the corresponding mean linear velocity (*v*). Mean submaximal values of *VO_2, VO_2/kg, VO_2 efficiency, VCO_2, Ve, RER, HR* and *GME* for both HBP and PRP were measured during the last minute of the 2-min (15W) submaximal exercise. During the maximal power exercise, the subject's mean values of *VO_2, VO_2/kg, VO_2 efficiency, VCO_2, Ve, RER, HR* and *GME* were calculated for both propulsion modes at each achieved resistance level to provide a comparison between the two propulsion modes. Peak values of *VO_2, VO_2/kg, VO_2 efficiency, VCO_2, Ve, RER* were found by calculating the highest mean value of each variable measured over a time interval of 30s, whereas the peak value of *HR* was defined as the highest mean value of *HR* measured over an interval of 10s. Peak power output was defined as the highest resistance level achieved during the maximal exercise, which was maintained for at least 30s.

Statistics

All analyses were performed using SPSS (IBM SPSS Statistics 26, SPSS, Inc., Chicago, USA). Mean and peak values were calculated using descriptive statistics. An ANOVA with a 2x2 design (mode: HBP, PRP; group: ND, PP) was used to determine the effect of propulsion mode and subject group on submaximal exercise responses. An ANOVA with a 2x4x2 design (mode: HBP, PRP; power output: 15W, 20W, 25W and 35W; group: ND, PP) was also used to evaluate the interaction between propulsion mode, power output, and subject group for the resistance levels achieved by all subjects during the maximal exercise tests. The effect of propulsion mode and subject group on peak performance was found using an ANOVA with a 2x2 design

Die approbierte gedruckte Originalversion dieser Dissertation ist an der TU Wien Bibliothek verfügbar.
The approved original version of this doctoral thesis is available in print at TU Wien Bibliothek.
TU WIEN Bibliothek Your knowledge hub

(mode: HBP, PRP; group: ND, PP). Statistical significance for all tests was set at $p<0.05$ with no adjustment for multiple comparisons.

Results

Submaximal exercise

There was a significant main effect of propulsion mode on all parameters except *HR*, indicating lower VO_2, VO_2/kg, *Ve*, *RER* and higher *GME* and VO_2 *efficiency* during HBP (Table 7). Mean values of VO_2 *efficiency* during HBP were 0.07 ml/kg/m lower for ND and 0.03 ml/kg/m lower for PP. Similarly, mean *GME* was 1.03% higher for ND and 2.75% higher for PP during HBP compared to PRP. There was a significant main effect of group on all parameters except *Ve* and *HR*, indicating that the mean values were significantly different between ND and PP. *HR* in both subject groups did not show any significant effects. A significant interaction effect was found for mode and group on *RER*, indicating that the changes in *RER* during the HBP and PRP tests were different between PP and ND.

Table 7: Mean (SD) submaximal values measured for HBP and PRP at 15W constant resistance for the PP and ND groups. Symbols appearing in the table are: gross mechanical efficiency (*GME*), oxygen uptake per unit distance travelled (VO_2 *efficiency*), weight-related oxygen uptake (VO_2/kg), oxygen uptake (VO_2), ventilation (*Ve*), respiratory exchange ratio (*RER*) and heart rate (*HR*).

	GME [%]	VO_2 eff. [mL/kg/m]	VO_2/kg [mL/min/kg]	VO_2 [mL/min]	Ve [l/min]	RER [-]	HR [bpm]
ND	n=9	n=9	n=9	n=9	n=9	n=9	n=9
HBP	7.59 (1.37)	0.12 (0.02)	9.94 (2.28)	620.04 (106.17)	20.42 (4.24)	0.83 (0.06)	110.00 (17.84)
PRP	6.56 (1.73)	0.19 (0.06)	10.94 (2.82)	738.93 (198.00)	24.74 (7.23)	0.87 (0.06)	108.80 (21.26)
PP	n=7	n=7	n=7	n=7	n=7	n=7	n=7
HBP	9.9 1(1.41)	0.08 (0.02)	6.72 (1.71)	486.72 (68.19)	17.35 (2.41)	0.68 (0.05)	96.10 (11.14)
PRP	7.16 (1.22)	0.11 (0.02)	8.89 (1.97)	649.70 (104.18)	23.76 (4.87)	0.84 (0.05)	111.33 (11.59)
Mode							
F-value	13.23	11.38	3.80	8.82	8.60	26.37	1.41
P-value	0.001	0.002	0.049	0.006	0.007	<0.001	0.245
Group							
F-value	7.92	17.68	10.48	5.50	1.22	21.07	0.92
P-value	0.009	<0.001	0.003	0.026	0.279	<0.001	0.345
Mode × Group							
F-value	2.70	1.52	0.52	0.22	0.33	7.78	1.93
P-value	0.111	0.229	0.478	0.646	0.573	0.009	0.176

bpm…beats per minute
green highlighted values indicate significance ($P<0.05$)

Die approbierte gedruckte Originalversion dieser Dissertation ist an der TU Wien Bibliothek verfügbar.
The approved original version of this doctoral thesis is available in print at TU Wien Bibliothek.
TU Bibliothek Your knowledge hub WIEN

Maximal exercise

Maximum power resistance levels were different between PP and ND. Both groups achieved higher power levels for HBP than PRP. Values for *GME* were higher in HBP than PRP for both the PP and ND groups (Figure 30).

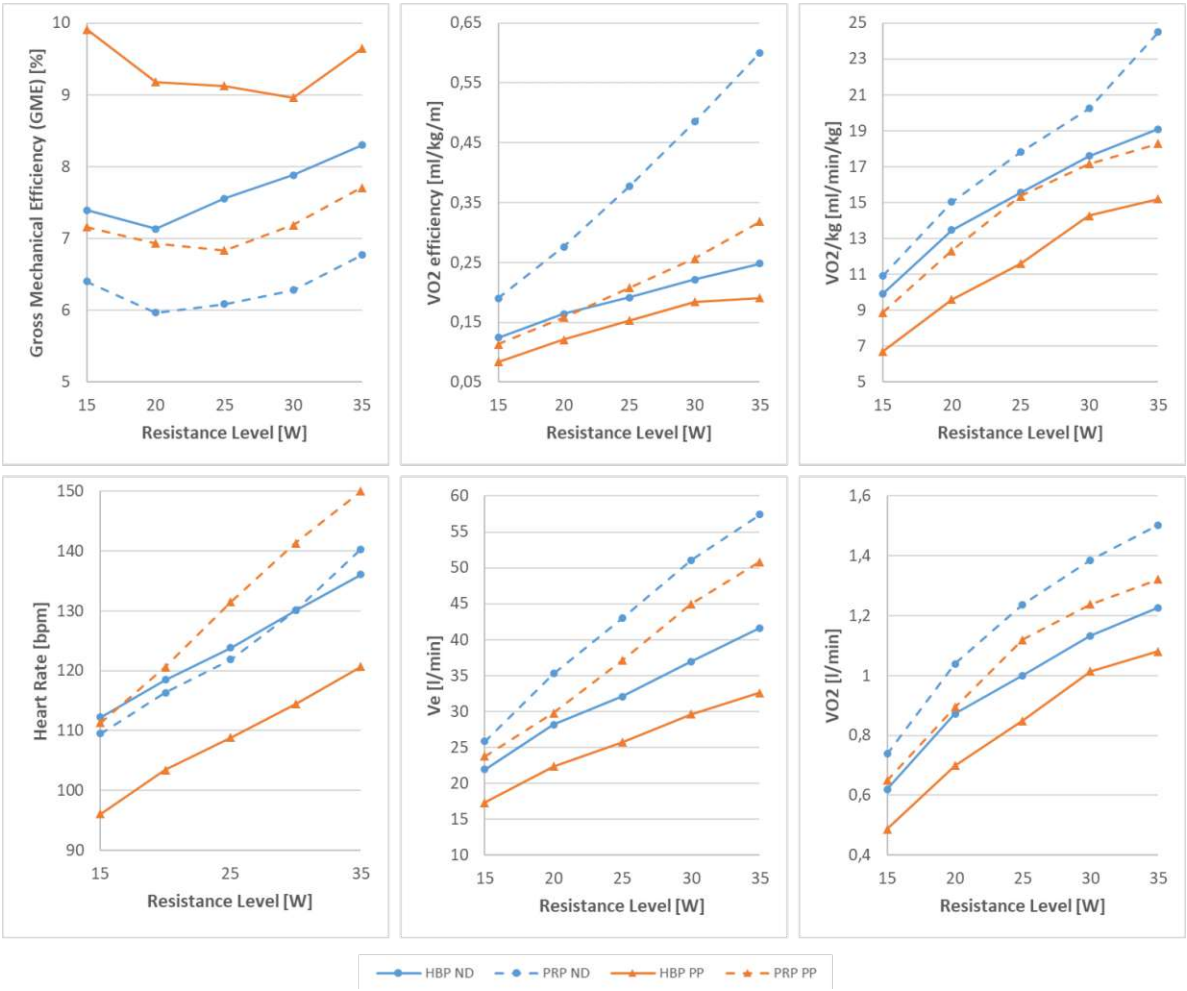

Figure 30: Dependence of gross mechanical efficiency (*GME*), oxygen uptake per unit distance travelled (*VO_2 efficiency*), weight-related oxygen uptake (*VO_2/kg*), heart rate (*HR*), ventilation (*Ve*) and oxygen uptake (*VO_2*) on resistance level measured for PP subjects (orange lines, triangle markers) and ND subjects (blue lines, circle markers) during HBP (solid line) and PRP (dashed lines).

Furthermore, *HR* increased as resistance level increased. A significant main effect of propulsion mode for all parameters in HBP was evident, indicating higher *GME* and *VO_2 efficiency* and lower *VO_2/kg*, *VO_2, Ve*, *HR* and *En* (Table 8).

Die approbierte gedruckte Originalversion dieser Dissertation ist an der TU Wien Bibliothek verfügbar.
The approved original version of this doctoral thesis is available in print at TU Wien Bibliothek.

Table 8: ANOVA results obtained for the maximal exercise tests (15W-35W) for the PP and ND subject groups. Symbols appearing in the table are: gross mechanical efficiency (*GME*), oxygen uptake per distance travelled (*VO_2 efficiency*), weight related oxygen uptake (*VO_2/kg*), oxygen uptake (*VO_2*), ventilation (*Ve*), heart rate (*HR*) and energy expenditure (*En*).

	Mode		Group		Mode×Group		Mode×PO		Mode×Group×PO	
	F-value	P-value	F-value	P-value	F-value	P-value	F-value	P-value	F-value	P-value
GME	68.410	<0.001	31.782	<0.001	3.127	0.079	0.049	0.995	0.386	0.818
VO_2 efficiency	37.194	<0.001	26.753	<0.001	9.375	0.003	2.584	0.040	0.676	0.610
VO_2/kg	24.859	<0.001	39.676	<0.001	0.098	0.755	0.668	0.615	0.400	0.808
VO_2	56.350	<0.001	24.057	<0.001	0.023	0.879	0.641	0.634	0.083	0.988
Ve	53.835	<0.001	10.167	0.002	0.049	0.825	1.968	0.103	0.042	0.997
HR	18.579	<0.001	1.955	0.164	12.999	<0.001	0.626	0.645	0.048	0.996
En	62.511	<0.001	30.945	<0.001	0.000	0.995	0.839	0.503	0.098	0.983

green highlighted values indicate significance (P<0.05)
PO…power output (resistance level)

HR was significantly higher for the PP group during PRP, whereas no significant differences were found with respect to propulsion mode for the ND group. Except for *HR,* there was also a significant main effect of group for all outcome variables, indicating higher *GME* and *VO_2 efficiency* and lower physiological responses for the PP group compared to the ND group. A significant interaction effect between propulsion mode and group was found for *VO_2 efficiency* and *HR*, suggesting that the differences between HBP and PRP were larger for *VO_2 efficiency* and smaller for *HR* in the ND group compared to the PP group. No interaction effects were found between propulsion mode, group, and power output, indicating that the combined effect of power output and propulsion mode was similar for both groups. In both groups, mean *RER* values were lower for HBP than PRP (Figure 31). As power resistance increased, *RER* values were above 1.0 for PRP but remained below 1.0 for HBP, indicating higher physical exhaustion during PRP.

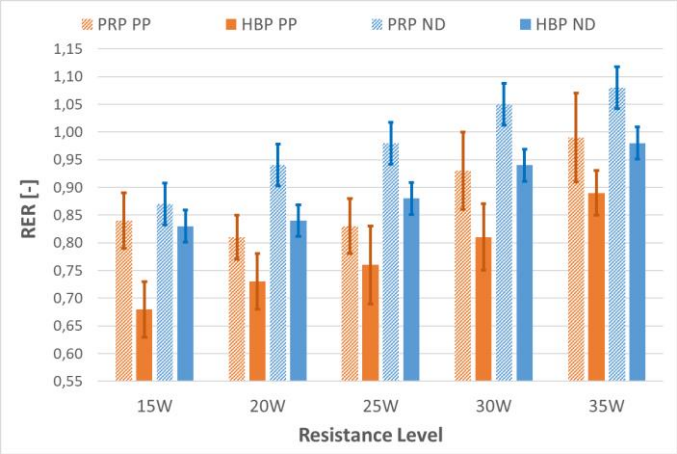

Figure 31: Mean RER values and standard deviations measured for HBP (solid infill) and PRP (diagonal stripes infill) in paraplegic (PP, orange) and non-disabled (ND, blue) subjects.

Die approbierte gedruckte Originalversion dieser Dissertation ist an der TU Wien Bibliothek verfügbar.
The approved original version of this doctoral thesis is available in print at TU Wien Bibliothek.
TU Bibliothek Your knowledge hub WIEN

Peak responses

A significant main effect was observed for propulsion mode on $PO_{(peak)}$, $Ve_{(peak)}$ and $HR_{(peak)}$; specifically, power output was higher and *Ve* and *HR* were lower for HBP than PRP (Table 9). No main effect was found for propulsion mode on peak oxygen uptake ($VO_2/kg_{(peak)}$, $VO_{2(peak)}$) and $RER_{(peak)}$. There was a significant main effect on group for all parameters except $HR_{(peak)}$. However, no interaction effect was found for propulsion mode and group on any of the outcome variables, as the ND and PP groups showed similar trends in peak values during HBP and PRP.

Table 9: Mean values and standard deviations for peak power output ($PO_{(peak)}$), peak weight-related oxygen uptake ($VO_2/kg_{(peak)}$), peak oxygen uptake ($VO_{2(peak)}$), peak ventilation ($Ve_{(peak)}$), peak respiratory exchange ratio ($RER_{(peak)}$), and peak heart rate ($HR_{(peak)}$). Results obtained from the ANOVA for propulsion mode (HBP vs. PRP), group (ND vs. PP) and interaction effects are also shown.

	$PO_{(peak)}$ [W]	$VO_2/kg_{(peak)}$ [mL/min/kg]	$VO_{2(peak)}$ [mL/min]	$Ve_{(peak)}$ [l/min]	$RER_{(peak)}$ [-]	$HR_{(peak)}$ [bpm]
ND	n=9	n=9	n=9	n=9	n=9	n=9
HBP	55,56 (7,68)	37,86 (30,70)	1615,42 (236,50)	59,69 (8,59)	1,09 (0,07)	157,67 (23,01)
PRP	46,67 (6,61)	34,41 (8,85)	1833,95 (541,13)	77,58 (26,71)	1,15 (0,09)	161,89 (21,12)
PP	n=7	n=7	n=7	n=7	n=7	n=7
HBP	46,43 (4,76)	19,42 (2,01)	1351,39 (178,50)	43,17 (7,05)	0,99 (0,06)	134,86 (7,13)
PRP	42,86 (4,88)	25,19 (8,13)	1541,17 (182,56)	57,79 (9,20)	1,04 (0,07)	158,86 (12,31)
Mode						
F-value	7,78	0,03	2,89	8,20	3,87	4,87
P-value	0,009	0,856	0,100	0,008	0,059	0,036
Group						
F-value	8,38	4,90	5,37	10,23	13,81	4,08
P-value	0,007	0,035	0,028	0,003	0,001	0,053
Mode×Group						
F-value	1,42	0,54	0,01	0,08	0,02	2,39
P-value	0,244	0,468	0,906	0,776	0,888	0,133

PO…power output
bpm…beats per minute
green highlighted values indicate significance (P<0.05)

Die approbierte gedruckte Originalversion dieser Dissertation ist an der TU Wien Bibliothek verfügbar.
The approved original version of this doctoral thesis is available in print at TU Wien Bibliothek.
TU WIEN Bibliothek Your knowledge hub

Discussion

The aim of this study was to measure metabolic cost and mechanical efficiency during wheelchair propulsion using a novel HBP device and to compare these performance indicators against those measured for conventional PRP. We investigated physiological parameters for both propulsion modes in a combined submaximal and maximal exercise test using both paraplegic (PP) and non-disabled (ND) subjects. The results of the submaximal test showed that higher *GME* and *VO_2 efficiency* were attained with lower physiological responses during HBP compared to PRP. This effect was also observed during the maximal exercise tests with continuously increasing resistance (i.e., increasing power output).

Furthermore, HBP showed higher peak power output and lower peak heart rate compared to PRP. In all tests, subjects showed significantly higher efficiency and lower physiological responses during HBP compared to PRP. Thus, our hypothesis that HPB is more efficient and less strenuous than conventional PRP was supported.

Our results for the submaximal and maximal tests showed higher *GME* and lower physiological responses with the HBP device, which is consistent with findings from previous studies that have focused on comparing submaximal arm-crank exercise with conventional PRP under similar conditions [19, 90, 98, 99]. Our measured values of *GME* and *VO_2 efficiency* for PRP are also consistent with data reported previously by others [11, 93]. The higher *GME* and *VO_2 efficiency* achieved by the PP group compared with the ND control group may be due to their familiarity with PRP as well as better upper-limb muscle conditioning resulting from everyday use of the wheelchair. However, the results of the maximal exercise indicate that the effects of propulsion mode and power output apply to both groups. Previous studies on arm-crank devices report higher peak power output compared to conventional PRP [19, 99]. Similar findings were observed during the propulsion mode with HBP, where mean peak power output values were 8.3% higher for the PP group and 19.0% higher for the ND group compared to PRP. Regarding peak oxygen uptake, we found significant differences between the subject groups but no significance was found between HBP and PRP, which is consistent with the results of other studies comparing arm-crank devices with PRP [19, 100–103].

Particularly for subjects with paraplegia, mean heart rates at power levels between 15W and 35W as well as $HR_{(peak)}$ were significantly reduced using the HBP device, which is also supported by lower *RER* values. This suggests a higher endurance capacity of the paraplegic

Die approbierte gedruckte Originalversion dieser Dissertation ist an der TU Wien Bibliothek verfügbar.
The approved original version of this doctoral thesis is available in print at TU Wien Bibliothek.
TU WIEN Bibliothek Your knowledge hub

subjects, which is also reflected in higher mean peak power output values achieved in HBP compared to PRP.

However, comparing the differences in *HR* values between both subject groups, no statistical significance was found - an observation that has also been reported previously and has been attributed to the normally higher *HR* in paraplegic persons [19].

Thus, independent of subject group, HBP was shown to achieve higher mechanical efficiencies and lower oxygen uptake at both submaximal and maximal workloads compared to PRP.

Although studies reported in the literature on alternative propulsion devices are not easily compared, the data on efficiency presented here, particularly our measurements of *GME and* VO_2 *efficiency,* place the HBP below the performance of the handcycle but above lever-propelled and PRP wheelchairs. Moreover, our findings indicate that propelling a wheelchair with this novel HBP device is more efficient and less strenuous than propelling a wheelchair with a push-rim. In addition, our previous study [95] showed that the HBP device may lower the probability of upper limb injuries by reducing joint loads and ergonomic joint ranges. To adapt to an individual user's wheelchair, the horizontal and vertical adjustment mechanisms shown in Figure 29 can be eliminated, leading to an even more compact and lightweight design of the crank mechanism that can also be swivelled for transfers. Therefore, we consider the novel wheelchair drive to be more suitable for indoor use than, for example, handcycles, making it an attractive alternative to push-rims for activities of daily living.

There are limitations that ought to be considered when interpreting the results of our study. The sample size (PP n=8; ND n=10) was relatively small. Because force application during wheelchair propulsion is highly individualized, especially for PRP, a larger number of test subjects may influence the findings reported here. Also, the age difference between the two groups may have affected the group comparison, as in general, younger subjects are more likely to have higher cardiorespiratory fitness. However, it is generally difficult to establish groups of able-bodied and paraplegic subjects that are comparable in terms of cardiorespiratory fitness, as it has been well investigated [104] that paraplegic subjects have lower cardiorespiratory fitness in comparison to able-bodied subjects. In any case, only group comparisons may have been influenced by the age difference, the effects of propulsion mode are not affected.

Die approbierte gedruckte Originalversion dieser Dissertation ist an der TU Wien Bibliothek verfügbar.
The approved original version of this doctoral thesis is available in print at TU Wien Bibliothek.
TU WIEN Bibliothek Your knowledge hub

Another improvement that is recommended for further studies is to make the test rig adjustable in the medial-lateral direction to account for individual differences in body anthropometry also in this dimension.

In summary, we found that both subject groups demonstrated significantly higher peak power output, higher mechanical efficiency, and lower physiological responses during handle-based propulsion compared to push-rim propulsion. Our results indicate that propelling the wheelchair with this novel HBP device is less strenuous and more efficient than conventional push-rim propulsion. Overall, the performance of the HBP was below that of the handbike, but it exceeded the performances of the lever-propelled and push-rim wheelchairs.

Acknowledgments

This work was supported by Austrian Science Fund (FWF) under Grant P 25507-B24. The authors acknowledge TU Wien Bibliothek for financial support through its Open Access Funding Programme.

Die approbierte gedruckte Originalversion dieser Dissertation ist an der TU Wien Bibliothek verfügbar.
The approved original version of this doctoral thesis is available in print at TU Wien Bibliothek.
TU WIEN Bibliothek Your knowledge hub

7 Conclusion and Outlook[7]

In this thesis, a manual wheelchair propulsion device (HBP) was developed and evaluated that follows an ergonomically optimized motion path for the arms obtained from musculoskeletal simulation **[Journal Publication I]**. The developed propulsion method is based on a length-adjusting crank and a sliding guide. Timing belts proved to be the ideal lubrication-free lightweight drive variant. Furthermore, a wheelchair-based test rig for manual wheelchair propulsion was developed, which allowed easy and reproducible testing of different manual wheelchair propulsion devices. The use of timing belts for the transmission of resistance torques instead of friction rolls allowed slip-less measurements with different propulsion methods. Both the various mounting possibilities for hand propelling devices as well as its connectivity have proved useful.

The results for the mean peak muscle activations showed, that push-rim propulsion leads to higher peak muscle activity compared to HBP at a similar wheelchair velocity. Moreover, the peak EMG values in push-rim propulsion indicated that most of the upper limb muscles were maximally recruited during propulsion whereas in HBP all muscles contributed evenly. **[Journal Publication II]**.

Our studies showed, that HBP offers a continuous cyclic motion at ergonomic joint ranges. Compared to push-rim propulsion, HBP stays with up to 30% reduced range of motion at the shoulder and up to 80% at the wrist within the recommended ergonomic ranges and average resultant peak forces were reduced by up to 20%. With lower net torques at both the shoulder and wrist this novel propulsion system shows high potential to reduce the risk of upper-extremity injuries. **[Journal Publication III]**

Independent of subject group, the novel HBP was shown to achieve higher mechanical efficiencies and lower oxygen uptake at both submaximal and maximal workloads compared with PRP. The here presented findings indicate that propelling a wheelchair with this novel HBP device is more efficient and less strenuous than propelling a wheelchair with a push-rim. **[Journal Publication IV]**

Overall, our hypotheses were supported and the results demonstrate that propelling the wheelchair with this novel HBP device is less strenuous, more joint-friendly and more efficient than conventional push-rim propulsion.

[7] This section is based on the discussions of Journal Publication I-IV

Die approbierte gedruckte Originalversion dieser Dissertation ist an der TU Wien Bibliothek verfügbar.
The approved original version of this doctoral thesis is available in print at TU Wien Bibliothek.
TU Bibliothek Your knowledge hub WIEN

There are some points that still need to be addressed: There are many different methods of propelling a wheelchair, but only a few are commercially available. Besides electric wheelchair propulsion, manual methods are limited to push-rim propulsion, lever propulsion, and the mounting of a third wheel equipped with a crank, the so-called handcycles. Due to the missing activity of the lower extremity, manual wheelchair propulsion is an important contribution for training the cardiovascular system. Thus, electric wheelchair propulsion is not a viable alternative. Although studies reported in the literature on alternative manual propulsion devices, are not easily compared, the data on efficiency place the here presented HBP below the performance of the handcycles but above lever propelled and PRP wheelchairs.

Since wheelchairs are very individual, a universal fixation that fits any wheelchair was problematic, hence the fixation of the drives needs to be adapted to the wheelchair. The here presented modular design supports easy wheelchair-specific adaptation. Furthermore, our research results have shown that some adjustment options are not essential for adaptation to the subjects, thus the HBP can be built much slimmer. Based on these findings, the drive was further developed in a follow-up project and is now significantly slimmer and offers the possibility to be swiveled away for transfers. Moreover, the methods demonstrated here, should provide the starting point for future studies focusing on effects on performance of a customized HBP-equipped active wheelchair.

Overall, the here presented scientific work can be concluded as a substantial contribution for people with special needs who are dependent on wheelchairs and can help to keep and enhance their independence and integration in daily life.

Die approbierte gedruckte Originalversion dieser Dissertation ist an der TU Wien Bibliothek verfügbar.
The approved original version of this doctoral thesis is available in print at TU Wien Bibliothek.
TU WIEN Bibliothek Your knowledge hub

List of References

[1] World Health Organization. Regional Office for South-East Asia, *Fact sheet on wheelchairs*. New Delhi: WHO Regional Office for South-East Asia, 2010. [Online]. Available: https://apps.who.int/iris/handle/10665/205041

[2] L. H. van der Woude, A. J. Dallmeijer, T. W. Janssen, and D. Veeger, "Alternative modes of manual wheelchair ambulation: an overview," *American journal of physical medicine & rehabilitation*, vol. 80, no. 10, pp. 765–777, 2001, doi: 10.1097/00002060-200110000-00012.

[3] K. A. Curtis *et al.,* "Effect of a standard exercise protocol on shoulder pain in long-term wheelchair users," *Spinal Cord*, vol. 37, no. 6, pp. 421–429, 1999, doi: 10.1038/sj.sc.3100860.

[4] R. A. Cooper *et al.,* "Engineering better wheelchairs to enhance community participation," *IEEE transactions on neural systems and rehabilitation engineering : a publication of the IEEE Engineering in Medicine and Biology Society*, vol. 14, no. 4, pp. 438–455, 2006, doi: 10.1109/TNSRE.2006.888382.

[5] M. P. Jensen, A. J. Hoffman, and D. D. Cardenas, "Chronic pain in individuals with spinal cord injury: a survey and longitudinal study," *Spinal Cord*, vol. 43, no. 12, pp. 704–712, 2005, doi: 10.1038/sj.sc.3101777.

[6] L. H. van der Woude, H. E. Veeger, A. J. Dallmeijer, T. W. Janssen, and L. A. Rozendaal, "Biomechanics and physiology in active manual wheelchair propulsion," *Medical Engineering & Physics*, vol. 23, no. 10, pp. 713–733, 2001, doi: 10.1016/S1350-4533(01)00083-2.

[7] M. L. Boninger, A. L. Souza, R. A. Cooper, S. G. Fitzgerald, A. M. Koontz, and B. T. Fay, "Propulsion patterns and pushrim biomechanics in manual wheelchair propulsion," *Archives of physical medicine and rehabilitation*, vol. 83, no. 5, pp. 718–723, 2002, doi: 10.1053/apmr.2002.32455.

[8] J. L. Mercer, M. Boninger, A. Koontz, D. Ren, T. Dyson-Hudson, and R. Cooper, "Shoulder joint kinetics and pathology in manual wheelchair users," *Clinical Biomechanics*, vol. 21, no. 8, pp. 781–789, 2006, doi: 10.1016/j.clinbiomech.2006.04.010.

[9] U. Arnet, S. van Drongelen, A. Scheel-Sailer, L. H. V. van der Woude, and D. H. E. J. Veeger, "Shoulder load during synchronous handcycling and handrim wheelchair propulsion in persons with paraplegia," *Journal of Rehabilitation Medicine*, vol. 44, no. 3, pp. 222–228, 2012, doi: 10.2340/16501977-0929.

[10] U. Arnet, S. van Drongelen, D. H. Veeger, and H. V. van der Woude L, "Force application during handcycling and handrim wheelchair propulsion: an initial comparison," *Journal of applied biomechanics*, vol. 29, no. 6, pp. 687–695, 2013, doi: 10.1123/jab.29.6.687.

[11] S. de Groot *et al.,* "Course of gross mechanical efficiency in handrim wheelchair propulsion during rehabilitation of people with spinal cord injury: a prospective cohort study," *Archives of physical medicine and rehabilitation*, vol. 86, no. 7, pp. 1452–1460, 2005, doi: 10.1016/j.apmr.2004.11.025.

[12] L. A. Zukowski, J. A. Roper, O. Shechtman, D. M. Otzel, J. Bouwkamp, and M. D. Tillman, "Comparison of metabolic cost, performance, and efficiency of propulsion using an ergonomic hand drive mechanism and a conventional manual wheelchair," *Archives of physical medicine and rehabilitation*, vol. 95, no. 3, pp. 546–551, 2014, doi: 10.1016/j.apmr.2013.08.238.

Die approbierte gedruckte Originalversion dieser Dissertation ist an der TU Wien Bibliothek verfügbar.
The approved original version of this doctoral thesis is available in print at TU Wien Bibliothek.
TU WIEN Bibliothek Your knowledge hub

[13] C. L. Flemmer and R. C. Flemmer, “A review of manual wheelchairs,” *Disability and rehabilitation. Assistive technology*, vol. 11, no. 3, pp. 177–187, 2016, doi: 10.3109/17483107.2015.1099747.

[14] P. S. Requejo *et al.,* “Shoulder muscular demand during lever-activated vs pushrim wheelchair propulsion in persons with spinal cord injury,” *The journal of spinal cord medicine*, vol. 31, no. 5, pp. 568–577, 2008, doi: 10.1080/10790268.2008.11754604.

[15] A. Rifai Sarraj *et al.,* “Evaluation of a wheelchair prototype with non-conventional, manual propulsion,” *Annals of physical and rehabilitation medicine*, vol. 53, no. 2, pp. 105–117, 2010, doi: 10.1016/j.rehab.2009.12.001.

[16] J. Lui, M. K. MacGillivray, A. W. Sheel, J. Jeyasurya, M. Sadeghi, and B. J. Sawatzky, “Mechanical efficiency of two commercial lever-propulsion mechanisms for manual wheelchair locomotion,” *Journal of rehabilitation research and development*, vol. 50, no. 10, pp. 1363–1372, 2013, doi: 10.1682/JRRD.2013.02.0034.

[17] L. H. V. van der Woude, S. de Groot, and T. W. J. JANSSEN, “Manual wheelchairs: Research and innovation in rehabilitation, sports, daily life and health,” *Medical Engineering & Physics*, vol. 28, no. 9, pp. 905–915, 2006, doi: 10.1016/j.medengphy.2005.12.001.

[18] J. Verellen, D. Theisen, and Y. Vanlandewijck, “Influence of crank rate in hand cycling,” *Medicine & Science in Sports & Exercise*, vol. 36, no. 10, pp. 1826–1831, 2004, doi: 10.1249/01.mss.0000142367.04918.5a.

[19] A. J. Dallmeijer, I. D. B. Zentgraaff, N. I. Zijp, and L. H. V. van der WOUDE, “Submaximal physical strain and peak performance in handcycling versus handrim wheelchair propulsion,” *Spinal Cord*, vol. 42, no. 2, pp. 91–98, 2004, doi: 10.1038/sj.sc.3101566.

[20] C. Kraaijenbrink, R. J. K. Vegter, A. H. R. Hensen, H. Wagner, and L. H. V. van der Woude, “Different cadences and resistances in sub-maximal synchronous handcycling in able-bodied men: Effects on efficiency and force application,” *PloS one*, vol. 12, no. 8, 1-15(e0183502), 2017, doi: 10.1371/journal.pone.0183502.

[21] L. H. van der Woude, I. Bosmans, B. Bervoets, and H. E. Veeger, “Handcycling: different modes and gear ratios,” *Journal of Medical Engineering & Technology*, vol. 24, no. 6, pp. 242–249, 2000, doi: 10.1080/030919000300037168.

[22] A. J. Dallmeijer, L. Ottjes, E. de Waardt, and L. H. V. van der WOUDE, “A physiological comparison of synchronous and asynchronous hand cycling,” *International Journal of Sports Medicine*, vol. 25, no. 8, pp. 622–626, 2004, doi: 10.1055/s-2004-817879.

[23] P. A. Smith, R. M. Glaser, J. S. Petrofsky, P. D. Underwood, G. B. Smith, and J. J. Richard, “Arm crank vs handrim wheelchair propulsion: metabolic and cardiopulmonary responses,” *Archives of physical medicine and rehabilitation*, vol. 64, no. 6, pp. 249–254, 1983.

[24] G. Mukherjee and A. Samanta, “Physiological response to the ambulatory performance of hand-rim and arm-crank propulsion systems,” *The Journal of Rehabilitation Research and Development*, vol. 38, no. 4, pp. 391–399, 2001.

[25] N. B. R. Kurup, “Novel handle based propulsion mechanism for wheelchair: Using forward dynamic optimization and kinematic-kinetic analysis,” Dissertation, Institut für Konstruktionswissenschaften, TU Wien, Wien, 2020. [Online]. Available: http:// hdl.handle.net/20.500.12708/78722

[26] M. Puchinger, N. B. R. Kurup, and M. Gföhler, “A Test Rig for Investigating Manual Wheelchair Propulsion Devices: TAR 2017 - Technically Assisted Rehabilitation - March 09-10, 2017,” *Current Directions in Biomedical Engineering*, vol. 3, no. 1, 12, 2017, doi: 10.1515/cdbme-2017-1001.

Die approbierte gedruckte Originalversion dieser Dissertation ist an der TU Wien Bibliothek verfügbar.
The approved original version of this doctoral thesis is available in print at TU Wien Bibliothek.
TU Bibliothek Your knowledge hub WIEN

[27] R. A. Cooper, “SMARTWheel: From concept to clinical practice,” *Prosthetics and orthotics international*, vol. 33, no. 3, pp. 198–209, 2009, doi: 10.1080/03093640903082126.
[28] Florian Stadler, “Entwicklung eines Sensorgriffes zu Erfassung der auftretenden Kräfte an der Hand bei Benutzung eines alternativen Rollstuhlantriebssystem,” Diplomarbeit, Institut für Konstruktionswissenschaften und Technische Logistik, TU Wien, Wien, 2015.
[29] S. S. Rao, E. L. Bontrager, J. K. Gronley, C. J. Newsam, and J. Perry, “Three-dimensional kinematics of wheelchair propulsion,” *IEEE Transactions on Rehabilitation Engineering*, vol. 4, no. 3, pp. 152–160, 1996, doi: 10.1109/86.536770.
[30] S. Wei, S.-L. Huang, C.-J. Jiang, and J.-C. Chiu, “Wrist kinematic characterization of wheelchair propulsion in various seating positions: implication to wrist pain,” *Clinical Biomechanics*, vol. 18, no. 6, S46-52, 2003, doi: 10.1016/S0268-0033(03)00084-6.
[31] Á. Gil-Agudo *et al.,* “Echographic and kinetic changes in the shoulder joint after manual wheelchair propulsion under two different workload settings,” *Frontiers in Bioengineering and Biotechnology*, vol. 2, p. 77, 2014, doi: 10.3389/fbioe.2014.00077.
[32] G. Desroches, R. Dumas, D. Pradon, P. Vaslin, F.-X. Lepoutre, and L. Chèze, “Upper limb joint dynamics during manual wheelchair propulsion,” *Clinical biomechanics (Bristol, Avon)*, vol. 25, no. 4, pp. 299–306, 2010, doi: 10.1016/j.clinbiomech.2009.12.011.
[33] I. M. Russell, S. Raina, P. S. Requejo, R. R. Wilcox, S. Mulroy, and J. L. McNitt-Gray, “Modifications in Wheelchair Propulsion Technique with Speed,” *Frontiers in Bioengineering and Biotechnology*, vol. 3, p. 171, 2015, doi: 10.3389/fbioe.2015.00171.
[34] C. Jayaraman, C. L. Beck, and J. J. Sosnoff, “Shoulder pain and jerk during recovery phase of manual wheelchair propulsion,” *Journal of Biomechanics*, vol. 48, no. 14, pp. 3937–3944, 2015, doi: 10.1016/j.jbiomech.2015.09.018.
[35] A. M. Koontz, R. A. Cooper, M. L. Boninger, A. L. Souza, and B. T. Fay, “Shoulder kinematics and kinetics during two speeds of wheelchair propulsion,” *The Journal of Rehabilitation Research and Development*, vol. 39, no. 6, pp. 635–649, 2002.
[36] A. M. Kwarciak, S. A. Sisto, M. Yarossi, R. Price, E. Komaroff, and M. L. Boninger, “Redefining the manual wheelchair stroke cycle: identification and impact of nonpropulsive pushrim contact,” *Archives of physical medicine and rehabilitation*, vol. 90, no. 1, pp. 20–26, 2009, doi: 10.1016/j.apmr.2008.07.013.
[37] U. Arnet, S. van Drongelen, L. H. V. van der Woude, and D. H. E. J. Veeger, “Shoulder load during handcycling at different incline and speed conditions,” *Clinical biomechanics (Bristol, Avon)*, vol. 27, no. 1, pp. 1–6, 2012, doi: 10.1016/j.clinbiomech.2011.07.002.
[38] M. M. Morrow, J. W. Rankin, R. R. NEPTUNE, and K. R. Kaufman, “A comparison of static and dynamic optimization muscle force predictions during wheelchair propulsion,” *Journal of Biomechanics*, vol. 47, no. 14, pp. 3459–3465, 2014, doi: 10.1016/j.jbiomech.2014.09.013.
[39] J. W. Rankin and R. R. NEPTUNE, “Musculotendon lengths and moment arms for a three-dimensional upper-extremity model,” *Journal of Biomechanics*, vol. 45, no. 9, pp. 1739–1744, 2012, doi: 10.1016/j.jbiomech.2012.03.010.
[40] J. W. Rankin, A. M. Kwarciak, W. M. Richter, and R. R. NEPTUNE, “The influence of wheelchair propulsion technique on upper extremity muscle demand: a simulation study,” *Clinical biomechanics (Bristol, Avon)*, vol. 27, no. 9, pp. 879–886, 2012, doi: 10.1016/j.clinbiomech.2012.07.002.
[41] J. S. Slowik, J. L. McNitt-Gray, P. S. Requejo, S. J. Mulroy, and R. R. NEPTUNE, “Compensatory strategies during manual wheelchair propulsion in response to

Die approbierte gedruckte Originalversion dieser Dissertation ist an der TU Wien Bibliothek verfügbar.
The approved original version of this doctoral thesis is available in print at TU Wien Bibliothek.
TU WIEN Bibliothek Your knowledge hub

weakness in individual muscle groups: A simulation study," *Clinical biomechanics (Bristol, Avon)*, vol. 33, pp. 34–41, 2016, doi: 10.1016/j.clinbiomech.2016.02.003.

[42] S. A. Kautz and M. L. Hull, "Dynamic optimization analysis for equipment setup problems in endurance cycling," *Journal of Biomechanics*, vol. 28, no. 11, pp. 1391–1401, 1995, doi: 10.1016/0021-9290(95)00007-5.

[43] J. W. Rankin and R. R. Neptune, "A theoretical analysis of an optimal chainring shape to maximize crank power during isokinetic pedaling," *Journal of Biomechanics*, vol. 41, no. 7, pp. 1494–1502, 2008, doi: 10.1016/j.jbiomech.2008.02.015.

[44] S. L. Delp *et al.,* "OpenSim: open-source software to create and analyze dynamic simulations of movement," *IEEE Transactions on Biomedical Engineering*, vol. 54, no. 11, pp. 1940–1950, 2007, doi: 10.1109/TBME.2007.901024.

[45] K. R. Saul *et al.,* "Benchmarking of dynamic simulation predictions in two software platforms using an upper limb musculoskeletal model," *Computer methods in biomechanics and biomedical engineering*, vol. 18, no. 13, pp. 1445–1458, 2015, doi: 10.1080/10255842.2014.916698.

[46] K. R. S. Holzbaur, W. M. Murray, and S. L. Delp, "A model of the upper extremity for simulating musculoskeletal surgery and analyzing neuromuscular control," *Annals of Biomedical Engineering*, vol. 33, no. 6, pp. 829–840, 2005, doi: 10.1007/s10439-005-3320-7.

[47] D. G. Thelen, "Adjustment of muscle mechanics model parameters to simulate dynamic contractions in older adults," *Journal of Biomechanical Engineering*, vol. 125, no. 1, pp. 70–77, 2003, doi: 10.1115/1.1531112.

[48] E. M. Arnold and S. L. Delp, "Fibre operating lengths of human lower limb muscles during walking," *Philosophical Transactions of the Royal Society B: Biological Sciences*, vol. 366, no. 1570, pp. 1530–1539, 2011, doi: 10.1098/rstb.2010.0345.

[49] J. W. Rankin, A. M. Kwarciak, W. Mark Richter, and R. R. NEPTUNE, "The influence of altering push force effectiveness on upper extremity demand during wheelchair propulsion," *Journal of Biomechanics*, vol. 43, no. 14, pp. 2771–2779, 2010, doi: 10.1016/j.jbiomech.2010.06.020.

[50] M. Sharif Shourijeh and J. McPhee, "Forward Dynamic Optimization of Human Gait Simulations: A Global Parameterization Approach," *Journal of Computational and Nonlinear Dynamics*, vol. 9, no. 3, 2014, doi: 10.1115/1.4026266.

[51] *Hairer E, Nørsett SP, Wanner G. 2008. Solving Ordinary Differential Equations I: Nonstiff Problems.Springer Science & Business Media*.

[52] D. H. von Seggern, *CRC Standard Curves and Surfaces with Mathematica, Second Edition,* 2nd ed. Boca Raton: Chapman & Hall/CRC, 2007.

[53] S. J. Mulroy, J. K. Gronley, C. J. Newsam, and J. Perry, "Electromyographic activity of shoulder muscles during wheelchair propulsion by paraplegic persons," *Archives of physical medicine and rehabilitation*, vol. 77, no. 2, pp. 187–193, 1996, doi: 10.1016/S0003-9993(96)90166-5.

[54] V. L. Goosey, I. G. Campbell, and N. E. Fowler, "Effect of push frequency on the economy of wheelchair racers," *Medicine & Science in Sports & Exercise*, vol. 32, no. 1, pp. 174–181, 2000, doi: 10.1097/00005768-200001000-00026.

[55] W. M. Richter, R. Rodriguez, K. R. Woods, and P. W. Axelson, "Stroke pattern and handrim biomechanics for level and uphill wheelchair propulsion at self-selected speeds," *Archives of physical medicine and rehabilitation*, vol. 88, no. 1, pp. 81–87, 2007, doi: 10.1016/j.apmr.2006.09.017.

Die approbierte gedruckte Originalversion dieser Dissertation ist an der TU Wien Bibliothek verfügbar.
The approved original version of this doctoral thesis is available in print at TU Wien Bibliothek.
TU WIEN Bibliothek Your knowledge hub

[56] Y. Vanlandewijck, D. Theisen, and D. Daly, “Wheelchair propulsion biomechanics: implications for wheelchair sports,” *Sports Medicine*, vol. 31, no. 5, pp. 339–367, 2001, doi: 10.2165/00007256-200131050-00005.

[57] P. Schantz, P. Björkman, M. Sandberg, and E. Andersson, “Movement and muscle activity pattern in wheelchair ambulation by persons with para-and tetraplegia,” *Scandinavian Journal of Rehabilitation Medicine*, vol. 31, no. 2, pp. 67–76, 1999, doi: 10.1080/003655099444560.

[58] J. W. Rankin, W. M. Richter, and R. R. NEPTUNE, “Individual muscle contributions to push and recovery subtasks during wheelchair propulsion,” *Journal of Biomechanics*, vol. 44, no. 7, pp. 1246–1252, 2011, doi: 10.1016/j.jbiomech.2011.02.073.

[59] M. G. Pandy, F. C. Anderson, and D. G. Hull, “A parameter optimization approach for the optimal control of large-scale musculoskeletal systems,” *Journal of Biomechanical Engineering*, vol. 114, no. 4, pp. 450–460, 1992, doi: 10.1115/1.2894094.

[60] J.-T. Lin, M. Huang, and S. Sprigle, “Evaluation of wheelchair resistive forces during straight and turning trajectories across different wheelchair configurations using free-wheeling coast-down test,” *Journal of rehabilitation research and development*, vol. 52, no. 7, pp. 763–774, 2015, doi: 10.1682/JRRD.2014.10.0235.

[61] J. H. Bednarczyk and D. J. Sanderson, “Limitations of kinematics in the assessment of wheelchair propulsion in adults and children with spinal cord injury,” *Physical Therapy*, vol. 75, no. 4, pp. 281–289, 1995, doi: 10.1093/ptj/75.4.281.

[62] J. S. Slowik, P. S. Requejo, S. J. Mulroy, and R. R. NEPTUNE, “The influence of wheelchair propulsion hand pattern on upper extremity muscle power and stress,” *Journal of Biomechanics*, vol. 49, no. 9, pp. 1554–1561, 2016, doi: 10.1016/j.jbiomech.2016.03.031.

[63] F. Ambrosio, M. L. Boninger, A. L. Souza, S. G. Fitzgerald, A. M. Koontz, and R. A. Cooper, “Biomechanics and strength of manual wheelchair users,” *The journal of spinal cord medicine*, vol. 28, no. 5, pp. 407–414, 2005, doi: 10.1080/10790268.2005.11753840.

[64] N. Babu Rajendra Kurup, M. Puchinger, and M. Gföhler, “Forward dynamic optimization of handle path and muscle activity for handle based isokinetic wheelchair propulsion: A simulation study,” *Computer methods in biomechanics and biomedical engineering*, vol. 22, no. 1, pp. 55–63, 2019, doi: 10.1080/10255842.2018.1527321.

[65] A. Faupin, P. Gorce, C. Meyer, and A. Thevenon, “Effects of backrest positioning and gear ratio on nondisabled subjects' handcycling sprinting performance and kinematics,” *Journal of rehabilitation research and development*, vol. 45, no. 1, pp. 109–116, 2008, doi: 10.1682/JRRD.2006.10.0139.

[66] S. L. Soltau, J. S. Slowik, P. S. Requejo, S. J. Mulroy, and R. R. NEPTUNE, “An Investigation of Bilateral Symmetry During Manual Wheelchair Propulsion,” *Frontiers in Bioengineering and Biotechnology*, vol. 3, p. 86, 2015, doi: 10.3389/fbioe.2015.00086.

[67] Pouran D Faghri, Kamyar Momeni, “Aging and Muscle Activity Patterns during Cycling,” *Int J Phys Med Rehabil*, vol. 03, no. 05, 2015, doi: 10.4172/2329-9096.1000307.

[68] S. Suzuki, S. Watanabe, and S. Homma, “EMG activity and kinematics of human cycling movements at different constant velocities,” *Brain Research*, vol. 240, no. 2, pp. 245–258, 1982, doi: 10.1016/0006-8993(82)90220-7.

[69] H. E. Veeger, E. M. Lute, K. Roeleveld, and L. H. van der Woude, “Differences in performance between trained and untrained subjects during a 30-s sprint test in a wheelchair ergometer,” *European Journal of Applied Physiology and Occupational Physiology*, vol. 64, no. 2, pp. 158–164, 1992, doi: 10.1007/BF00717954.

Die approbierte gedruckte Originalversion dieser Dissertation ist an der TU Wien Bibliothek verfügbar.
The approved original version of this doctoral thesis is available in print at TU Wien Bibliothek.
TU WIEN Bibliothek Your knowledge hub

[70] W. M. Keyserling, D. S. Stetson, B. A. Silverstein, and M. L. Brouwer, “A checklist for evaluating ergonomic risk factors associated with upper extremity cumulative trauma disorders,” *Ergonomics*, vol. 36, no. 7, pp. 807–831, 1993, doi: 10.1080/00140139308967945.

[71] D. H. Veeger, L. A. Rozendaal, and F. C. T. van der Helm, “Load on the shoulder in low intensity wheelchair propulsion,” *Clinical Biomechanics*, vol. 17, no. 3, pp. 211–218, 2002, doi: 10.1016/S0268-0033(02)00008-6.

[72] A. M. Koontz *et al.,* “Investigation of the performance of an ergonomic handrim as a pain-relieving intervention for manual wheelchair users,” *Assistive technology : the official journal of RESNA*, vol. 18, no. 2, 123-43; quiz 145, 2006, doi: 10.1080/10400435.2006.10131912.

[73] J. L. Collinger *et al.,* “Shoulder biomechanics during the push phase of wheelchair propulsion: a multisite study of persons with paraplegia,” *Archives of physical medicine and rehabilitation*, vol. 89, no. 4, pp. 667–676, 2008, doi: 10.1016/j.apmr.2007.09.052.

[74] A. Gil-Agudo, A. Del Ama-Espinosa, E. Pérez-Rizo, S. Pérez-Nombela, and B. Crespo-Ruiz, “Shoulder joint kinetics during wheelchair propulsion on a treadmill at two different speeds in spinal cord injury patients,” *Spinal Cord*, vol. 48, no. 4, pp. 290–296, 2010, doi: 10.1038/sc.2009.126.

[75] McLaurin, “Lever drive system for wheelchairs,” *J Rehabil Res Develop*, vol. 23, p. 52, 1986.

[76] A. R. Sarraj and R. Massarelli, “Design History and Advantages of a New Lever-Propelled Wheelchair Prototype,” *International Journal of Advanced Robotic Systems*, vol. 8, no. 3, p. 26, 2011, doi: 10.5772/10669.

[77] J. Rasmussen, S. T. Christensen, M. Gföhler, M. Damsgaard, and T. Angeli, “Design optimization of a pedaling mechanism for paraplegics,” *Struct Multidisc Optim*, vol. 26, 1-2, pp. 132–138, 2004, doi: 10.1007/s00158-003-0324-5.

[78] N. B. R. Kurup, M. Puchinger, T. Keck, and M. Gfoehler, “Wrist Kinematics and Kinetics during Wheelchair Propulsion with a Novel Handle-based Propulsion Mechanism,” *Annual International Conference of the IEEE Engineering in Medicine and Biology Society. IEEE Engineering in Medicine and Biology Society. Annual International Conference*, vol. 2018, pp. 2146–2149, 2018, doi: 10.1109/EMBC.2018.8512658.

[79] N. Babu Rajendra Kurup, M. Puchinger, and M. Gfoehler, “A preliminary muscle activity analysis: Handle based and push-rim wheelchair propulsion,” *Journal of Biomechanics*, vol. 89, pp. 119–122, 2019, doi: 10.1016/j.jbiomech.2019.04.011.

[80] M. L. Boninger, R. A. Cooper, R. N. Robertson, and S. D. Shimada, “Three-dimensional pushrim forces during two speeds of wheelchair propulsion,” *American journal of physical medicine & rehabilitation*, vol. 76, no. 5, pp. 420–426, 1997, doi: 10.1097/00002060-199709000-00013.

[81] B. Odle, J. Reinbolt, G. Forrest, and T. Dyson-Hudson, “Construction and evaluation of a model for wheelchair propulsion in an individual with tetraplegia,” *Medical & Biological Engineering & Computing*, vol. 57, no. 2, pp. 519–532, 2019, doi: 10.1007/s11517-018-1895-z.

[82] B. Odle, G. Forrest, J. Reinbolt, and T. Dyson-Hudson, “Development of an OpenSim Shoulder Model for Manual Wheelchair Users With Tetraplegia,” in 2011.

[83] G. Wu *et al.,* “ISB recommendation on definitions of joint coordinate systems of various joints for the reporting of human joint motion--Part II: shoulder, elbow, wrist and hand,” *Journal of Biomechanics*, vol. 38, no. 5, pp. 981–992, 2005, doi: 10.1016/j.jbiomech.2004.05.042.

Die approbierte gedruckte Originalversion dieser Dissertation ist an der TU Wien Bibliothek verfügbar.
The approved original version of this doctoral thesis is available in print at TU Wien Bibliothek.
TU WIEN Bibliothek Your knowledge hub

[84] K. R. Saul, S. Hayon, T. L. Smith, C. J. Tuohy, and S. Mannava, “Postural dependence of passive tension in the supraspinatus following rotator cuff repair: a simulation analysis,” *Clinical biomechanics (Bristol, Avon)*, vol. 26, no. 8, pp. 804–810, 2011, doi: 10.1016/j.clinbiomech.2011.04.005.

[85] J. W. Wannop, J. T. Worobets, and D. J. Stefanyshyn, “Normalization of ground reaction forces, joint moments, and free moments in human locomotion,” *Journal of applied biomechanics*, vol. 28, no. 6, pp. 665–676, 2012, doi: 10.1123/jab.28.6.665.

[86] M. P. Kadaba, H. K. Ramakrishnan, M. E. Wootten, J. Gainey, G. Gorton, and G. V. Cochran, “Repeatability of kinematic, kinetic, and electromyographic data in normal adult gait,” *Journal of orthopaedic research : official publication of the Orthopaedic Research Society*, vol. 7, no. 6, pp. 849–860, 1989, doi: 10.1002/jor.1100070611.

[87] M. L. Boninger, R. A. Cooper, S. D. Shimada, and T. E. Rudy, “Shoulder and elbow motion during two speeds of wheelchair propulsion: a description using a local coordinate system,” *Spinal Cord*, vol. 36, no. 6, pp. 418–426, 1998, doi: 10.1038/sj.sc.3100588.

[88] M. L. Boninger, R. A. Cooper, R. N. Robertson, and T. E. Rudy, “Wrist biomechanics during two speeds of wheelchair propulsion: an analysis using a local coordinate system,” *Archives of physical medicine and rehabilitation*, vol. 78, no. 4, pp. 364–372, 1997, doi: 10.1016/S0003-9993(97)90227-6.

[89] H. E. Veeger, L. S. Meershoek, L. H. van der Woude, and J. M. Langenhoff, “Wrist motion in handrim wheelchair propulsion,” *The Journal of Rehabilitation Research and Development*, vol. 35, no. 3, pp. 305–313, 1998.

[90] L. H. van der Woude, G. de GROOT, A. P. Hollander, G. J. van Ingen Schenau, and R. H. ROZENDAL, “Wheelchair ergonomics and physiological testing of prototypes,” *Ergonomics*, vol. 29, no. 12, pp. 1561–1573, 1986, doi: 10.1080/00140138608967269.

[91] L. H. van der Woude, H. E. Veeger, R. H. ROZENDAL, and A. J. Sargeant, “Optimum cycle frequencies in hand-rim wheelchair propulsion. Wheelchair propulsion technique,” *European Journal of Applied Physiology and Occupational Physiology*, vol. 58, no. 6, pp. 625–632, 1989, doi: 10.1007/BF00418509.

[92] K. A. M. Samuelsson, H. Tropp, and B. Gerdle, “Shoulder pain and its consequences in paraplegic spinal cord-injured, wheelchair users,” *Spinal Cord*, vol. 42, no. 1, pp. 41–46, 2004, doi: 10.1038/sj.sc.3101490.

[93] C. E. Beekman, L. Miller-Porter, and M. Schoneberger, “Energy Cost of Propulsion in Standard and Ultralight Wheelchairs in People With Spinal Cord Injuries,” *Physical Therapy*, vol. 79, no. 2, pp. 146–158, 1999, doi: 10.1093/ptj/79.2.146.

[94] M. T. Hopman, W. M. van Teeffelen, J. Brouwer, S. Houtman, and R. A. Binkhorst, “Physiological responses to asynchronous and synchronous arm-cranking exercise,” *European Journal of Applied Physiology and Occupational Physiology*, vol. 72, 1-2, pp. 111–114, 1995, doi: 10.1007/BF00964124.

[95] M. Puchinger, P. Stefanek, K. Gstaltner, M. G. Pandy, and M. Gfohler, “In Vivo Biomechanical Assessment of a Novel Handle-Based Wheelchair Drive,” *IEEE transactions on neural systems and rehabilitation engineering : a publication of the IEEE Engineering in Medicine and Biology Society*, vol. 29, pp. 1669–1678, 2021, doi: 10.1109/TNSRE.2021.3105388.

[96] L. J. M. Valent *et al.,* “Effects of hand cycle training on physical capacity in individuals with tetraplegia: a clinical trial,” *Physical Therapy*, vol. 89, no. 10, pp. 1051–1060, 2009, doi: 10.2522/ptj.20080340.

[97] L. GARBY and A. ASTRUP, “The relationship between the respiratory quotient and the energy equivalent of oxygen during simultaneous glucose and lipid oxidation and

Die approbierte gedruckte Originalversion dieser Dissertation ist an der TU Wien Bibliothek verfügbar.
The approved original version of this doctoral thesis is available in print at TU Wien Bibliothek.
TU WIEN Bibliothek Your knowledge hub

lipogenesis," *Acta Physiologica Scandinavica*, vol. 129, no. 3, pp. 443–444, 1987, doi: 10.1111/j.1365-201X.1987.tb10613.x.

[98] M. N. Sawka, R. M. Glaser, S. W. Wilde, and T. C. von Luhrte, "Metabolic and circulatory responses to wheelchair and arm crank exercise," *Journal of applied physiology: respiratory, environmental and exercise physiology*, vol. 49, no. 5, pp. 784–788, 1980, doi: 10.1152/jappl.1980.49.5.784.

[99] H. Tropp, K. Samuelsson, and L. Jorfeldt, "Power output for wheelchair driving on a treadmill compared with arm crank ergometry," *British Journal of Sports Medicine*, vol. 31, no. 1, pp. 41–44, 1997, doi: 10.1136/bjsm.31.1.41.

[100] R. M. Glaser, M. N. Sawka, M. F. Brune, and S. W. Wilde, "Physiological responses to maximal effort wheelchair and arm crank ergometry," *Journal of applied physiology: respiratory, environmental and exercise physiology*, vol. 48, no. 6, pp. 1060–1064, 1980, doi: 10.1152/jappl.1980.48.6.1060.

[101] T. J. McConnell, M. A. Horvat, T. A. Beutel-Horvat, and L. A. Golding, "Arm crank versus wheelchair treadmill ergometry to evaluate the performance of paraplegics," *Paraplegia*, vol. 27, no. 4, pp. 307–313, 1989, doi: 10.1038/sc.1989.46.

[102] G. Martel, L. Noreau, and J. Jobin, "Physiological responses to maximal exercise on arm cranking and wheelchair ergometer with paraplegics," *Paraplegia*, vol. 29, no. 7, pp. 447–456, 1991, doi: 10.1038/sc.1991.61.

[103] E. M. Gass, L. A. Harvey, and G. C. Gass, "Maximal physiological responses during arm cranking and treadmill wheelchair propulsion in T4-T6 paraplegic men," *Paraplegia*, vol. 33, no. 5, pp. 267–270, 1995, doi: 10.1038/sc.1995.60.

[104] G. J. Farkas, P. S. Gordon, A. M. Swartz, A. S. Berg, and D. R. Gater, "Influence of mid and low paraplegia on cardiorespiratory fitness and energy expenditure," *Spinal cord series and cases*, vol. 6, no. 1, pp. 1–10, 2020, doi: 10.1038/s41394-020-00363-5.

Die approbierte gedruckte Originalversion dieser Dissertation ist an der TU Wien Bibliothek verfügbar.
The approved original version of this doctoral thesis is available in print at TU Wien Bibliothek.
TU WIEN Bibliothek Your knowledge hub

Appendix

Die approbierte gedruckte Originalversion dieser Dissertation ist an der TU Wien Bibliothek verfügbar.
The approved original version of this doctoral thesis is available in print at TU Wien Bibliothek.
TU WIEN Bibliothek Your knowledge hub

Die approbierte gedruckte Originalversion dieser Dissertation ist an der TU Wien Bibliothek verfügbar.
The approved original version of this doctoral thesis is available in print at TU Wien Bibliothek.

Granted Patent

Mechanischer Rollstuhlantrieb und Rollstuhl mit einem solchen mechanischen Rollstuhlantrieb

English title: Mechanical Wheelchair Drive and Wheelchair having such a Mechanical Wheelchair Drive

Markus Puchinger, Nithin B. R. Kurup, Margit Gföhler

EP 3 823 576 B1, PCT/AT2019/060235, WO 2020/014720

*Registered: **16.07.2019**, Granted: 16.02.2022*

(19) Europäisches Patentamt
European Patent Office
Office européen des brevets

(11) **EP 3 823 576 B1**

(12) **EUROPÄISCHE PATENTSCHRIFT**

(45) Veröffentlichungstag und Bekanntmachung des Hinweises auf die Patenterteilung:
16.02.2022 Patentblatt 2022/07

(21) Anmeldenummer: **19745031.5**

(22) Anmeldetag: **16.07.2019**

(51) Internationale Patentklassifikation (IPC):
A61G 5/02 *(2006.01)*

(52) Gemeinsame Patentklassifikation (CPC):
A61G 5/023; A61G 5/026

(86) Internationale Anmeldenummer:
PCT/AT2019/060235

(87) Internationale Veröffentlichungsnummer:
WO 2020/014720 (23.01.2020 Gazette 2020/04)

(54) **MECHANISCHER ROLLSTUHLANTRIEB UND ROLLSTUHL MIT EINEM SOLCHEN MECHANISCHEN ROLLSTUHLANTRIEB**

MECHANICAL WHEELCHAIR DRIVE AND WHEELCHAIR HAVING SUCH A MECHANICAL WHEELCHAIR

ENTRAÎNEMENT MÉCANIQUE DE FAUTEUIL ROULANT ET FAUTEUIL ROULANT COMPRENANT UN TEL ENTRAÎNEMENT MÉCANIQUE DE FAUTEUIL ROULANT

(84) Benannte Vertragsstaaten:
AL AT BE BG CH CY CZ DE DK EE ES FI FR GB GR HR HU IE IS IT LI LT LU LV MC MK MT NL NO PL PT RO RS SE SI SK SM TR

(30) Priorität: **16.07.2018 AT 506092018**

(43) Veröffentlichungstag der Anmeldung:
26.05.2021 Patentblatt 2021/21

(73) Patentinhaber: **Technische Universität Wien**
1040 Wien (AT)

(72) Erfinder:
- **GFÖHLER, Margit**
  1040 Wien (AT)
- **KURUP, Nithin Babu Rajendra**
  1040 Wien (AT)
- **PUCHINGER, Markus**
  1040 Wien (AT)

(74) Vertreter: **SONN Patentanwälte OG**
Riemergasse 14
1010 Wien (AT)

(56) Entgegenhaltungen:
DE-U1- 8 803 670 US-B1- 6 910 701

Anmerkung: Innerhalb von neun Monaten nach Bekanntmachung des Hinweises auf die Erteilung des europäischen Patents im Europäischen Patentblatt kann jedermann nach Maßgabe der Ausführungsordnung beim Europäischen Patentamt gegen dieses Patent Einspruch einlegen. Der Einspruch gilt erst als eingelegt, wenn die Einspruchsgebühr entrichtet worden ist. (Art. 99(1) Europäisches Patentübereinkommen).

Printed by Jouve, 75001 PARIS (FR)

Die approbierte gedruckte Originalversion dieser Dissertation ist an der TU Wien Bibliothek verfügbar.
The approved original version of this doctoral thesis is available in print at TU Wien Bibliothek.
TU Bibliothek Your knowledge hub WIEN

Beschreibung

[0001] Die Erfindung betrifft einen mechanischen Rollstuhlantrieb mit einem drehbar gelagerten Hebel, einem an dem Hebel befestigten Griff und einer Kraftübertragungseinheit zur Übertragung einer Drehbewegung des Hebels auf ein Rollstuhlrad.

[0002] Da der mechanische Rollstuhlantrieb zur Montage an einem Rollstuhl geeignet ist, betrifft die Erfindung des Weiteren einen Rollstuhl mit einer Sitzfläche, einer Rückenlehne, Fußstützen und zumindest zwei Rollstuhlrädern.

[0003] Vielfach werden im Alltag eingesetzte Rollstühle von den beeinträchtigten Personen von Hand angetrieben. Zu diesem Zweck weisen die Rollstuhlräder typischerweise entlang ihres Umfangs leicht zu greifende Greifringe auf, mit deren Hilfe das jeweilige Rollstuhlrad direkt durch zug- bzw. stoßartige Bewegungen angetrieben und auch gebremst werden kann.

[0004] Auf Grund ihrer Wendigkeit und ihres geringen Gewichts sind mittels Greifring antreibbare Rollstühle vergleichsweise leicht im Alltag einsetzbar und stellen daher für viele Menschen mit Behinderung den bevorzugten Rollstuhltyp dar. Da diese Rollstühle mit Muskelkraft angetrieben werden, wird bei dieser Art der Fortbewegung zugleich auch die körperliche Fitness der beeinträchtigten Personen zumindest im Bereich des Oberkörpers erhalten bzw. verbessert.

[0005] Allerdings muss bei der Verwendung von Rollstühlen, die mittels Greifringen angetrieben werden, in Kauf genommen werden, dass der zum Antrieb erforderliche Bewegungsablauf die Gelenke der oberen Extremitäten stark belastet, was bei Personen, die regelmäßig auf die Benutzung eines Rollstuhles angewiesen sind, zu Langzeitschäden, chronischen Schmerzen oder sonstigen Beeinträchtigungen führen kann. Zudem werden durch den sich ständig wiederholenden Bewegungsablauf die Muskelgruppen im Schulter-, Oberarm- und Handgelenksbereich eher einseitig belastet und dadurch zusammenwirkende Muskeln (Agonisten und Antagonisten) ungleichmäßig beansprucht, was ebenfalls zu Beeinträchtigung oder chronischen Schmerzen führen kann. Dadurch kann die Bewegungsfreiheit der Personen, die ohnehin bereits auf einen Rollstuhl angewiesen sind, noch stärker eingeschränkt werden.

[0006] Neben diesen den Bewegungsapparat betreffenden Nachteilen hat sich darüber hinaus in Simulationen herausgestellt, dass der Bewegungsablauf zum Antreiben eines Rollstuhles mit Greifringen ineffizient ist, da ein beträchtlicher Teil der muskulären Antriebsleistung nicht auf die Rollstuhlräder übertragen wird.

[0007] Aus dem Stand der Technik sind zwar elektrische Rollstuhlantriebe bekannt, die einige der vorstehenden Nachteile vermeiden. Allerdings hängt deren Reichweite primär von der Kapazität der Energiespeicher ab und der elektrische Antrieb bringt nicht nur ein höheres Zusatzgewicht mit sich, sondern wirkt sich auch auf die Größe und damit auch auf die Wendigkeit des Rollstuhles negativ aus.

[0008] Daneben sind aus dem Stand der Technik, wie unter anderem aus der DE 3413312 A1, sogenannte Handhebelrollstühle bekannt, bei denen der Antrieb des Rollstuhles mittels eines verschwenkbaren Hebels erfolgt. Dabei werden zum Antrieb des Rollstuhls zwei im Wesentlichen senkrecht angeordnete Hebel nach vorne gedrückt bzw. verschwenkt und das erzeugte Drehmoment auf die Rollstuhlräder übertragen. Zum Rückstellen des Hebels ist dieser durch einen Freilaufmechanismus freigegeben.

[0009] Zwar ist diese Art des Antriebs für die Zurücklegung von weiten Strecken durchaus geeignet, jedoch ist die Wendigkeit auf Grund der Anordnung der Hebel eingeschränkt. Darüber hinaus muss der Hebel nach jeder Verschwenkung zurückgestellt werden, was keine kontinuierliche Antriebsbewegung erlaubt und die Handhabung erschwert. Weiters ist der zum Vortrieb nutzbare Winkelbereich des Hebels begrenzt, was sich in Kombination mit der erforderlichen Hebelrückstellung einschränkend auf die erreichbare Geschwindigkeit auswirkt.

[0010] Aus dem Sportbereich sind des Weiteren Rennrollstühle mit einem zusätzlichen Vorderrad bekannt, welches mit einer Handkurbel und einer Kette angetrieben wird. Allerdings sind diese Rennrollstühle wegen des zusätzlichen Vorderrades und der damit einhergehenden reduzierten Wendigkeit nicht alltagstauglich.

[0011] Darüber hinaus sind aus dem Stand der Technik Rollstühle mit Kurbelantrieben bekannt. Unter anderem zeigen die US 4,758,013 A, US 6,910,701 B1, WO 2004/110329 A1 und US 5,037,120 A solche Rollstühle, bei denen die Drehbewegung einer Kurbel mit Hilfe einer Kette auf das Rollstuhlrad übertragen wird. Nachteiligerweise ist der Kurbelantrieb nicht an die Körpergröße der antreibenden Person anpassbar.

[0012] Die WO 2014/199110 A1 offenbart ebenfalls einen Kurbelantrieb für einen Rollstuhl, welcher direkt im Mittelpunkt des Rollstuhlrades befestigbar ist und darüber hinaus über eine Gangschaltung verfügt. Der Hebel ist längenveränderbar, sodass der Benutzer in Kombination mit den unterschiedlichen Gängen die für ihn passende Einstellung finden kann. Nachteilig ist jedoch, dass durch die vergleichsweise tiefe Anordnung des Hebels nur wenig Muskelleistung auf die Rollstuhlräder übertragen werden kann und die Gelenke der oberen Extremitäten stark belastet werden.

[0013] Ein weiterer Rollstuhl ist aus DE 88 03 670 U1 bekannt.

[0014] Der Erfindung liegt somit die Aufgabe zugrunde, zumindest einzelne Nachteile des Standes der Technik zu reduzieren bzw. zur Gänze zu beseitigen. Die Erfindung setzt sich daher insbesondere zum Ziel, einen alltagstauglichen mechanischen Rollstuhlantrieb bzw. einen damit ausgestatteten Rollstuhl zu schaffen, der das Risiko von Langzeitschäden für Gelenke und Muskeln bei gleichzeitiger Erhöhung der Fortbewegungseffizienz minimiert. Die Erfindung ist in Anspruch 1 definiert.

Die approbierte gedruckte Originalversion dieser Dissertation ist an der TU Wien Bibliothek verfügbar.
The approved original version of this doctoral thesis is available in print at TU Wien Bibliothek.
TU Bibliothek Your knowledge hub WIEN

[0015] Die gestellte Aufgabe wird dabei dadurch gelöst, dass der Hebel längenveränderbar und entlang einer in sich geschlossenen und von der Kreisform abweichenden Führung einer Führungsplatte führbar ist, sodass eine Längenveränderung des Hebels während der Drehbewegung stattfindet. Dadurch wird bei dem erfindungsgemäßen Rollstuhlantrieb eine kontinuierliche, von der Kreisform abweichende und zugleich geführte Drehbewegung ermöglicht und auf das Rollstuhlrad übertragen, wodurch die Muskeln und Gelenke einer antreibenden Person weitgehend geschont werden und ein kontinuierlicher, d.h. im Wesentlichen ruckelfreier, Antrieb des Rollstuhls erfolgt. Der Erfindung liegt dabei die Erkenntnis zugrunde, dass eine von der Kreisform abweichende Führung des längenveränderbaren Hebels während der Drehbewegung eine im Vergleich zum Stand der Technik gleichmäßigere Beanspruchung sowohl der als Agonisten als auch der als Antagonisten wirkenden Muskeln der oberen Extremitäten bewirkt und die Gelenke weniger stark auslenkt. Insbesondere ist es durch die von der Kreisform abweichende Führung möglich, die beteiligten Muskeln und Gelenke nur innerhalb von Bereichen zu belasten und auszulenken, innerhalb deren keine (Langzeit-)Schäden auftreten. Vorzugsweise ist die Führung der Führungsplatte daher derart an die Gelenke einer Person angepasst, dass die Gelenke während der Drehbewegung möglichst gering ausgelenkt werden. Zu diesem Zweck kann die Führung derart ausgestaltet sein, dass der Hebel im Gebrauchszustand des Rollstuhlantriebs in einer im Wesentlichen parallelen Stellung zu einer Rückenlehne des Rollstuhls eine kürzere Länge aufweist als in einer Stellung im Wesentlichen senkrecht zur Rückenlehne des Rollstuhls. Für eine kontinuierliche Drehbewegung weist die Führung insbesondere keine Unstetigkeitsstellen auf. Um die Längenveränderbarkeit des Hebels zu ermöglichen, kann dieser teleskopartig ausgebildet sein oder zumindest zwei ineinander verschiebbare Schienenelemente aufweisen. Damit der Hebel während der Drehbewegung durch die Führung der Führungsplatte geführt werden kann, ist die Führung vorzugsweise als in sich geschlossene Kulissenführung ausgebildet, durch welche ein an dem Hebel befestigter Führungsstift geführt wird. Alternativ kann die Führung auch als in sich geschlossene Führungsschiene ausgebildet sein, durch welche ein an dem Hebel befestigter Führungsschlitten oder Haken geführt wird. Es versteht sich von selbst, dass der Führungsstift, der Führungsschlitten oder der Haken zur besseren Führung durch zusätzliche Lagerungsmittel gelagert sein können. "In sich geschlossen" bedeutet in diesem Zusammenhang, dass die Führung keinen Anfang und auch kein Ende aufweist und dadurch eine geschlossene Drehbewegung ermöglicht. Um während der Drehbewegung eine Änderung der Handstellung zu ermöglichen, ohne dabei den Griff freigeben zu müssen, ist der Griff an dem Hebel vorzugsweise drehbar befestigt. Die Führungsplatte ist im Gebrauchszustand des Rollstuhlantriebs im Wesentlichen senkrecht zu einer Sitzfläche des Rollstuhls angeordnet.

[0016] Um eine kompakte Ausführung des Rollstuhlantriebs zu ermöglichen, ist in einer bevorzugten Ausführungsform vorgesehen, dass der Hebel einen in einem Befestigungspunkt der Führungsplatte drehbar gelagerten Hebelteil und einen entlang der Führung geführten, ausziehbaren Hebelteil aufweist. Vorzugsweise ist der drehbar gelagerte Hebelteil in dem Befestigungspunkt über ein Kugellager oder ein Drehgelenk mit der Führungsplatte verbunden. Der drehbare bzw. der ausziehbare Hebelteil können insbesondere teleskop- oder schienenartig ineinander geschoben werden. Bevorzugt wird hierbei zur Minimierung der Reibung eine Linearführung mit Kugelumlauflagerung verwendet. Der Griff ist vorzugsweise an dem ausziehbaren Hebelteil befestigt.

[0017] Damit der Rollstuhlantrieb an die jeweilige Körpergröße der antreibenden Person angepasst werden kann, ist es günstig, wenn eine horizontale Justiereinrichtung zur verstellbaren Befestigung der Führungsplatte und des Hebels entlang einer Horizontalen vorgesehen ist. Dadurch ist es möglich, die Führungsplatte und den Hebel im Gebrauchszustand horizontal an verschiedenen Stellen zu befestigen. Eine Horizontale ist dabei eine im Gebrauchszustand des Rollstuhlantriebs zu einer Bodenfläche im Wesentlichen parallel verlaufende und in Fahrtrichtung des Rollstuhls weisende gedachte Linie. Die Befestigung kann dabei mit Hilfe von Befestigungsmitteln, wie beispielsweise Befestigungsstifte, Klammern oder Rasthaken, an dafür vorgesehenen Stellen erfolgen.

[0018] In einer bevorzugten Ausführungsform ist zudem eine vertikale Justiereinrichtung zur verstellbaren Befestigung der Führungsplatte und des Hebels entlang einer Vertikalen vorgesehen. Dadurch ist es möglich, die Führungsplatte und den Hebel im Gebrauchszustand vertikal an verschiedenen Stellen zu befestigen. Eine Vertikale ist dabei eine im Gebrauchszustand des Rollstuhlantriebs zu einer Bodenfläche im Wesentlichen senkrecht angeordnete gedachte Linie. Die Befestigung kann dabei mit Hilfe von Befestigungsmitteln, wie beispielsweise Befestigungsstifte, Klammern oder Rasthaken, an dafür vorgesehenen Stellen erfolgen.

[0019] Um die horizontale und/oder die vertikale Justiereinrichtung rasch und individuell einstellen zu können, ist es vorteilhaft, wenn die Justiereinrichtung eine Schiene mit Befestigungslöchern und einen entlang der Schiene gleitenden Schlitten mit einem Fixierstift aufweist, wobei der Fixierstift zur Fixierung des Schlittens in die Befestigungslöcher einführbar ist und die Führungsplatte und der Hebel mittelbar oder unmittelbar mit dem Schlitten verbunden sind. Dabei ist in einer besonders bevorzugten Ausführungsform vorgesehen, dass jeweils die vertikale und die horizontale Justiereinrichtung eine Schiene und einen Schlitten aufweisen und die vertikale Justiereinrichtung, insbesondere deren Schiene samt deren Schlitten, auf dem Schlitten der horizontalen Justiereinrichtung befestigt ist und die Führungs-

Die approbierte gedruckte Originalversion dieser Dissertation ist an der TU Wien Bibliothek verfügbar.
The approved original version of this doctoral thesis is available in print at TU Wien Bibliothek.
TU WIEN Bibliothek Your knowledge hub

platte und der Hebel auf dem Schlitten der vertikalen Justiereinrichtung befestigt ist. Dadurch ist im Gebrauchszustand des Rollstuhlantriebs eine Verstellbarkeit des Rollstuhlantriebs in einer Ebene senkrecht zu einer Bodenfläche gegeben. In dieser besonders bevorzugten Ausführungsform sind die Führungsplatte und der Hebel unmittelbar mit dem Schlitten der vertikalen Justiereinrichtung und mittelbar über den Schlitten und die Schiene der vertikalen Justiereinrichtung mit dem Schlitten der horizontalen Justiereinrichtung verbunden. Es ist auch denkbar, die Rollen der vertikalen und horizontalen Justiereinrichtung zu vertauschen, sodass die horizontale Justiereinrichtung, insbesondere deren Schiene samt deren Schlitten, auf dem Schlitten der vertikalen Justiereinrichtung befestigt ist und die Führungsplatte und der Hebel auf dem Schlitten der horizontalen Justiereinrichtung befestigt ist.

[0020] Um ein Rollstuhlrad auf besonders einfache Weise anzutreiben, ist in einer bevorzugten Ausführungsform vorgesehen, dass die Kraftübertragungseinheit durch einen Riemenantrieb gebildet wird. Dadurch kann auf ein kompliziertes und fehleranfälliges Getriebe mit Zahnrädern verzichtet und Verschleißteile einfach ausgetauscht werden.

[0021] Um die Baugröße des Rollstuhlantriebs gering zu halten, ist es günstig, wenn ein Riemen die Drehbewegung des Hebels über eine erste Rolle, insbesondere ein erstes Zahnriemenrad, aufnimmt und an eine zweite Rolle, insbesondere ein zweites Zahnriemenrad, zur Übertragung der Drehbewegung an ein Rollstuhlrad abgibt. Vorzugsweise wird der Riemen dabei durch ein in sich geschlossenes Band mit einer profilierten Innenseite, vorzugsweise einem Zahnriemen, gebildet. Die erste Rolle kann insbesondere direkt mit dem Hebel verdrehsicher verbunden sein und so die Drehbewegung des Hebels auf den Riemen übertragen. Die zweite Rolle ist ebenfalls mit dem Riemen verbunden und zur Übertragung der Drehbewegung an ein Rollstuhlrad eingerichtet, wobei die Kraftübertragung an das Rollstuhlrad vorzugsweise über einen Riementrieb mit Spannvorrichtung erfolgt. Bei der Übertragung der Drehbewegung des Hebels auf das Rollstuhlrad kann bei der ersten und/ oder der zweiten Rolle zusätzlich eine Übersetzung vorgesehen sein. Beispielsweise kann die zweite Rolle verdrehsicher mit einer Übersetzungsrolle verbunden sein, welche einen anderen Durchmesser aufweist und so den Riemen übersetzend mit dem Riementrieb bzw. direkt mit dem Rollstuhlrad verbindet, wobei der Riementrieb bzw. das Rollstuhlrad mit der Übersetzungsrolle in Kontakt ist.

[0022] Um einen möglichst kompakten Rollstuhlantrieb zu schaffen, sind in einer besonders bevorzugten Ausführungsform Umlenkrollen vorgesehen, sodass der Riemen im Wesentlichen entlang einer Außenseite des Rollstuhlantriebs, insbesondere entlang der Schienen, führbar ist. Diese Umlenkrollen sind, sofern Justiereinrichtungen vorhanden sind, insbesondere an den Schlitten angebracht.

[0023] Um insbesondere bei Bergabfahrten des Rollstuhls Verletzungen zu vermeiden, ist es günstig, wenn die Kraftübertragungseinheit einen vorzugsweise deaktivierbaren Freilaufmechanismus zur Übertragung der Drehbewegung des Hebels in nur eine Drehrichtung aufweist. Vorteilhafterweise entspricht die übertragene Drehrichtung des Hebels der Vorwärtsdrehrichtung des Rollstuhlrades im Gebrauchszustand. Durch den Freilaufmechanismus wird insbesondere bei geneigten Bodenflächen die Sicherheit erhöht, da in diesem Fall die Rotation des Rollstuhlrades nicht auf die Rotation des Hebels übertragen wird.

[0024] Um insbesondere bei Verwendung eines Freilaufmechanismus dennoch ein sicheres Bremsen des Rollstuhles zu ermöglichen, ist es vorteilhaft, wenn an dem Griff ein Betätigungshebel für eine Bremsvorrichtung des Rollstuhlrades vorgesehen ist. Der Betätigungshebel kann wiederum über einen Seilzug, einen Bowdenzug oder eine Hydraulikleitung mit einer Bremsvorrichtung des Rollstuhlrades verbunden sein. Die Bremsvorrichtung kann dabei beispielsweise eine Scheiben- oder Trommelbremse aufweisen.

[0025] Um bestehende Rollstühle mit dem erfindungsgemäßen Rollstuhlantrieb nachzurüsten, kann zumindest eine Befestigungsvorrichtung zur Befestigung an einem Rollstuhl, insbesondere an einer Armlehnenhalterung eines Rollstuhls, vorgesehen sein. Demnach kann der erfindungsgemäße Rollstuhlantrieb an Stelle einer Armlehne eines Rollstuhles befestigt werden.

[0026] Mit dem erfindungsgemäßen Rollstuhlantrieb werden insbesondere die zur Durchführung der Drehbewegung benötigten Gelenke und Muskeln der oberen Extremitäten geschont und die von den Muskeln erzeugte und auf die Rollstuhlräder übertragene Leistung optimiert bzw. erhöht. Um die Muskeln und Gelenke nur in jenen Bereichen, d.h. Streckungs- und Beugungswinkel, anzusprechen, die bei regelmäßiger Verwendung des Rollstuhlantriebs keine (dauerhaften) Schäden oder Schmerzen hervorrufen, ist es günstig, wenn die Führung einer im Wesentlichen tropfenförmigen geschlossenen Kurve mit einem breiten und einem schmalen Endkurvenbereich entspricht, wobei die Endkurvenbereiche jeweils einen Scheitelpunkt aufweisen und der schmale Endkurvenbereich der geschlossenen Kurve im montierten Zustand des Rollstuhlantriebs in Richtung einer Rückenlehne des Rollstuhles zeigt. Diese Kurvenform stellt das Ergebnis einer Optimierungsaufgabe dar, bei der die von der Muskulatur auf das Rollstuhlrad übertragene Leistung unter Reduzierung der Gelenksauslenkung maximiert wurde. Die Endkurvenbereiche können dabei durch Kreisbögen angenähert werden. Der schmale Endkurvenbereich der Kurve weist erfindungsgemäß einen kleineren angenäherten Kurvenradius auf als der breite Endkurvenbereich.

[0027] Eine besonders effiziente Kurvenform hinsichtlich der Kraftübertragung und der Gelenksschonung ergibt sich, wenn im montierten Zustand des Rollstuhlantriebs eine zwischen den Scheitelpunkten des breiten

Die approbierte gedruckte Originalversion dieser Dissertation ist an der TU Wien Bibliothek verfügbar.
The approved original version of this doctoral thesis is available in print at TU Wien Bibliothek.
TU WIEN Bibliothek Your knowledge hub

und des schmalen Endkurvenbereichs verlaufende Längsachse zumindest 5°, bevorzugt zumindest 10°, vorzugsweise im Wesentlichen 15°, aber nicht mehr als 30°, zur Horizontalen, insbesondere mit dem breiten Endkurvenbereich nach unten, geneigt ist. Im Gebrauchszustand ist daher der breite Endkurvenbereich vorzugsweise zu einer Bodenfläche hin geneigt.

[0028] Eine besonders günstige Ausführungsform ergibt sich, wenn die Kurve im Wesentlichen durch folgende mathematische Gleichungen beschreibbar ist:

$$X_1 = A\cos(\theta)$$

$$Y_1 = B\sin(\theta)\sin^n(0{,}5 * \theta)$$

$$\begin{pmatrix} X \\ Y \end{pmatrix} = \begin{pmatrix} \cos(\beta) & -\sin(\beta) \\ \sin(\beta) & \cos(\beta) \end{pmatrix} \begin{pmatrix} X_1 \\ Y_1 \end{pmatrix}$$

, wobei θ als Laufkoordinate einem Winkel entspricht, die Koordinaten X und Y den Verlauf der Führung in einem kartesischen Koordinatensystem beschreiben, der Parameter β zwischen -20° und 30°, die Parameter A und B zwischen 0,01 m und 0,25 m und der Parameter n zwischen 0,2 und 0,9 festgelegt werden. Die Laufkoordinate θ weist vorzugsweise Werte zwischen 0 und 2*π bzw. zwischen 0° und 360° auf. Die durch die angegebenen Gleichungen beschriebene Kurve entspricht im Wesentlichen einem besonders günstigen Verlauf der Führung. Dieser kann, je nach Betrachtungsweise, auch gespiegelt sein. Die tatsächliche Orientierung der durch die Kurve beschriebene Führung ist im montierten Zustand des Rollstuhlantriebs aber dergestalt, dass der schmale Endkurvenbereich in Richtung einer Rückenlehne des Rollstuhles zeigt und die Längsachse vorzugsweise mit dem breiten Endkurvenbereich nach unten, d.h. zu einer Bodenfläche hin, geneigt ist. Der Verlauf der Führung kann zweckmäßigerweise geringfügig von der durch die obigen Gleichungen beschriebenen Kurve abweichen, um beispielsweise Unstetigkeiten zu glätten. Insbesondere in dem schmalen Endkurvenbereich ist es für die Drehbewegung des Hebels günstig, wenn die Kurve bzw. die Führung abgeflacht ist.

[0029] Die eingangs gestellte Aufgabe wird zudem durch einen Rollstuhl gelöst, bei dem ein mechanischer Rollstuhlantrieb vorgesehen ist, der mit zumindest einem Rollstuhlrad verbunden ist und bei dem der Rollstuhlantrieb gemäß obiger Beschreibung ausgebildet ist.

[0030] In einer bevorzugten Ausführungsform ist vorgesehen, dass an dem Rollstuhl zwei Rollstuhlräder vorgesehen sind, die mit jeweils einem Rollstuhlantrieb verbunden sind.

[0031] Die Erfindung wird nachstehend anhand von bevorzugten Ausführungsformen weiter erläutert. Darin zeigen:

Fig. 1 einen erfindungsgemäßen Rollstuhlantrieb in einer Schrägansicht;

Fig. 2 eine Führungsplatte samt Führung und einen längenveränderbaren Hebel in seitlicher Ansicht;

Fig. 3 eine besonders bevorzugte Ausführungsform einer Kurve, durch welche die Führung beschrieben werden kann;

Fig. 4 einen Rollstuhl mit einem erfindungsgemäßen Rollstuhlantrieb; und

Fig. 5 einen Rollstuhl mit einem erfindungsgemäßen Rollstuhlantrieb in Explosionsdarstellung.

[0032] In Fig. 1 ist ein mechanischer Rollstuhlantrieb 1 für einen Rollstuhl 2 in einer bevorzugten Ausführungsform dargestellt. Der Rollstuhlantrieb 1 weist einen längenveränderbaren Hebel 3 auf, der aus einem drehbar gelagerten Hebelteil 4 und einem ausziehbaren Hebelteil 5 besteht, an welchen wiederum ein vorzugsweise drehbarer Griff 6 befestigt ist. Mittels einer Kraftübertragungseinheit 7 kann die Drehbewegung des Hebels 3 auf ein Rollstuhlrad 34 (nicht gezeigt) übertragen werden. Um den Rollstuhl zu bremsen, kann der Griff 6 einen Betätigungshebel 40 für eine Bremsvorrichtung 41 des Rollstuhlrades 34 aufweisen (vgl. Fig. 4). Der Betätigungshebel 40 kann dabei beispielsweise über einen Seilzug (nicht gezeigt) mit der Bremsvorrichtung 41 verbunden sein.

[0033] Um während der Drehbewegung eine Längenveränderung des Hebels 3 zu bewerkstelligen, ist der drehbar gelagerte Hebelteil 4 in einem Befestigungspunkt 10 einer Führungsplatte 9 drehbar gelagert und der ausziehbare Hebelteil 5 in einer in sich geschlossenen Führung 8 der Führungsplatte 9 geführt. Vorzugsweise wird die Führung 8 durch eine Kulissenführung 11 gebildet, in welcher ein am ausziehbaren Hebelteil 5 befestigter Führungsstift 12 gleitet. Alternativ kann die Führung 8 auch als in sich geschlossene Führungsschiene ausgebildet sein, an welcher ein an dem ausziehbaren Hebelteil 5 befestigter Führungsschlitten oder Haken entlanggleitet. Der der Führungsstift 12, der Führungsschlitten oder der Haken können zur besseren Führung durch zusätzliche Lagerungsmittel gelagert sein.

[0034] Um den Rollstuhlantrieb 1 an den jeweiligen Benutzer anpassen zu können, sind vorzugsweise eine horizontale Justiereinrichtung 13 und eine vertikale Justiereinrichtung 14 vorgesehen. Durch die horizontale Justiereinrichtung 13 kann die Führungsplatte 9 und der Hebel 3 entlang einer Horizontalen, d.h. im Gebrauchszustand im Wesentlichen in Fahrtrichtung des Rollstuhls, an verschiedenen Stellen befestigt werden. Durch die vertikale Justiereinrichtung 14 kann die Führungsplatte 9 und der Hebel 3 entlang einer Vertikalen, d.h. im Gebrauchszustand im Wesentlichen im rechten Winkel zu einer Bodenfläche, an verschiedenen Stellen befestigt werden. In der gezeigten Ausführungsform weisen die Justiereinrichtungen 13, 14 jeweils Schienen 15 mit Befestigungslöchern 16 und Schlitten 17 mit Befestigungs-

Die approbierte gedruckte Originalversion dieser Dissertation ist an der TU Wien Bibliothek verfügbar.
The approved original version of this doctoral thesis is available in print at TU Wien Bibliothek.
TU WIEN Bibliothek Your knowledge hub

stiften 18 auf. Zudem ist die Schiene 15 der vertikalen Justiereinrichtung 14 mit dem Schlitten 17 der horizontalen Justiereinrichtung 13 verbunden. Um die Führungsplatte 9 und den Hebel 3 an die Körpergröße einer Person anzupassen, müssen lediglich die Befestigungsstifte 18 aus den Befestigungslöchern 16 entnommen und die Schlitten 17 entlang der Schienen 15 an eine geeignete Position verschoben werden. Anschließend werden die Befestigungsstifte 18 wieder durch dazu vorgesehene Durchgangslöcher der Schlitten 17 und in die Befestigungslöcher 16 eingeführt, um so die Schlitten 17 zu fixieren.

[0035] Wie des Weiteren der Fig. 1 zu entnehmen ist, wird die Kraftübertragungseinheit 7 durch einen Riemenantrieb 19 gebildet, wobei ein Riemen 20, vorzugsweise ein Zahnriemen, die Drehbewegung des Hebels 3 von einer ersten Rolle (nicht sichtbar), insbesondere ein Zahnriemenrad, auf eine zweite Rolle 22, ebenfalls insbesondere ein Zahnriemenrad, überträgt. Zu diesem Zweck ist die erste Rolle drehfest mit dem Hebel 3 verbunden. Wie insbesondere aus Fig. 4 hervorgeht, ist die zweite Rolle 22 vorzugsweise über einen Riementrieb 23 mit einer Spannvorrichtung 24 mit einem Rollstuhlrad 34 verbunden. Die zweite Rolle 22 kann jedoch auch direkt mit dem Rollstuhlrad 34 verbunden sein. Um die Drehbewegung zu übersetzen, kann, wie in dem gezeigten Ausführungsbeispiel, die zweite Rolle 22 drehfest mit einer Übersetzungsrolle 39 verbunden sein, welche einen anderen Durchmesser aufweist und den Riemen 20 übersetzend mit dem Riementrieb 23 bzw. dem Rollstuhlrad 34 verbindet. In diesem Fall ist der Riementrieb 23 bzw. das Rollstuhlrad 34 mit der Übersetzungsrolle 39 in Kontakt.

[0036] Damit der Rollstuhlantrieb 1 möglichst kompakt ausgeführt werden kann, kann der Riemen 20 über Umlenkrollen 26 geführt werden, welche in der gezeigten Ausführungsform an den Schlitten 17 und den Schienen 15 befestigt sind, sodass der Riemen 20 im Wesentlichen entlang der Außenseite des Rollstuhlantriebs 1, insbesondere entlang der Schienen 15, führbar ist.

[0037] Um den Rollstuhlantrieb 1 an einem Rollstuhl 2 montieren zu können (vgl. Fig. 4), kann zumindest eine Befestigungsvorrichtung 27 insbesondere zur Befestigung an einer Armlehnenhalterung 28 des Rollstuhls 2 vorgesehen sein. Die Befestigungsvorrichtung 27 weist beispielsweise eine Montagestange zum Einführen in die Armlehnenhalterung 28 auf.

[0038] Wie aus Fig. 2 hervorgeht, ist die Führung 8 der Führungsplatte 9 in sich geschlossen und weicht von einer Kreisform ab. Der an dem ausziehbaren Hebelteil 5 befestigte Führungsstift gleitet in der Führung 8 und bewirkt somit während der Drehbewegung die Längenveränderung. Durch die von der Kreisform abweichende Kurvenform werden die Gelenke der antreibenden Person geschont und zugleich die von den Muskeln auf das Rollstuhlrad 34 übertragene Leistung erhöht. Zudem werden die an der Drehbewegung beteiligten Muskeln gleichmäßiger belastet und eine kontinuierliche, d.h. ruckelfreie, Fortbewegung ermöglicht.

[0039] Fig. 3 zeigt eine geschlossene Kurve C in einem kartesischen Koordinatensystem, welche dem Verlauf der Führung 8 in einer besonders bevorzugten Ausführungsform entspricht. Im Ursprung des Koordinatensystems käme der Befestigungspunkt 10 des Hebels 3 zu liegen. Die dargestellte Kurve C ist dabei im Wesentlichen durch folgende Gleichungen beschreibbar:

$$X_1 = A\cos(\theta)$$

$$Y_1 = B\sin(\theta)\sin^n(0{,}5 * \theta)$$

$$\begin{pmatrix} X \\ Y \end{pmatrix} = \begin{pmatrix} \cos(\beta) & -\sin(\beta) \\ \sin(\beta) & \cos(\beta) \end{pmatrix} \begin{pmatrix} X_1 \\ Y_1 \end{pmatrix}$$

, wobei θ als Laufkoordinate einem Winkel zwischen 0 und 2*pi bzw. 0° und 360° entspricht. Die Koordinaten X und Y beschreiben den Verlauf der Führung 8 in dem kartesischen Koordinatensystem. In der gezeigten Darstellung wurden der Parameter β zu 15,95°, der Parameter A zu 0,151 m, der Parameter B zu 0,152 m und der Parameter n zu 0,7 gewählt. Der Verlauf der durch die Gleichungen beschriebene Kurve, welche der punktierten Linie entspricht, kann zur Vermeidung von Unstetigkeiten und zur besseren Führung des Hebels 3 zur durchgezogenen Linie hin abgeflacht sein.

[0040] Die dargestellte Kurve C weist im Wesentlichen einen tropfenförmigen Verlauf auf und besitzt einen breiten 29 und einem schmalen Endkurvenbereich 30. Die Endkurvenbereiche 29, 30 weisen jeweils einen Scheitelpunkt 31 auf, welche durch eine Längsachse 32 miteinander verbunden sind. Die Längsachse ist um einen Winkel β von vorzugsweise 15° in mathematisch positive Richtung geneigt, sodass der breite Endkurvenbereich 29 nach unten geneigt ist. Im montierten Zustand des Rollstuhlantriebs 1 zeigt der schmale Endkurvenbereich 30 der geschlossenen Kurve C bevorzugt in Richtung einer Rückenlehne 33 des Rollstuhles 2 (vgl. Fig. 4). Dadurch ergibt sich eine besonders gelenkschonende Drehbewegung.

[0041] In Fig. 4 sind zwei Rollstuhlantriebe 1 jeweils in Verbindung mit jeweils einem Rollstuhlrad 34 eines Rollstuhls 2 dargestellt. Der Rollstuhl 2 kann, wie aus dem Stand der Technik bekannt, eine Sitzfläche 35, eine Rückenlehne 33 und zwei Fußablagen 36 aufweisen. Durch die Verwendung von zwei Rollstuhlantrieben 1 ist jedes Rollstuhlrad 34 einzeln über jeweils einen Rollstuhlantrieb 1 antreibbar. Wie in Fig. 4 ersichtlich, ist jeder der beiden Rollstuhlantriebe 1 jeweils über die Befestigungsvorrichtungen 27 mit dem Rollstuhl 2 verbunden. Die Drehbewegung eines Hebels 3 wird über einen Riemen 20 , eine erste Rolle und eine zweite Rolle 22 auf ein Rollstuhlrad 34 übertragen. Zu diesem Zweck kann jeweils ein Rollstuhlrad 34 über einen Riementrieb 23 mit

Die approbierte gedruckte Originalversion dieser Dissertation ist an der TU Wien Bibliothek verfügbar.
The approved original version of this doctoral thesis is available in print at TU Wien Bibliothek.
TU Bibliothek Your knowledge hub WIEN

Spannvorrichtung 24 mit der zweiten Rolle 22 verbunden sein. Es ist aber auch denkbar, dass die zweite Rolle unmittelbar mit einem Rollstuhlrad 34 verbunden ist. Auch eine Übersetzung mit Hilfe einer mit der zweiten Rolle 22 verbunden Übersetzungsrolle 39 ist möglich.

[0042] Fig. 5 zeigt den Rollstuhl 2 mit einem Rollstuhlantrieb 1 nochmals in Explosionsdarstellung. In der Darstellung ist ein zweiter Riemen 37 des Riementriebs 23 samt Spannvorrichtung 24 zu erkennen.

Patentansprüche

1. Mechanischer Rollstuhlantrieb (1) mit einem drehbar gelagerten Hebel (3), einem an dem Hebel (3) befestigten Griff (6) und einer Kraftübertragungseinheit (7) zur Übertragung einer Drehbewegung des Hebels (3) auf ein Rollstuhlrad (34), **dadurch gekennzeichnet, dass** der Hebel (3) längenveränderbar und entlang einer in sich geschlossenen und von der Kreisform abweichenden Führung (8) einer Führungsplatte (9) führbar ist, sodass eine Längenveränderung des Hebels (3) während der Drehbewegung stattfindet.

2. Mechanischer Rollstuhlantrieb (1) nach Anspruch 1, **dadurch gekennzeichnet, dass** der Hebel (3) einen in einem Befestigungspunkt (10) der Führungsplatte (9) drehbar gelagerten Hebelteil (4) und einen entlang der Führung (8) geführten, ausziehbaren Hebelteil (5) aufweist.

3. Mechanischer Rollstuhlantrieb (1) nach Anspruch 1 oder 2, **dadurch gekennzeichnet, dass** eine horizontale Justiereinrichtung (13) zur verstellbaren Befestigung der Führungsplatte (9) und des Hebels (3) entlang einer Horizontalen vorgesehen ist.

4. Mechanischer Rollstuhlantrieb (1) nach einem der Ansprüche 1 bis 3, **dadurch gekennzeichnet, dass** eine vertikale Justiereinrichtung (14) zur verstellbaren Befestigung der Führungsplatte (9) und des Hebels (3) entlang einer Vertikalen vorgesehen ist.

5. Mechanischer Rollstuhlantrieb (1) nach Anspruch 3 oder 4, **dadurch gekennzeichnet, dass** die Justiereinrichtung (13, 14) eine Schiene (15) mit Befestigungslöchern (16) und einen entlang der Schiene gleitenden Schlitten (17) mit einem Fixierstift (18) aufweist, wobei der Fixierstift (18) zur Fixierung des Schlittens (17) in die Befestigungslöcher (16) einführbar ist und die Führungsplatte (9) und der Hebel (3) mittelbar oder unmittelbar mit dem Schlitten (17) verbunden sind.

6. Mechanischer Rollstuhlantrieb (1) nach einem der Ansprüche 1 bis 5, **dadurch gekennzeichnet, dass** die Kraftübertragungseinheit (7) durch einen Riemenantrieb gebildet wird.

7. Mechanischer Rollstuhlantrieb (1) nach Anspruch 6, **dadurch gekennzeichnet, dass** ein Riemen (20) die Drehbewegung des Hebels (3) über eine erste Rolle, insbesondere ein erstes Zahnriemenrad, aufnimmt und an eine zweite Rolle (22), insbesondere ein zweites Zahnriemenrad, zur Übertragung der Drehbewegung an ein Rollstuhlrad (34) abgibt, wobei vorzugsweise Umlenkrollen (26) vorgesehen sind, sodass der Riemen (20) im Wesentlichen entlang einer Außenseite des Rollstuhlantriebs, insbesondere entlang der Schienen (15), führbar ist.

8. Mechanischer Rollstuhlantrieb nach einem der Ansprüche 1 bis 7, **dadurch gekennzeichnet, dass** die Kraftübertragungseinheit (7) einen vorzugsweise deaktivierbaren Freilaufmechanismus zur Übertragung der Drehbewegung des Hebels (3) in nur eine Drehrichtung aufweist.

9. Mechanischer Rollstuhlantrieb (1) nach einem der Ansprüche 1 bis 8, **dadurch gekennzeichnet, dass** an dem Griff (6) ein Betätigungshebel (40) für eine Bremsvorrichtung (41) des Rollstuhlrades (34) vorgesehen ist.

10. Mechanischer Rollstuhlantrieb (1) nach einem der Ansprüche 1 bis 9, **dadurch gekennzeichnet, dass** zumindest eine Befestigungsvorrichtung (27) zur Befestigung an einem Rollstuhl (2), insbesondere an einer Armlehnenhalterung (28) eines Rollstuhls, vorgesehen ist.

11. Mechanischer Rollstuhlantrieb (1) nach einem der Ansprüche 1 bis 10, **dadurch gekennzeichnet, dass** die Führung (8) einer im Wesentlichen tropfenförmigen geschlossenen Kurve (C) mit einem breiten (29) und einem schmalen Endkurvenbereich (30) entspricht, wobei die Endkurvenbereiche (29, 30) jeweils einen Scheitelpunkt (31) aufweisen und der schmale Endkurvenbereich (30) der geschlossenen Kurve (C) im montierten Zustand des Rollstuhlantriebs (1) in Richtung einer Rückenlehne (33) des Rollstuhles (2) zeigt.

12. Mechanischer Rollstuhlantrieb (1) nach Anspruch 11, **dadurch gekennzeichnet, dass** im montierten Zustand des Rollstuhlantriebs (1) eine zwischen den Scheitelpunkten (31) des breiten (29) und des schmalen Endkurvenbereichs (30) verlaufende Längsachse (32) zumindest 5°, bevorzugt zumindest 10°, vorzugsweise im Wesentlichen 15°, aber nicht mehr als 30°, zur Horizontalen, insbesondere mit dem breiten Endkurvenbereich nach unten, geneigt ist.

13. Mechanischer Rollstuhlantrieb (1) nach Anspruch

Die approbierte gedruckte Originalversion dieser Dissertation ist an der TU Wien Bibliothek verfügbar.
The approved original version of this doctoral thesis is available in print at TU Wien Bibliothek.
TU Bibliothek Your knowledge hub WIEN

12, **dadurch gekennzeichnet, dass** die Kurve (C) im Wesentlichen durch folgende mathematische Gleichungen beschreibbar ist:

$$X_1 = A\cos(\theta)$$

$$Y_1 = B\sin(\theta)\sin^n(0{,}5 * \theta)$$

$$\begin{pmatrix} X \\ Y \end{pmatrix} = \begin{pmatrix} \cos(\beta) & -\sin(\beta) \\ \sin(\beta) & \cos(\beta) \end{pmatrix} \begin{pmatrix} X_1 \\ Y_1 \end{pmatrix}$$

, wobei θ einem Winkel entspricht, die Koordinaten X und Y den Verlauf der Führung in einem kartesischen Koordinatensystem beschreiben, der Parameter β zwischen -20° und 30°, die Parameter A und B zwischen 0,01 m und 0,25 m und der Parameter n zwischen 0,2 und 0,9 festgelegt werden.

14. Rollstuhl (2) mit einer Sitzfläche (35), einer Rückenlehne (33) und zumindest zwei Rollstuhlrädern (34), **dadurch gekennzeichnet, dass** ein mechanischer Rollstuhlantrieb (1) vorgesehen ist, der mit zumindest einem Rollstuhlrad (34) verbunden ist und der Rollstuhlantrieb (1) nach einem der Ansprüche 1 bis 13 ausgebildet ist.

15. Rollstuhl (2) nach Anspruch 14, **dadurch gekennzeichnet, dass** an dem Rollstuhl zwei Rollstuhlräder (34) vorgesehen sind, die mit jeweils einem Rollstuhlantrieb (1) verbunden sind.

Claims

1. Mechanical wheelchair drive (1) comprising a rotatably mounted lever (3), a handle (6) fastened to the lever (3) and a force transfer unit (7) for transferring a rotational motion of the lever (3) to a wheelchair wheel (34), **characterized in that** the lever (3) has a variable length and can be guided along a closed guide (8) of a guide plate (9), which guide (8) deviates from the circular form, so that a length variation of the lever (3) takes place during the rotational motion.

2. Mechanical wheelchair drive (1) according to Claim 1, **characterized in that** the lever (3) has a lever part (4) mounted rotatably at a fastening point (10) of the guide plate (9) and an extendable lever part (5) guided along the guide (8).

3. Mechanical wheelchair drive (1) according to Claim 1 or 2, **characterized in that** a horizontal adjusting device (13) is provided for the adjustable fastening of the guide plate (9) and the lever (3) along a horizontal.

4. Mechanical wheelchair drive (1) according to one of Claims 1 to 3, **characterized in that** a vertical adjusting device (14) is provided for the adjustable fastening of the guide plate (9) and the lever (3) along a vertical.

5. Mechanical wheelchair drive (1) according to Claim 3 or 4, **characterized in that** the adjusting device (13, 14) comprises a rail (15) with fastening holes (16) and a carriage (17) with a fixing pin (18), which carriage (17) slides along the rail, wherein the fixing pin (18) can be introduced into the fastening holes (16) for fixing the carriage (17) and wherein the guide plate (9) and the lever (3) are connected indirectly or directly to the carriage (17).

6. Mechanical wheelchair drive (1) according to one of Claims 1 to 5, **characterized in that** the force transfer unit (7) is formed by a belt drive.

7. Mechanical wheelchair drive (1) according to Claim 6, **characterized in that** a belt (20) receives the rotational motion of the lever (3) via a first roller, in particular a first toothed belt wheel, and delivers it to a second roller (22), in particular a second toothed belt wheel, for transfer of the rotational motion to a wheelchair wheel (34), wherein preferably deflecting rollers (26) are provided so that the belt (20) can be guided substantially along an outer side of the wheelchair drive, in particular along the rails (15) .

8. Mechanical wheelchair drive according to one of Claims 1 to 7, **characterized in that** the force transfer unit (7) comprises a preferably de-activatable freewheeling mechanism for transferring the rotational motion of the lever (3) in only one direction of rotation.

9. Mechanical wheelchair drive (1) according to one of Claims 1 to 8, **characterized in that** an actuating lever (40) for a braking device (41) of the wheelchair drive (34) is provided on the handle (6) .

10. Mechanical wheelchair drive (1) according to one of Claims 1 to 9, **characterized in that** at least one fastening device (27) is provided for fastening on a wheelchair (2), in particular on an armrest holder (28) of a wheelchair.

11. Mechanical wheelchair drive (1) according to one of Claims 1 to 10, **characterized in that** the guide (8) corresponds to a substantially droplet-shaped closed curve (C) having a wide (29) and a narrow end curve region (30), wherein the end curve regions (29, 30) each have a vertex point (31) and the narrow end curve region (30) of the closed curve (C) in the mounted state of the wheelchair drive (1) points in the direction of a backrest (33) of the wheelchair (2).

Die approbierte gedruckte Originalversion dieser Dissertation ist an der TU Wien Bibliothek verfügbar.
The approved original version of this doctoral thesis is available in print at TU Wien Bibliothek.
TU WIEN Bibliothek Your knowledge hub

12. Mechanical wheelchair drive (1) according to Claim 11, **characterized in that** in the mounted state of the wheelchair drive (1) a longitudinal axis (32) running between the vertex points (31) of the wide (29) and the narrow end curve region (30) is inclined by at least 5°, preferably at least 10°, preferably substantially 15° but no more than 30° with respect to the horizontal, in particular with the wide end curve region downwards.

13. Mechanical wheelchair drive (1) according to Claim 12, **characterized in that** the curve (C) can be described substantially by the following mathematical equations:

$$X_1 = A\cos(\theta)$$

$$Y_1 = B\sin(\theta)\sin^n(0{,}5 * \theta)$$

$$\begin{pmatrix} X \\ Y \end{pmatrix} = \begin{pmatrix} \cos(\beta) & -\sin(\beta) \\ \sin(\beta) & \cos(\beta) \end{pmatrix} \begin{pmatrix} X_1 \\ Y_1 \end{pmatrix}$$

wherein θ corresponds to an angle, the coordinates X and Y describe the course of the guide in a Cartesian coordinate system, the parameter β is specified between -20° and 30°, the parameters A and B are specified between 0.01 m and 0.25 m and the parameter n is specified between 0.2 and 0.9.

14. Wheelchair (2) having a seat surface (35), a backrest (33) and at least two wheelchair wheels (34), **characterized in that** a mechanical wheelchair drive (1) is provided, which is connected to at least one wheelchair wheel (34) and the wheelchair drive (1) is configured according to one of Claims 1 to 13.

15. Wheelchair (2) according to Claim 14, **characterized in that** two wheelchair wheels (34) are provided on the wheelchair which are each connected to a wheelchair drive (1).

Revendications

1. Entraînement mécanique de fauteuil roulant (1) comprenant un levier (3) rotatif, une poignée (6) fixée au levier (3) et une unité de transmission de force (7) destinée à transmettre un mouvement de rotation du levier (3) à une roue de fauteuil roulant (34), **caractérisé en ce que** le levier (3) est réglable en longueur et peut être guidé le long d'un guide (8) fermé sur luimême et de forme non circulaire d'une plaque de guidage (9), de sorte que la longueur du levier (3) varie au cours du mouvement de rotation.

2. Entraînement mécanique de fauteuil roulant (1) selon la revendication 1, **caractérisé en ce que** le levier (3) présente une partie de levier (4) logée de manière rotative en un point de fixation (10) de la plaque de guidage (9) et une partie de levier (5) extensible guidée le long du guide (8).

3. Entraînement mécanique de fauteuil roulant (1) selon la revendication 1 ou 2, **caractérisé en ce qu'**un dispositif d'ajustement horizontal (13) est prévu pour fixer de manière réglable la plaque de guidage (9) et le levier (3) le long d'un axe horizontal.

4. Entraînement mécanique de fauteuil roulant (1) selon l'une des revendications 1 à 3, **caractérisé en ce qu'**un dispositif d'ajustement vertical (14) est prévu pour fixer de manière réglable la plaque de guidage (9) et le levier (3) le long d'un axe vertical.

5. Entraînement mécanique de fauteuil roulant (1) selon la revendication 3 ou 4, **caractérisé en ce que** le dispositif d'ajustement (13, 14) présente un rail (15) pourvu de trous de fixation (16) et un chariot (17) coulissant le long du rail et pourvu d'une broche de fixation (18), dans lequel la broche de fixation (18) peut être introduite dans les trous de fixation (16) pour fixer le chariot (17), et la plaque de guidage (9) et le levier (3) sont reliés directement ou indirectement au chariot (17).

6. Entraînement mécanique de fauteuil roulant (1) selon l'une des revendications 1 à 5, **caractérisé en ce que** l'unité de transmission de force (7) est formée d'une courroie d'entraînement.

7. Entraînement mécanique de fauteuil roulant (1) selon la revendication 6, **caractérisé en ce qu'**une courroie (20) reçoit le mouvement de rotation du levier (3) par l'intermédiaire d'une première poulie, en particulier une première poulie crantée, et le transmet à une deuxième poulie (22), en particulier une deuxième poulie crantée, pour transmettre le mouvement de rotation à une roue de fauteuil roulant (34), dans lequel il est de préférence prévu des poulies de renvoi (26), de sorte que la courroie (20) peut être guidée essentiellement le long d'un côté extérieur de l'entraînement de fauteuil roulant, en particulier le long des rails (15).

8. Entraînement mécanique de fauteuil roulant selon l'une des revendications 1 à 7, **caractérisé en ce que** l'unité de transmission de force (7) présente un mécanisme à roue libre, de préférence désactivable, destiné à transmettre le mouvement de rotation du levier (3) dans un seul sens de rotation.

9. Entraînement mécanique de fauteuil roulant (1) selon l'une des revendications 1 à 8, **caractérisé en**

Die approbierte gedruckte Originalversion dieser Dissertation ist an der TU Wien Bibliothek verfügbar.
The approved original version of this doctoral thesis is available in print at TU Wien Bibliothek.
TU WIEN Bibliothek Your knowledge hub

ce qu'un levier de commande (40) d'un dispositif de freinage (41) de la roue de fauteuil roulant (34) est prévu sur la poignée (6).

10. Entraînement mécanique pour fauteuil roulant (1) selon l'une des revendications 1 à 9, **caractérisé en ce qu'**il est prévu au moins un dispositif de fixation (27) pour la fixation à un fauteuil roulant (2), en particulier à un support d'accoudoir (28) d'un fauteuil roulant.

11. Entraînement mécanique de fauteuil roulant (1) selon l'une des revendications 1 à 10, **caractérisé en ce que** le guide (8) correspond à une courbe fermée (C) sensiblement en forme de goutte présentant une zone de courbe d'extrémité large (29) et une zone de courbe d'extrémité étroite (30), dans lequel les zones de courbe d'extrémité (29, 30) présentent chacune un sommet (31) et la zone de courbe d'extrémité étroite (30) de la courbe fermée (C) est dirigée vers un dossier (33) du fauteuil roulant (2) lorsque l'entraînement de fauteuil roulant (1) est monté.

12. Entraînement mécanique de fauteuil roulant (1) selon la revendication 11, **caractérisé en ce que**, lorsque l'entraînement de fauteuil roulant (1) est monté, un axe longitudinal (32) s'étendant entre les sommets (31) de la zone de courbe d'extrémité large (29) et de la zone de courbe d'extrémité étroite (30) est incliné d'au moins 5°, préférablement d'au moins 10°, de préférence essentiellement de 15°, mais pas de plus de 30°, par rapport à l'horizontale, en particulier avec la zone de courbe d'extrémité large vers le bas.

13. Entraînement mécanique de fauteuil roulant (1) selon la revendication 12, **caractérisé en ce que** la courbe (C) peut être décrite essentiellement par les équations mathématiques suivantes :

$$X_1 = A\cos(\theta)$$

$$Y_1 = B\sin(\theta)\sin^n(0{,}5 * \theta)$$

$$\begin{pmatrix} X \\ Y \end{pmatrix} = \begin{pmatrix} \cos(\beta) & -\sin(\beta) \\ \sin(\beta) & \cos(\beta) \end{pmatrix} \begin{pmatrix} X_1 \\ Y_1 \end{pmatrix}$$

, où θ correspond à un angle, les coordonnées X et Y décrivent le parcours du guide dans un système de coordonnées cartésiennes, le paramètre β est fixé entre -20° et 30°, les paramètres A et B entre 0,01 m et 0,25 m et le paramètre n entre 0,2 et 0,9.

14. Fauteuil roulant (2) comprenant une assise (35), un dossier (33) et au moins deux roues de fauteuil roulant (34), **caractérisé en ce qu'**il est prévu un entraînement mécanique de fauteuil roulant (1) qui est relié à au moins une roue de fauteuil roulant (34) et **en ce que** l'entraînement de fauteuil roulant (1) est conçu selon l'une des revendications 1 à 13.

15. Fauteuil roulant (2) selon la revendication 14, **caractérisé en ce que** deux roues de fauteuil roulant (34) sont prévues sur le fauteuil roulant, lesquelles sont reliées chacune à un entraînement de fauteuil roulant (1).

Die approbierte gedruckte Originalversion dieser Dissertation ist an der TU Wien Bibliothek verfügbar.
The approved original version of this doctoral thesis is available in print at TU Wien Bibliothek.
TU Bibliothek Your knowledge hub WIEN

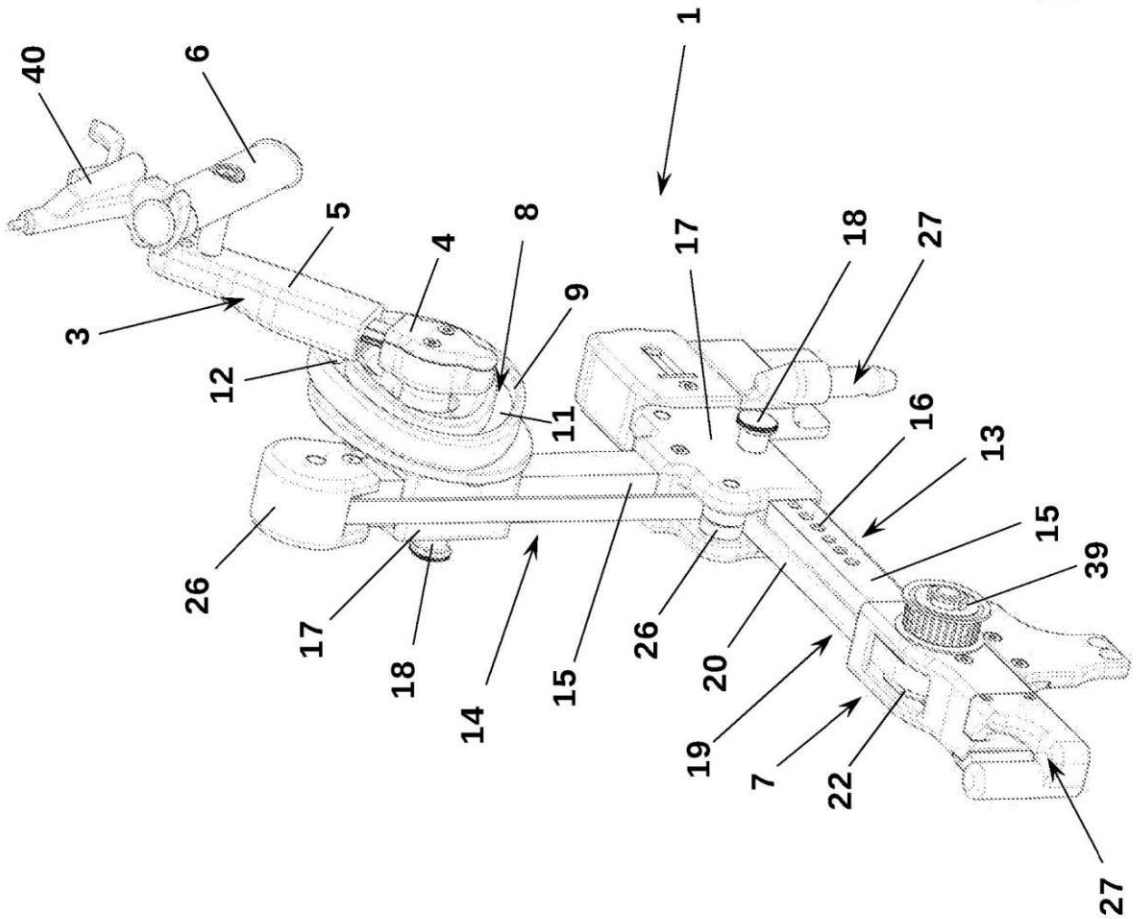

Fig. 1

Die approbierte gedruckte Originalversion dieser Dissertation ist an der TU Wien Bibliothek verfügbar.
The approved original version of this doctoral thesis is available in print at TU Wien Bibliothek.

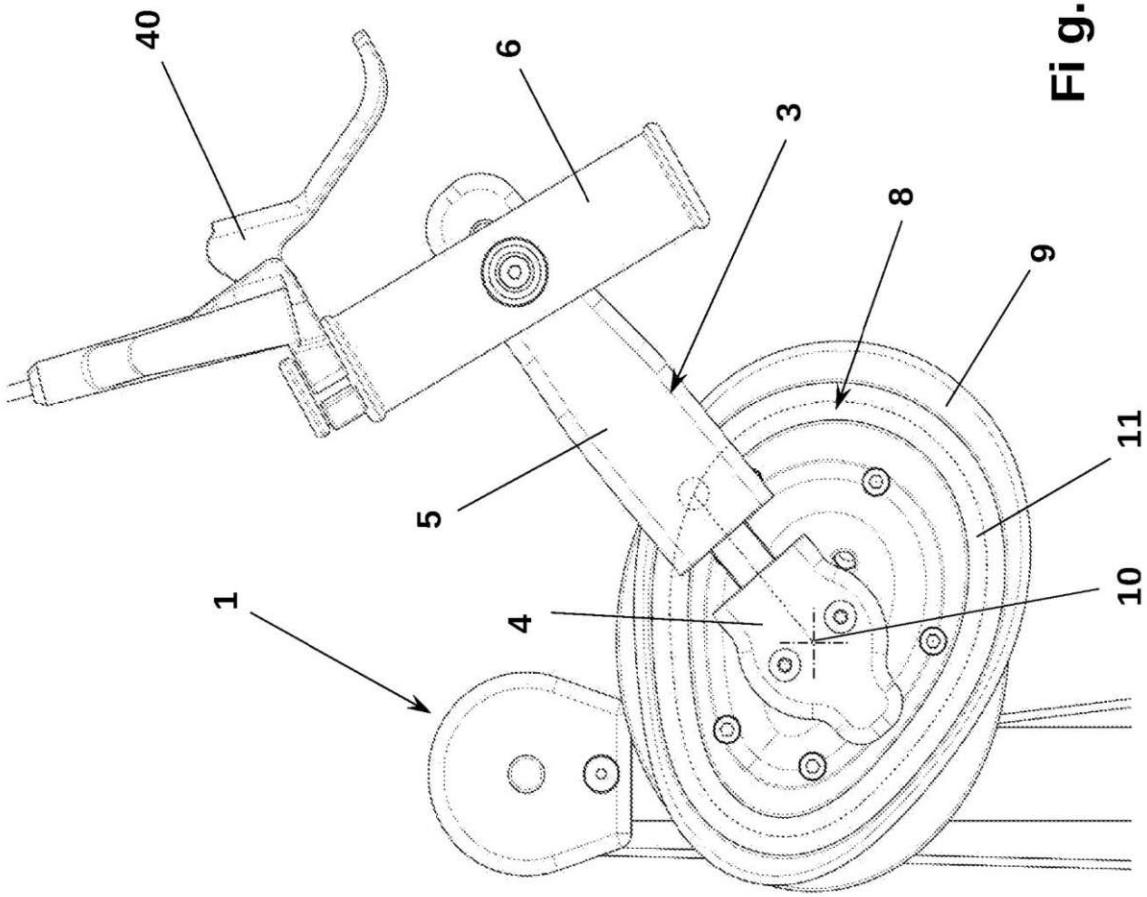

Fig. 2

Die approbierte gedruckte Originalversion dieser Dissertation ist an der TU Wien Bibliothek verfügbar.
The approved original version of this doctoral thesis is available in print at TU Wien Bibliothek.

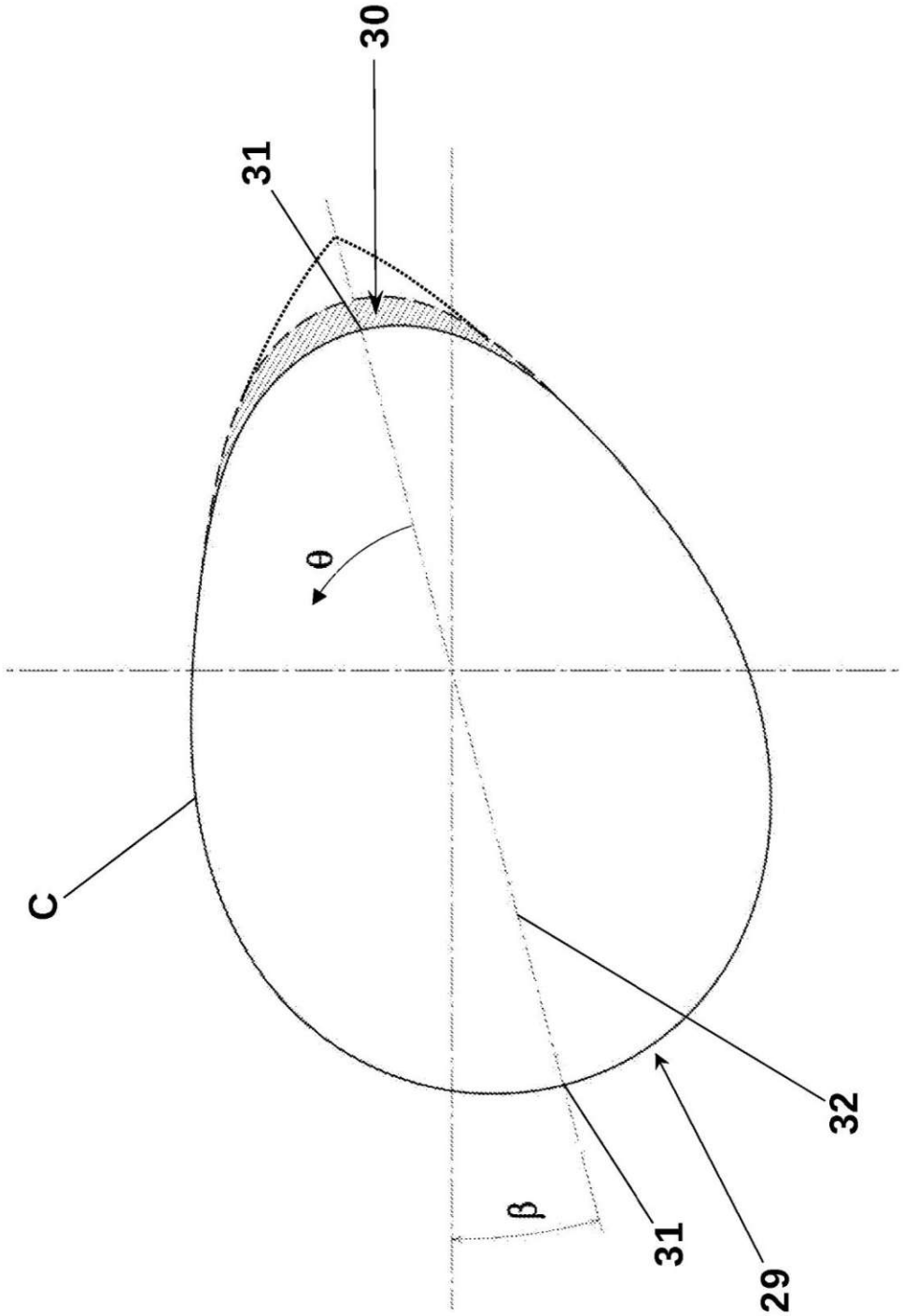

Fig. 3

Die approbierte gedruckte Originalversion dieser Dissertation ist an der TU Wien Bibliothek verfügbar.
The approved original version of this doctoral thesis is available in print at TU Wien Bibliothek.

EP 3 823 576 B1

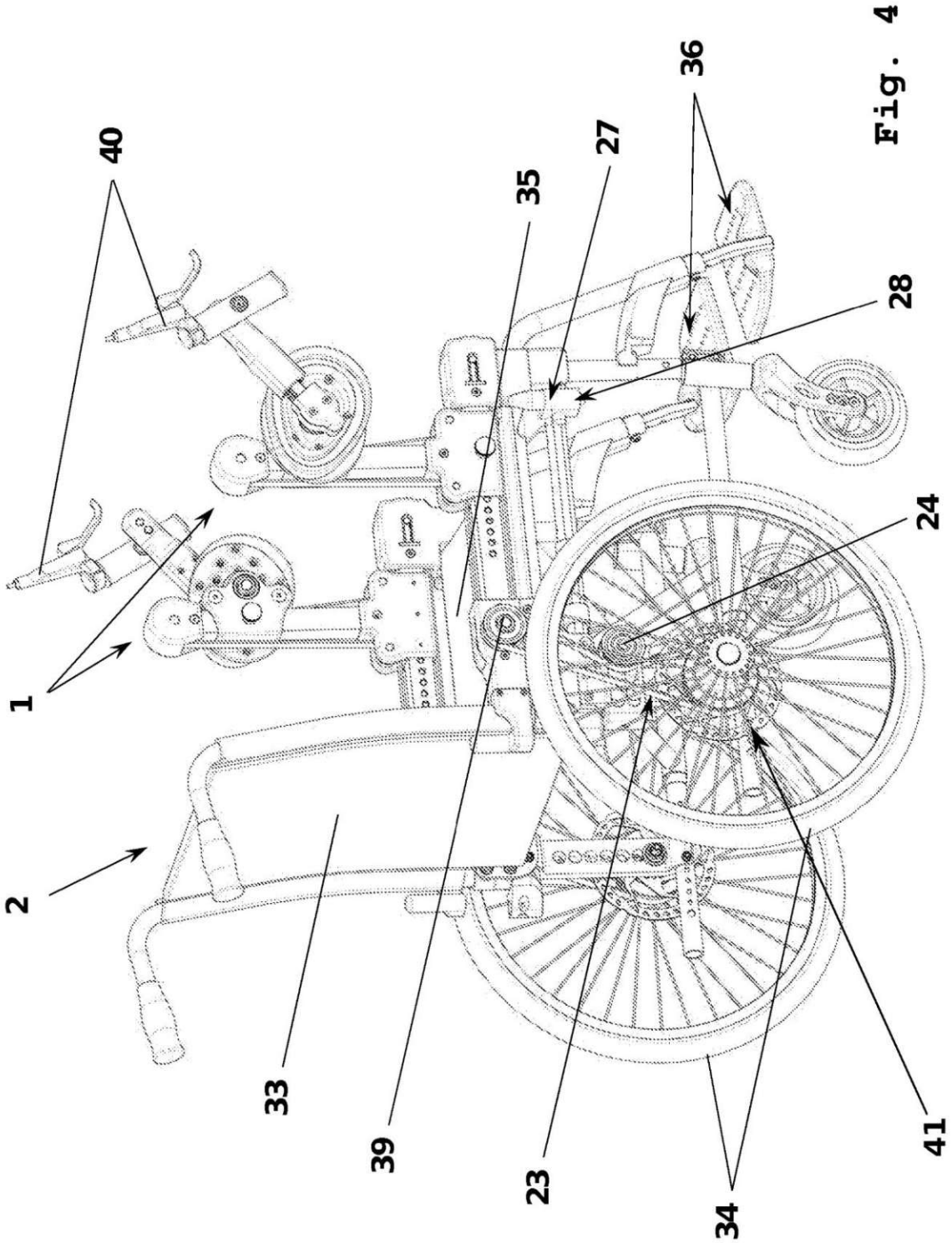

Fig. 4

Die approbierte gedruckte Originalversion dieser Dissertation ist an der TU Wien Bibliothek verfügbar.
The approved original version of this doctoral thesis is available in print at TU Wien Bibliothek.

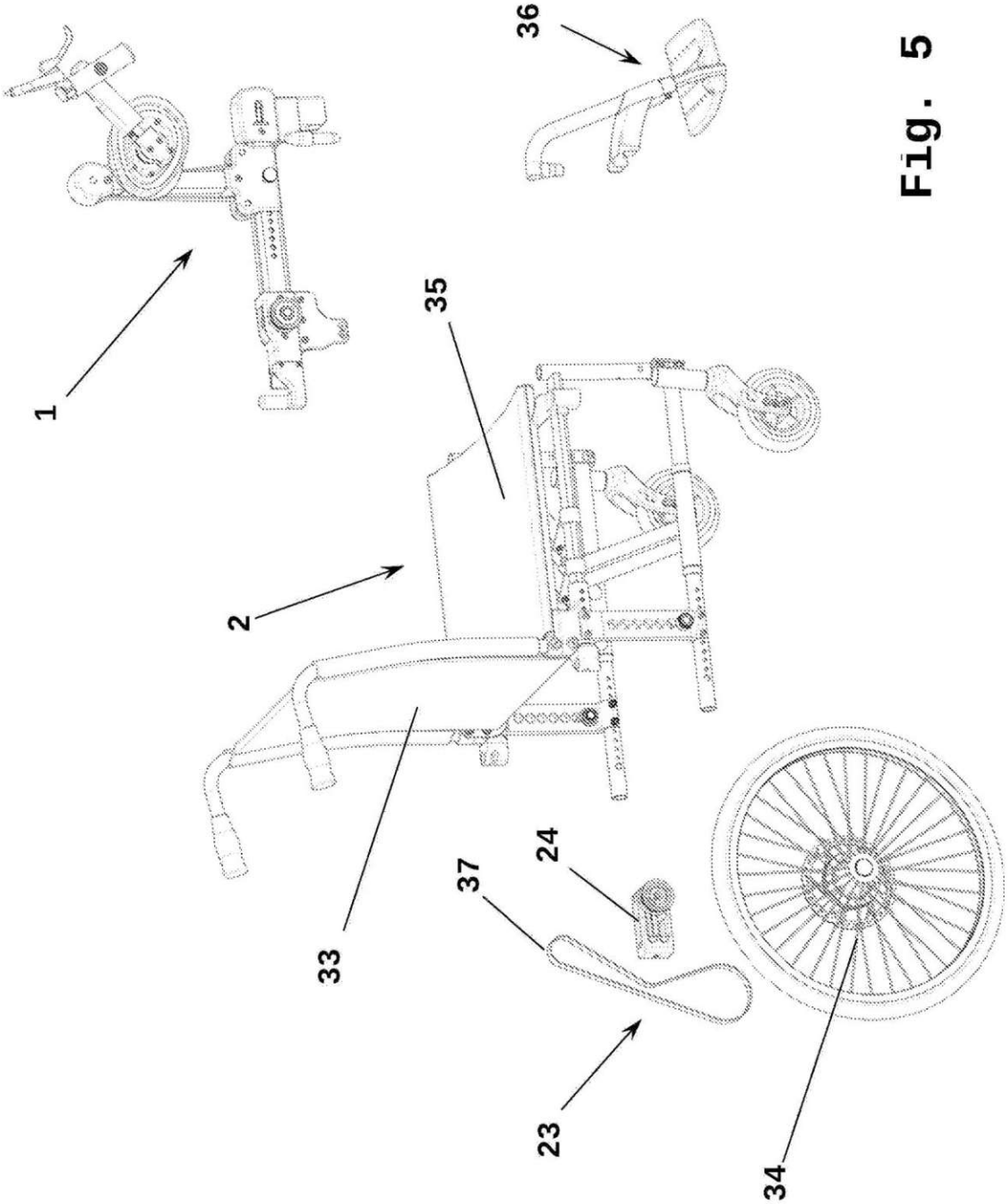

Fig. 5

Die approbierte gedruckte Originalversion dieser Dissertation ist an der TU Wien Bibliothek verfügbar.
The approved original version of this doctoral thesis is available in print at TU Wien Bibliothek.

EP 3 823 576 B1

IN DER BESCHREIBUNG AUFGEFÜHRTE DOKUMENTE

Diese Liste der vom Anmelder aufgeführten Dokumente wurde ausschließlich zur Information des Lesers aufgenommen und ist nicht Bestandteil des europäischen Patentdokumentes. Sie wurde mit größter Sorgfalt zusammengestellt; das EPA übernimmt jedoch keinerlei Haftung für etwaige Fehler oder Auslassungen.

In der Beschreibung aufgeführte Patentdokumente

- DE 3413312 A1 **[0008]**
- US 4758013 A **[0011]**
- US 6910701 B1 **[0011]**
- WO 2004110329 A1 **[0011]**
- US 5037120 A **[0011]**
- WO 2014199110 A1 **[0012]**
- DE 8803670 U1 **[0013]**

Die approbierte gedruckte Originalversion dieser Dissertation ist an der TU Wien Bibliothek verfügbar.
The approved original version of this doctoral thesis is available in print at TU Wien Bibliothek.
TU WIEN Bibliothek Your knowledge hub

MARKUS PUCHINGER

Diplom Ingenieur

PERSÖNLICHES

Geburtsdatum: [redacted]

Geburtsort: [redacted]

Staatsangehörigkeit: [redacted]

Familienstand: [redacted]

[redacted]

KONTAKT

BERUFSERFAHRUNG

St. Pölten seit 09/2019	**HTBLuVA St. Pölten** **Lehrer für Tages- und Abendschule** Abteilung Maschinenbau
WIEN 04/2017 – 07/2021 09/2013 – 07/2021	**Technische Universität Wien** **Universitätsassistent** **Projektassistent** am Institut für Konstruktionswissenschaften und Technische Logistik / Rehabilitationstechnik

AUSBILDUNG

WIEN seit 04/2015	**Technische Universität Wien** **Doktorstudium Maschinenbau**
WIEN 01/2013 – 04/2015	**Technische Universität Wien** **Masterstudium Maschinenbau** (mit ausgezeichnetem Erfolg abgeschlossen)
WIEN 02/2007 – 01/2013	**Technische Universität Wien** **Bachelorstudium Maschinenbau**
ALLENTSTEIG / ST. PÖLTEN 09/2006 - 03/2007	**Präsenzdienst** **Schreiber / Presseabteilung**
ST. PÖLTEN 09/2001 – 06/2006	**HTBLuVA St. Pölten** **Automatisierungstechnik und Mechatronik** (mit ausgezeichnetem Erfolg abgeschlossen)
ST. PÖLTEN 09/1997 – 06/2001	**BRG und BORG St. Pölten** **Unterstufengymnasium mit Schwerpunkt Musik**

KENNTNISSE

MS Word®	
MS Excel®	
MS Power Point ®	
Solid Works	
CATIA®	
Creo®	
LabVIEW®	
MatLAB®	
MathCad	
3D Druck	
C++	

Sprachen

Deutsch	
Englisch	

PATENTE

Patente

07/2019 EP3823576B1:
Mechanischer (gelenkschonender) Rollstuhlantrieb
WO 2020/014720:
Mechanical Wheelchair Drive and Wheelchair having such a Mechanical Wheelchair Drive

INTERESSEN

Oldtimerfahrzeuge, Skisport, Radsport, Wandern

Die approbierte gedruckte Originalversion dieser Dissertation ist an der TU Wien Bibliothek verfügbar.
The approved original version of this doctoral thesis is available in print at TU Wien Bibliothek.
TU Bibliothek, Your knowledge hub WIEN

PUBLIKATIONEN

M. Puchinger, N. Kurup, K. Gstaltner, M. Pandy, and M. Gföhler, “Metabolic Cost and Mechanical Efficiency of a Novel Handle-Based Device for Wheelchair Propulsion,” *Journal of Rehabilitation Medicine*, vol. 54, 2022, doi: 10.2340/jrm.v54.1503

E. Ambrosini *et al.,* “A Robotic System with EMG-Triggered Functional Eletrical Stimulation for Restoring Arm Functions in Stroke Survivors,” *Neurorehabilitation and Neural Repair*, vol. 35, no. 4, pp. 334–345, 2021, doi: 10.1177/1545968321997769

M. Gföhler *et al.,* “Development of a mobile, compact desalination Plant operated by muscle power,” in 2021, p. 1

M. Gföhler, M. Puchinger, and K. Gstaltner, “,,KURT“ - ein gelenkschonender manueller Rollstuhlantrieb,” *Orthopädie Technik*, 07/21, no. 7, pp. 30–35, 2021

M. Puchinger, P. Stefanek, K. Gstaltner, M. Pandy, and M. Gföhler, “In Vivo Biomechanical Assessment of a Novel Handle-Based Wheelchair Drive,” *IEEE Transactions on Neural Systems and Rehabilitation Engineering*, vol. 29, pp. 1669–1678, 2021, doi: 10.1109/tnsre.2021.3105388

E. Ambrosini, M. Russold, M. Puchinger, and M. Gföhler, “A Hybrid Robotic System for Arm Training of Stroke Survivors: Concept and First Evaluation,” *IEEE Transactions on Biomedical Engineering*, vol. 66, no. 12, pp. 3290–3300, 2019, doi: 10.1109/tbme.2019.2900525

N. Babu Rajendra Kurup, M. Puchinger, and M. Gfoehler, “A preliminary muscle activity analysis: Handle based and push-rim wheelchair propulsion,” *Journal of Biomechanics*, vol. 89, pp. 119–122, 2019, doi: 10.1016/j.jbiomech.2019.04.011

M. Puchinger, J. Zajc, M. Russold, and M. Gföhler, “The Evolution Of The Retrainer Passive Arm Exoskeleton,” in 2019, p. 208

J. Zajc, M. Puchinger, M. Russold, and M. Gföhler, “Patient Testing A Control Strategy For An Upper Arm Rehabilitation Device,” in 2019, p. 209

N. Babu Rajendra Kurup, M. Puchinger, and M. Gföhler, “Forward dynamic optimization of handle path and muscle activity for handle based isokinetic wheelchair propulsion: A simulation study,” *Computer Methods in Biomechanics and Biomedical Engineering*, vol. 22, no. 1, pp. 55–63, 2018, doi: 10.1080/10255842.2018.1527321

N. Babu Rajendra Kurup, M. Puchinger, and M. Gföhler, “Preliminary analysis of kinematics and muscle activity on a novel handle based wheelchair propulsion mechanism,” in 2018, p. 1

S. Dalla Gasperina, M. Gandolla, M. Puchinger, M. Gföhler, and A. Pedrocchi, “Multi-modal human-machine control interfaces of upper limb motorized exoskeletons for severely impaired patients,” in 2018, p. 6

N. B. R. Kurup, M. Puchinger, T. Keck, and M. Gfoehler, “Wrist Kinematics and Kinetics during Wheelchair Propulsion with a Novel Handle-based Propulsion Mechanism,” in 2018

D. Pohselt, M. Gföhler, and M. Puchinger, “Ein Stützarm aus dem 3-D-Drucker,” *Die Presse*, 14/07, 2018

M. Puchinger, N. Babu Rajendra Kurup, and M. Gföhler, “A Novel Device for Manual Wheelchair Propulsion - first experimental results,” in 2018, p. 1

M. Puchinger, N. Babu Rajendra Kurup, and M. Gföhler, “Passive light-weight arm exoskeleton: possible applications,” in 2018, pp. 21–25

M. Puchinger, N. Babu Rajendra Kurup, and M. Gföhler, “Performance of a manual wheelchair propulsion device optimized for the musculoskeletal system of the upper limbs - preliminary results,” in 2018, p. 1

M. Puchinger, N. Babu Rajendra Kurup, T. Keck, J. Zajc, M. Russold, and M. Gföhler, “The RETRAINER Light-Weight Arm Exoskeleton: Effect of Adjustable Gravity Compensation on Muscle Activations and Forces,” in 2018, p. 6

J. Zajc, M. Puchinger, M. Russold, and M. Gföhler, “Comparison of Three Control Strategies for an Upper Arm Rehabilitation Device,” in 2018, pp. 162–166

E. Ambrosini, M. Gföhler, and M. Puchinger, “The combined action of a passive exoskeleton and an EMG-controlled neuroprosthesis for upper limb stroke rehabilitation: First results of the RETRAINER project,” in 2017, 2017

N. Babu Rajendra Kurup, M. Puchinger, and M. Gföhler, “Dynamically Optimized Muscle Activity Patterns From A Novel Handle Based Propulsion Movement For A Wheelchair,” in German Sport University Cologne, Köln (Cologne), 2017, p. 4

M. Gandolla *et al.,* “Upper limb assistive devices for muscular dystrophy patients: Proposed approaches,” in 6/4, 2017

M. Gandolla, M. Gföhler, and M. Puchinger, “BRIDGE — Behavioural reaching interfaces during daily antigravity activities through upper limb exoskeleton: Preliminary results,” in 2017, 2017

M. Puchinger, N. Babu Rajendra Kurup, and M. Gföhler, “A Test Rig for Investigating Manual Wheelchair Propulsion Devices,” in Current Directions in Biomedical Engineering - Abstracts - TAR-Conference 2017 - Berlin, March 9-10, 2017, p. 12

M. Bulgheroni, M. Gföhler, and M. Puchinger, “Reaching And Grasping Training Based On Robotic Hybrid Assistance For Neurological Patients,” in 2016, pp. 21–24

M. Puchinger and M. Gföhler, “The ReTrainer arm exoskeleton - a modular lightweight device that combines adjustable gravity compensation, lockable joints and neuromuscular electrical stimulation,” in 2016, pp. 11–14

Die approbierte gedruckte Originalversion dieser Dissertation ist an der TU Wien Bibliothek verfügbar.
The approved original version of this doctoral thesis is available in print at TU Wien Bibliothek.
TU Bibliothek Your knowledge hub WIEN